

AD-780 429

THE NOL LARGE SCALE GAP TEST. III.  
COMPILATION OF UNCLASSIFIED DATA AND  
SUPPLEMENTARY INFORMATION FOR INTER-  
PRETATION OF RESULTS

Donna Price, et al

Naval Ordnance Laboratory  
White Oak, Maryland

8 March 1974

DISTRIBUTED BY:

**NTIS**

National Technical Information Service  
U. S. DEPARTMENT OF COMMERCE  
5285 Port Royal Road, Springfield Va. 22151

## UNCLASSIFIED

SECURITY CLASSIFICATION OF THIS PAGE (When Data Entered)

REPORT DOCUMENTATION PAGE		READ INSTRUCTIONS BEFORE COMPLETING FORM
1. REPORT NUMBER NOLTR 74-40	2. GOVT ACCESSION NO.	3. RECIPIENT'S CATALOG NUMBER AD 780429
4. TITLE (and Subtitle) The NOL Large Scale Gap Test. III. Compilation of Unclassified Data and Supplementary Information for Interpretation of Results		5. TYPE OF REPORT & PERIOD COVERED Final
7. AUTHOR(s) Donna Price A. R. Clairmont, Jr. J. O. Erkman		6. PERFORMING ORG. REPORT NUMBER
9. PERFORMING ORGANIZATION NAME AND ADDRESS Naval Ordnance Laboratory (Code 231) White Oak Silver Spring, Maryland 20910		8. CONTRACT OR GRANT NUMBER(s)
11. CONTROLLING OFFICE NAME AND ADDRESS Chief of Naval Material Navy Department Washington, D. C. 20360		10. PROGRAM ELEMENT, PROJECT, TASK AREA & WORK UNIT NUMBERS 61152N, ZR000-01, R013-09-010, MAT 03L000-15923
14. MONITORING AGENCY NAME & ADDRESS (if different from Controlling Office)		12. REPORT DATE 8 March 1974
		13. NUMBER OF PAGES 89
		15. SECURITY CLASS. (of this report) UNCLASSIFIED
		15a. DECLASSIFICATION/DOWNGRADING SCHEDULE
16. DISTRIBUTION STATEMENT (of this Report) Approved for public release; distribution unlimited.		
17. DISTRIBUTION STATEMENT (of the abstract entered in Block 20, if different from Report)		
18. SUPPLEMENTARY NOTES		
19. KEY WORDS (Continue on reverse side if necessary and identify by block number) Explosives Sensitivity Shock Sensitivity Gap Test Critical Diameter NATIONAL TECHNICAL INFORMATION SERVICE Department of Defense Springfield, VA 22114		
20. ABSTRACT (Continue on reverse side if necessary and identify by block number) The objectives of this report are to bring up to date the compilations of all unclassified NOL large-scale gap test (LSGT) results, to describe exactly the present standardized test, and to review or report all NOL studies made on the test or modifications of it. The topics presented include standardized test procedure, best test calibration, effect of temperature and porosity on sensitivity, and the effect on test values of modifying the test. A comparison between the NOL large scale and small		

DD FORM 1 JAN 73 1473

EDITION OF 1 NOV 65 IS OBSOLETE  
S/N 0102-014-6601

UNCLASSIFIED

SECURITY CLASSIFICATION OF THIS PAGE (When Data Entered)

UNCLASSIFIED

SECURITY CLASSIFICATION OF THIS PAGE(When Data Entered)

20. Abstract (Cont.)

scale gap test values is given, and also the relationship of the former to the wedge test data. Finally an appendix is devoted to the compilation of critical diameter ( $d_c$ ) measurements and to showing that there is no general relationship between the LSGT results and  $d_c$ .

This report supersedes NOLTR 65-177.

UNCLASSIFIED

SECURITY CLASSIFICATION OF THIS PAGE(When Data Entered)

THE NOL LARGE SCALE GAP TEST. III. COMPILATION  
OF UNCLASSIFIED DATA AND SUPPLEMENTARY  
INFORMATION FOR INTERPRETATION OF RESULTS

Prepared by:  
Donna Price  
A. R. Clairmont, Jr.  
J. O. Erkman

ABSTRACT: The objectives of this report are to bring up to date the compilations of all unclassified NOL large-scale gap test (LSGT) results, to describe exactly the present standardized test, and to review or report all NOL studies made on the test or modifications of it. The topics presented include standardized test procedure, best test calibration, effect of temperature and porosity on sensitivity, and the effect on test values of modifying the test. A comparison between the NOL large scale and small scale gap test values is given, and also the relationship of the former to the wedge test data. Finally an appendix is devoted to the compilation of critical diameter ( $d_c$ ) measurements and to showing that there is no general relationship between the LSGT results and  $d_c$ .

This report supersedes NOLTR 65-177. (AD-368687L)

NAVAL ORDNANCE LABORATORY  
WHITE OAK, MARYLAND

NOLTR 74-40

8 March 1974

THE NOL LARGE SCAPE GAP TEST. III. COMPILATION OF UNCLASSIFIED  
DATA AND SUPPLEMENTARY INFORMATION FOR INTERPRETATION OF RESULTS

The writing and compilations of this report were carried out under Task IR-159, Transition from Deflagration to Detonation, of NOL's Independent Research Program. The report itself is a compendium of the results of test work carried out under numerous projects. It is believed that assembling all such information in a single report is an important contribution to the study of shock sensitivity of explosives and propellants.

ROBERT WILLIAMSON II  
Captain, USN  
Commander

*Carl Boyars*  
CARL BOYARS  
By direction

CONTENTS

	Page
I. INTRODUCTION . . . . .	1
II. STANDARDIZED LSGT PROCEDURE . . . . .	2
III. CALIBRATION OF THE LSGT . . . . .	8
IV. LSGT RESULTS . . . . .	14
V. EFFECT OF TEMPERATURE AND POSOSITY ON LSGT RESULTS . . .	18
A. Temperature . . . . .	18
B. Porosity . . . . .	19
VI. EFFECT OF CHANGING LSGT ELEMENTS . . . . .	24
A. Donor . . . . .	24
B. Gap Material . . . . .	25
C. Confinement . . . . .	27
D. Witness . . . . .	32
1. Steel Plate . . . . .	32
2. Explosive Witness; Modified and Extended Tests . . .	34
VII. COMPARISON OF NOL LARGE SCALE AND SMALL SCALE GAP TEST VALUES . . . . .	36
VIII. RELATIONSHIP OF LSGT RESULTS TO WEDGE TEST DATA . . .	38
IX. SUMMARY . . . . .	52
X. REFERENCES . . . . .	53
APPENDIX A - GLOSSARY . . . . .	A-1
APPENDIX B - DENSITY OF EXPLOSIVE COMPONENTS . . . . .	B-1
APPENDIX C - COMPILATION OF LSGT RESULTS . . . . .	C-1
APPENDIX D - SUMMARY OF NOL MEASUREMENTS OF CRITICAL DIAMETER FOR DETONATION . . . . .	D-1

## CONTENTS (Cont.)

## ILLUSTRATIONS

Figure	Title	Page
1	Cross Section of LSGT Assembly . . . . .	4
2	Witness Plate Damage from a Detonation (GO) . . . . .	5
3	Witness Plate Damage from a Strong Chemical Reaction (NO GO) . . . . .	5
4	LSGT Results for Pressed Charges of Organic HE . . . . .	20
5	LSGT Results for Pressed Charges of AP and AP/Fuel Mixtures . . . . .	21
6	LSGT Results for Two Composite Propellant Models . . . . .	21
7	Effect of Confinement on 50% Gap in LSGT . . . . .	30
8	Variation of Initiating Pressure of Cast Comp B with Reciprocal Effective Charge Diameter . . . . .	33
9	Extended Gap Test Assembly . . . . .	35
10	Comparison of Extended, Modified, and Regular LSGT Results for 7 $\mu$ AP . . . . .	37
11	Correlation of SSGT and LSGT Values . . . . .	40
12	Reciprocal Run Length vs Pressure for Unconfined DINA . . . . .	44
13	Reciprocal Run Length vs Pressure for Confined DINA . . . . .	44
14	Shock to Detonation Transition for Cast Pentolite and DINA . . . . .	49
15	Shock to Detonation Transition for Other TNT Based Cast Explosives . . . . .	49
16	Approximate Particle Size Distribution of Three Classes of RDX . . . . .	50
D-1	Detonation Failure Limit Curves for TNT . . . . .	D-5
D-2	Detonability Curves (Group 1) . . . . .	D-7
D-3	Detonability Curves (Group 2) . . . . .	D-7
D-4	Minima in Detonability Curves . . . . .	D-9
D-5	Critical Diameter vs %TMD for Composite Model . . . . .	D-10
D-6	Relations $d_C$ vs $P_g$ for Group 1 HE . . . . .	D-11
D-7	Relations $d_C$ vs $P_g$ for Group 2 HE . . . . .	D-12

## TABLES

Table	Title	Page
1	Determination of 50% Point from Various Test Patterns Shown by a Detonable Material . . . . .	6
2	Pressure-Distance Data from Current LSGT Calibrations . . . . .	12
3	Hugoniot Data for Essentially Non-Porous Explosives . . . . .	13
4	LSGT Results at 25°C for Simple Double Base Propellants . . . . .	17

CONTENTS (Cont.)

TABLES (Cont.)

Table	Title	Page
5	50% Gap Thickness for Various Attenuators . . . . .	26
6	Data Showing Effect of Confinement on 50% Gap and $P_i$ . . . . .	29
7	Effect Of Confinement on Test Results for Comp B . . . . .	31
8	Comparison of LSGT and SSGT Results at Same Relative Density . . . . .	39
9	Data for Shock-to-Detonation Transition in Cast DINA . . . . .	43
10	Wedge Test Data for Cast Charges . . . . .	47
11	Critical Initiating Pressure ( $P_i$ ) from LSGT Data . . . . .	48
D-1	NOL Determinations of Critical Diameter at Only One Density . . . . .	D-2



## I. INTRODUCTION

The NOL Large Scale Gap Test (LSGT) is essentially a modification of that first developed by Eyster, Smith, and Walton (1) for high explosives. As in all gap tests, an attenuator is placed between a standard high explosive booster and the test material; the thickness of the gap (attenuator) is varied until detonation is achieved in 50% of the trials, and this 50% gap is the measured quantity. The major changes from the earlier test are confinement of test charge and use of polymethyl methacrylate (PMMA) rather than wax as the gap material. The first permits extension of the quantitative scale to many propellants and most explosives; the second is a matter of convenience.

The usefulness of the present test has been greatly extended by its calibration which gives the shock pressure on axis as a function of the gap length. In conjunction with Hugoniot data for the test material, the measured 50% gap can be interpreted as a critical initiating pressure for detonation of the test material. The test now offers, therefore, one of a number of methods for studying shock-to-detonation transitions, and has frequently been so used, in addition to its use in routine screening of materials for their shock sensitivity. In either case, however, valid test results for transition to detonation can be obtained only if detonation of the test material can be achieved, i.e., the material is in a state supercritical\* for detonation. Because the standard LSGT is uninstrumented, supplementary information about detonability of the test material should be available for adequate interpretation of the test results.

A major purpose of the present report is to describe exactly the present standardized test conditions and to bring up to date the compilation of all unclassified NOL large scale gap test results. All of the work on the present test, particularly modifications of it, will be summarized whether reported before or not; hence this report can serve as a single accessible source of work carried out on the standardized test. The reader will find some difference between earlier references (2) and this one; in such cases, the present report supersedes any earlier ones.

\*In other words, it is in such a state that it is potentially detonable.

- (1) E. A. Eyster, L. C. Smith, and S. R. Walton, "The Sensitivity of High Explosives to Pure Shocks", NOLM 10,336, 14 Jul 1949.
- (2) I. Jaffe, A. R. Clairmont, Jr., and D. Price, "Large Scale Shock Sensitivity Test. Compilation of NOL Data for Propellants and Explosives", NOLTR 61-4, 15 May 1961 and NOLTR 65-177, 15 Nov 1965.

In addition to adding the test results accumulated in the past eight years, the present listing contains revised values of the 50% pressure ( $P_G$ ) for all previously reported results. The bases of the revision are current improved Hugoniot data for the PMMA attenuator and calibration data for the LSGT set up. As in previous compilations, results are reported only for solid test samples; the LSGT is not designed for testing the shock sensitivity of liquids.

Although no single measurement can be a completely adequate measure of the complex reaction of a given explosive to various strength shocks, i.e., shock sensitivity, a standardized gap test can be used to obtain values which do give much useful information. Gap test results have been used here to show the relative sensitivities of explosives and propellants as well as the manner in which variables such as temperature and porosity affect explosive detonability and change sensitivity behavior.

## II. STANDARDIZED LSGT PROCEDURE

The earliest version of the NOL standardized large-scale gap test for solids was first described in 1958 (3). Since that time, the basic elements of the test have remained the same, but the method of assembling it has been improved. The assembly time is now much shorter and the amount of burning cardboard (assembly containers) after a firing has been much reduced. The early assembly method has been reported (3); the present method will be described here.

Figure 1 shows schematically the actual assembly just before the charge is fired; it also shows the more important dimensions. As shown there, a J-2 blasting cap (Hercules) is used to initiate the standard donor which consists of two pressed 50/50 pentolite pellets of  $\rho_0 = 1.56 \pm 0.01$  g/cc. The gap is made up of 0.025 cm (0.010 in.) thick cellulose acetate cards or, if larger than 1.25 cm, of 1.27 or 2.54 cm thick PMMA discs and of cards. These two materials have shown equivalence as shock attenuators (4). The test material or acceptor is cast, pressed, or machined to fit a cold drawn, mechanical steel (MT-1015) seamless tube of 0.56 cm thick walls. The ends of the acceptor are machined or cut so that they are flat and flush with the ends of the tube. A cold rolled, mild steel witness plate is placed 1.59 mm beyond the end of the acceptor.

- (3) A. B. Amster, R. L. Beauregard, G. J. Bryan, and E. K. Lawrence, "Detonability of Solid Propellants. I. Test Methods and Instrumentation," NAVORD 5788, 3 Feb 1958.
- (4) I. Jaffe, R. L. Beauregard and A. B. Amster, "The Attenuation of Shock in Lucite", NAVORD 6876, 27 May 1960. Also ARS Journal 32, 22-25 (1962).

For assembly, a cardboard spacer (a short tube 4.76 cm I.D. x 0.15 cm thick x 1.91 cm long) is first placed around the end of the acceptor tube. The test components (acceptor, gap, donor, and wooden block used to hold the detonator) are then slipped into a cardboard container (5.10 cm I.D. x 5.66 cm O.D. x 21.6 cm long). There the spacer serves to hold the acceptor firmly in the center of the larger container and also to provide a standoff of the charge from the witness plate. The completed assembly is then suspended (with the witness plate at the bottom\*) by a light wooden frame in a section of a liner from a 16-inch gun barrel. The pieces labeled A in Figure 1 are notched to fit the witness plate snugly. Cross pieces, B, rest on the top of the liner. The liner serves to trap the fragments of the steel tube holding the test charge. The trajectories of these fragments are nearly radial so that few fragments escape. The witness plate is blasted toward blocks of aluminum and steel on the bombproof floor. Fired in this way, the gap test causes no damage to the bombproof itself.

At firing, the detonation of the pentolite sends a shock through the gap and into the acceptor. If the transmitted shock initiates a reaction in the test material, the effect of that reaction is shown as damage to the witness plate. The plate is recovered after the shot. The criterion for a positive result or "go" is that a neat hole be punched in the plate, e.g., Figure 2. Any other result is negative or "no-go". If a reaction is of sufficient vigor to damage the plate by bulging or denting it, as shown in Figure 3, but does not punch a hole, the test result is still considered negative or a "no-go". Similarly, a broken plate or one with a poor quality hole is considered a "no-go".

Methods of obtaining additional information about shock induced reactions which bulge but do not punch the witness plate (or which punch it with a ragged rather than a clean-cut hole) will be described in Section VI D. Such ambiguous results seldom occur in testing military explosives.

Twelve charges are usually required to obtain a 50% point (critical gap). This is a gap at which a charge will detonate in 50% of the trials, and the larger the critical gap, the more sensitive the test material. The test procedure is a modification of the Bruceton "up and down" technique (3). For an unknown material, the first test is made at zero gap. If no detonation occurs, two additional tests are made at zero gap. If detonation occurs, the next test is made at 50 cards and thereafter the number of cards is doubled until a negative result (no-go) is obtained. Subsequent tests are made by dividing the gap between the closest go and no go in half until one positive and one negative result, differing by one card, can be obtained. At this point, the schedule outlined in Table 1 (3) is followed.

\*The equivalence of results for the upright and inverted forms of the test (for distances of 10 inches or more between the witness plate and the floor) was established in reference (2).

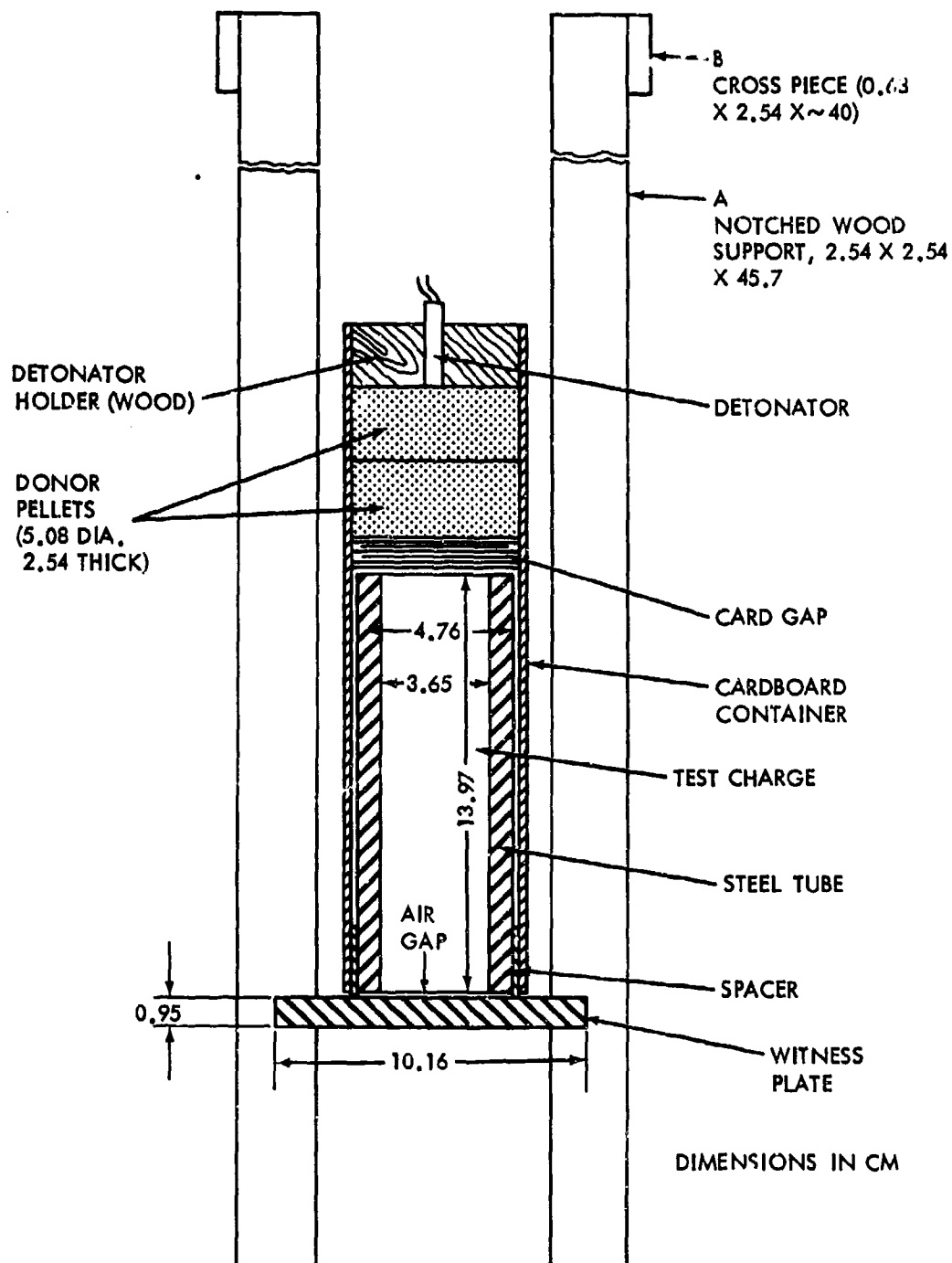


FIG. 1 CROSS SECTION OF GAP TEST ASSEMBLY

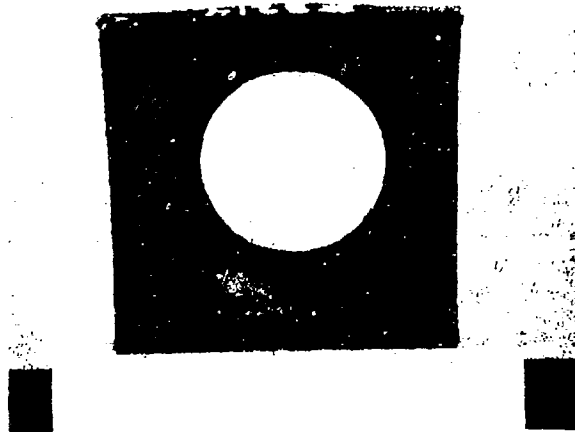


FIG. 2 WITNESS PLATE DAMAGE FROM A DETONATION (GO)

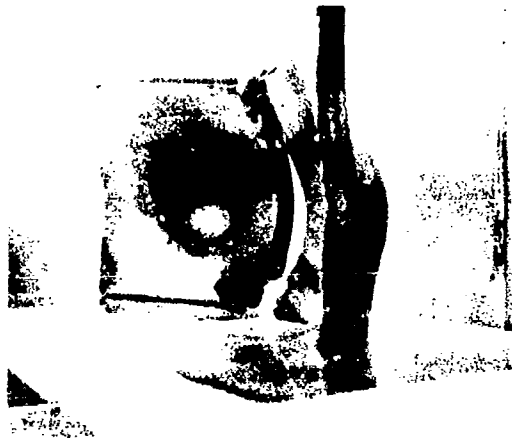


FIG. 3 WITNESS PLATE DAMAGE FROM A STRONG CHEMICAL REACTION (NO GO).

Table 1

DETERMINATION OF 50% POINT FROM VARIOUS TEST PATTERNS  
SHOWN BY DETONABLE MATERIAL

N = an integer  
+ = detonation  
- = no detonation  
.... = no tests needed

Basic Test Pattern		Results of Supplementary Tests			
$\frac{\text{Number of Cards}}{N}$	$\frac{\text{Number of Cards}}{N+1}$	Additional Tests to Establish 50% Point	$\frac{\text{Number of Cards}}{N-1}$	$\frac{\text{Number of Cards}}{N+2}$	50% Point
++	--	None	....	....	$N+1/2^*$
+-	-+	None	....	....	$N+1/2^*$
+-	--	Two tests at N-1	--	....	N-1 a
			++	....	N
			-+	....	$N-1/2^*$
++	-+	Two tests at N+2	....	--	N+1
			....	++	N+2 b
			....	-+	$N+1.5^*$

\*Reported to the nearest card

a It is assumed that during the course of testing detonation occurred at N-2

b It is assumed that during the course of testing no detonation occurred at N+3

The criterion now used to classify the test results is not the one originally selected. The choice of the present criterion was made to improve the test reliability; the reliability was then investigated by carrying out a 50-shot test on cast Comp B. The 50 charges were obtained by combining five different preparations (of 10 charges each) made from the same batch of explosive. It was found (2) that the standard deviation of the population was 3.3 cards (0.084 cm). Hence, at the 95% confidence limit, the 50% gap value was  $201 + 1.1$  cards for a 50-shot test or  $201 + 3.3$  cards for a 10-shot test with the same population distribution. However, it was also shown (2) that this large value for the standard deviation of the population resulted from variation in the casting house procedure from preparation to preparation. It was estimated that a 10-shot test made on charges from a single controlled preparation would yield a 50% value to within less than 1 card (0.025 cm) at the 95% confidence level. By contrast, after firing many 10 to 12 shot tests on samples prepared outside NOL, we find the 50% gap measured with the present standardized procedure and at controlled temperature is reproducible to better than  $+ 2$  cards (0.0508 cm). The present test procedure is, therefore, quite satisfactory from a statistical standpoint.

There is some additional information, of both historical and current interest, about the standardized test of Figure 1. The small stand-off (1.59 mm air space) between the acceptor and the witness plate was originally introduced in the gap testing of liquid propellants (5) and carried over to the design of the present test for solids. Subsequent study has shown that this slight stand-off frequently prevents the witness plate from shattering and thereby facilitates interpretation of test results. Moreover, the presence of the stand-off has no effect on the 50% point for Comp B although the punched witness plate from the standard test is somewhat more bent than that from the test run without the stand-off. PMMA/cellulose acetate was initially chosen as the gap material because (1) it is stable to changes in temperature and humidity, (2) it matches the impedance of solid non-porous test materials better than most other commonly used attenuators, and (3) it is much more convenient to use than molded wax (1). Additional advantages, particularly over metal gaps, are that PMMA forms no damaging fragments and apparently has no moderately large amplitude elastic wave preceding the plastic (shock) wave; such a situation complicates the estimation of the shock wave transmitted from the gap to the test material which has already been pre-compressed by the elastic wave. The disadvantage of PMMA is its viscoelastic behavior and the resultant uncertainty of its relaxation times. Hence in the low pressure range there is still uncertainty about whether a pressure lower than the equilibrium value should be used. The latter has been used throughout the present work.

(5) G. D. Edwards and T. K. Rice, "Liquid Monopropellants; Detonation Sensitivity", NavOrd 2884, 25 Oct 1953.

## III. CALIBRATION OF THE LSGT

In the gap test, the gap thickness is varied to obtain the 50% point. Of course, varying the attenuator thickness varies the shock pressure at the end of the gap. Since the thickness (shock path-length from donor to end of gap) and shock strength or amplitude are not simply related, it is necessary to carry out a calibration, i.e., to determine the pressure  $P$  as a function of gap thickness  $x$ .

The basic hydrodynamic shock relation used is

$$P = \rho_0 U u \quad (1)$$

where the density  $\rho_0$  is 1.185 g/cc for PMMA;  $U, u$  are the shock and particle velocities, respectively; and  $P$  is the pressure\*. Many materials exhibit the linear relation

$$U = a + bu \quad (2)$$

where  $a$  and  $b$  are constants. When this is so, Equation (2) can be combined with Equation (1) to give

$$P = \rho_0 U(U-a)/b \quad (3)$$

so that the desired  $P$  vs  $x$  curve can be computed, through Equation (3), by obtaining experimentally the  $U$  vs  $x$  curve. It was by this method that our first calibration curve was obtained with tetryl Lot 1878-5. (The LSGT originally used tetryl,  $\rho_0 = 1.51$  g/cc, as the standard booster.) Subsequent work showed that three later batches of tetryl donors gave a  $U$  vs  $x$  curve differing from that of the first batch; it also made clear that the method of obtaining  $P$  vs  $x$  from  $U$  vs  $x$ , as outlined above, was inadequate in the lower pressure region. The difference between the first batch of tetryl pellets (1878-5) and the succeeding three batches might arise from chemical or physical differences or both, but it is more likely that the earlier work suffered from the poorer experimental techniques and data reduction then used. On this assumption in 1965, the same calibration curve was used for the first four batches of tetryl boosters (2). Values that appear in parentheses in the present compilation are those

\*Throughout this report shocked materials (attenuator and acceptor) have been treated as liquids. Because their solid structure does have some effect, our treatment is an approximation; a completely rigorous treatment would consider stress components in shocked solids.



obtained with boosters from the first batch of tetryl (Test Nos.  $\leq 440$ ) to which the present tetryl calibration curve has now been assigned.

The first major improvement of the LSGT calibration was obtained by measuring both  $U$  vs  $x$  and  $u_{fs}$  vs  $x$  (6). From the free surface velocity  $u_{fs}$ , the  $u$  vs  $x$  curve was obtained from the frequently used approximation

$$u_{fs} \approx 2u. \quad (4)$$

Substitution of  $U$  vs  $x$  and  $u$  vs  $x$  in Equation (1) gave the desired calibration for PMMA shocked with the standard tetryl donor. The same work also showed that Equation (2) is inadequate to represent the PMMA Hugoniot over the entire pressure range of the gap test. If the  $U, u$  curve is approximated as two straight lines, the lower pressure segment has a much smaller slope than that at higher pressures.

Shortly after the above work, tetryl pellets had to be discontinued as the standard donor because the source of supply, NOS, Macon, Georgia was closed. Since then (Test Nos.  $\geq 770$  in the compilation), the standard donor has been 50/50 pentolite pressed to a density of  $1.56 \pm 0.01$  g/cc. These pellets are supplied by NAD, Crane, Indiana (Federal Stock No. 1375-991-8891)\*. Hence we now require two calibrations of the LSGT, one with each of the standard donors.

The second major improvement of the LSGT calibration has been completed quite recently (7). It is the resultant of a number of factors, but the dominant one is our new ability to measure particle velocity directly to  $\pm 0.03$  mm/ $\mu$ sec by the electromagnetic velocity (EMV) method. Thus we found that  $u$  in PMMA of the LSGT after the shock had traveled 20 mm was about 10% greater than the value we had obtained with the free surface velocity approximation. A second very important factor was the availability of precise Hugoniot measurements on PMMA in the lower pressure region. These in conjunction with our own measurements of  $u$  and of  $U$  allowed us to represent the most consistent Hugoniot for PMMA as

\*The specification calls for a density of 1.56 - 1.57 g/cc. It is doubtful that the density can be controlled this closely. An exact check of the production density is complicated by the barrel shape of the pellets. See appendix of reference (7).

- (6) T. P. Liddiard, Jr. and D. Price, "Recalibration of the Standard Gap Test", NOLTR 65-43, 20 Aug 1965.
- (7) J. O. Erkman, D. J. Edwards, A. R. Clairmont, Jr., and D. Price, "Calibration of the NOL Large Scale Gap Test; Hugoniot Data for Polymethyl Methacrylate", NOLTR 73-15, 4 Apr 1973.

$$U = 2.7228 + 4.0667 u - 10.9051 u^2 + 10.6912 u^3, \quad 0.03 \leq u \leq 0.5363 \quad (5)$$

$$U = 2.561 + 1.595 u, \quad u > 0.5363 \quad (6)$$

where both  $u$  and  $U$  are in units of mm/ $\mu$ sec. Equation (6) applies at pressures above 21.7 kbar and is Equation (2) with the range of  $u$  restricted. The coefficients differ very little from those that have been used the last eight years (2.57, 1.61). Equation (5), on the other hand, reflects the viscoelastic behavior of PMMA at lower pressures, and will probably be modified as more is learned about the relaxation times of PMMA in that region. It should be mentioned here that our PMMA in the LSGT is bar stock Plexiglas II UVA produced by Rohm and Haas.

Our present calibration procedure consists of measuring  $u$  (by the EMV method) vs  $x$  and obtaining  $P$  vs  $x$  by use of the PMMA Hugoniot, Equations (5) and (6). The LSGT calibration with tetryl donors so obtained can be represented as

$$u = 1.7342 \exp(-0.01852 x) + 0.6602 \exp(-0.2794 x) \quad \text{for } x \leq 34.65 \text{ mm} \quad (7)$$

and

$$u = 0.0921 + 3.7038 \exp(-0.0435 x) \quad \text{for } x > 34.65 \text{ mm} \quad (8)$$

For pentolite donor charges, the results are

$$u = 1.7735 \exp(-0.01841 x) + 0.8765 \exp(-0.3495 x) \quad \text{for } x \leq 36.00 \text{ mm} \quad (9)$$

and

$$u = 0.0905 + 4.0877 \exp(-0.04451 x) \quad \text{for } x > 36.00 \text{ mm} \quad (10)$$

Table 2 gives the pressures at 5 - 10 mm intervals of  $x$  for each donor in the LSGT. It should be noted that at  $x \leq 10$  mm, the values are considered nominal only. In that region ( $x < 10$  mm) of very rapid attenuation of the donor induced shock,  $u$  cannot be measured very reliably.

At  $x > 10$  mm, the maximum estimated error for an individual measurement of  $u$  is  $\pm 6\%$ . Replicate measurements over the range of 0.2 - 1.5 mm/ $\mu$ sec show differences of 4% or less and therefore suggest the  $\pm 6\%$  is pessimistic; however, replicates at 0.15 mm/ $\mu$ sec show a difference of 11%. Error in the pressure  $P$  must be at least as large as that in  $u$  and probably somewhat larger. Our recent (still unreported) error analysis in  $P$  for  $P > 21.5$  kbar ( $x < 50$  mm) showed errors of 10 - 12%. Error in  $P$ , like that in  $u$ , would be expected to be largest on a percentage basis at lowest pressures (e.g.,  $x \sim 100$  mm).

From Table 2 it can be seen that for  $x \geq 5$  mm the difference between  $P$  derived from the measured  $u$  for pentolite and tetryl loading is experimentally insignificant. This is indicated both by our error analysis and by the range found for replicate measurements. However, most pentolite data were consistently above the analogous tetryl data. Hence we have presented two distinct calibration ( $P, x$ ) curves with the small differences between them shown in Table 2. Even so, for practical purposes, we can use the same calibration curve for both tetryl and pentolite at  $x > 51$  mm (200 cards).

Despite the fact that the new results for tetryl are in some ranges significantly larger than the early ones, the two (old and new)  $P$  vs  $x$  curves do not cross. Therefore the relative ranking of explosives by gap sensitivity will not be changed although the 50% pressures ( $P_g$ ) will be, in some cases. The same situation also exists for the old and new calibrations with pentolite.

The gap test calibration provides only the shock pressure at the end of the 50% gap; to obtain the value of the pressure transmitted to the test material across the PMMA/acceptor interface, it is necessary to know Hugoniot data for the unreacted charge. Such data are now available for a number of essentially non-porous explosives (ca. 0 - 5% voids); Table 3 presents representative data. In other words, there are now available sufficient Hugoniot data to permit a fair estimate (on the basis of density and composition) for almost any non-porous charge of interest. The critical initiating pressure for most non-porous charges tested is about 15 - 30% higher than the pressure in the PMMA at the end of the 50% gap; the latter pressure generally orders the non-porous test materials for shock sensitivity in the same way as does the initiating pressure (11).

(11) D. Price and I. Jaffe, "Large Scale Gap Test: Interpretation of Results for Propellants", ARS Journal 31, 595 (1961).

Table 2  
PRESSURE-DISTANCE DATA FROM CURRENT  
CALIBRATIONS

<u>x,mm</u>	<u>P, Kbar</u>	
	<u>Tetryl</u>	<u>Pentolite</u>
0	181.0	213.1
5	110.4	113.0
10	86.4	88.2
15	73.3	75.4
20	63.6	65.8
25	55.7	57.7
30	48.9	50.7
35	42.6	44.6
40	32.9	35.1
45	25.8	27.3
50	20.6	21.5
55	16.9	17.5
60	14.1	14.5
70	10.3	10.4
80	7.8	7.8
90	6.2	6.1
100	5.2	5.1

Table 3  
HUGONIOT DATA FOR ESSENTIALLY NON-POROUS EXPLOSIVES

Form	Composition	Density g/cc	% TMD	Hugoniot Data*		Ref
				a	b	
TNT	Cast	1.614		2.390	2.050	8
Comp B-3	Cast	1.72	60/40 RDX/TNT	2.710	1.860	8
TATB	Pressed	1.847	95.3	2.340	2.316	8
DATB	Pressed	1.780	96.9	2.449	1.892	8
TNB	Pressed	1.640	97.2	2.318	2.025	8
HBXs	Cast		RDX / TNT / Al / Wax			8
HBX-1		1.750	40 38 17 5	2.936	1.651	8
HBX-3		1.850	31 29 35 5	3.134	1.605	8
H-6		1.760	44.76 29.53 20.95 4.76	2.832	1.695	8
Pentolite	Cast	1.67	50/50 PETN/TNT	2.83	1.91	9**
Comp B	Cast	1.70	60/40/1 RDX/TNT/Wax	2.95	1.58	9
Comp B-3	Cast	1.70	60/40 RDX/TNT	3.03	1.73	9
TNT	Cast	1.63		2.57	1.88	9
Octol	Cast	1.80	75/25 HMX/TNT	3.01	1.72	9
TNT	Cast	1.62		2.274	2.652	U<3.7 10
Tritonal	Cast	1.73	80/20 TNT/Al	2.987	1.363	U>3.7 10
H-6	Cast	1.76	45/30/20/5 RDX/TNT/Al/Wax	2.313	2.769	U<3.8 10
				2.654	1.984	U<3.7 10
EJC	Cast		CMDR propellant, 18% Al***	1.900	1.724	2.550 8
FFP-1	Cast		44.5/40/15.5 Energetic binder/AP/Al	1.760	1.327	2.430 8

\*In form U (mm/usec) = a + bu

\*\*Reference 9 gives only name of "military explosives". It is assumed that they are cast and have composition shown.

\*\*\*A composite modified double base propellant made up of NC, NG, AP and Al.

(8) N. L. Coleburn and T. P. Liddiard, Jr., "Hugoniot Equations of State of Several Unreacted Explosives", J. Chem. Phys. 44 (5), 1929 (1966).

(9) V. M. Boyle, R. L. Jameson, and M. Sutanoff, "Determination of Shock Hugoniot for Several Condensed Phase Explosives", Fourth Symposium (International) on Detonation, ACR-126 (ONR), U.S. Gov. Print. Office, Washington, 1967; p 241.

(10) V. M. Boyle, W. G. Smothers, and L. E. Ervin, "The Shock Hugoniot of Unreacted Explosives", Fifth Symposium (International) on Detonation, ACR-184 (ONR), U.S. Gov. Print. Office, Washington, 1972; p 251.

Pressed explosives are much more shock sensitive than cast. Hence direct measurement of their Hugoniot under conditions of no decomposition is difficult to impossible. For this reason, data for only three pressed charges have been given in Table 3 and those are relatively shock insensitive materials. However, it may be possible soon to measure the non-reactive Hugoniot on the less sensitive voidless explosive and then derive from it the Hugoniot of the same explosive at different porosities (12). Until more and valid non-reactive Hugoniot are available for derivation of the initiating pressure  $P_i$ , the relative shock sensitivity of a charge in the LSGT is expressed as  $P_g$  because for many explosives  $P_i$  values cannot yet be derived.  $P_g$  is subject to change with improved calibration (as is  $P_i$ ); nevertheless it is physically much more directly related to the true initiating pressure than is the 50% gap thickness which remains unchanged with calibration. This point will be discussed in more detail in Section V B.

#### IV. LSGT RESULTS

All gap test values which have been obtained in the configuration of Figure 1 have been critically reviewed. In particular, some earlier results obtained at "ambient" temperature have been discarded when other temperature-controlled tests on the same material are available. Where no later tests have been made, however, the early result has been tabulated. The present compilation (Appendices B and C) supersedes all previously published standardized large scale gap test values at this Laboratory.

The explosives are listed alphabetically according to their abbreviations, and mixtures (composite explosives) are listed according to the abbreviation of their major component. The chemical name of each explosive is given after the abbreviation in Appendix B or C or both. This list includes some results in which the witness plate damage was not caused by a steady-state detonation. Wherever this situation has been recognized, it is noted in the comments and references given to the supplementary work. It does not occur frequently with military explosives, those chiefly based on pure organic high explosives which are C-H-N-O materials. It is most apt to occur for inorganic oxidizers such as ammonium perchlorate (AP) and ammonium nitrate (AN) and their mixtures, particularly if the material is either highly compacted or of very large particle size. It can also occur in the LSGT configuration for coarse grained weak organic explosives, e.g., DNT. When it is suspected that a non-steady state reaction has been induced in the test material by the relatively strong boosting, a single shot in a double length tube has frequently demonstrated that the induced reaction is indeed fading and not steady state (e.g., witness plate undamaged). If the test results are

(12) J. O. Erkman, "Porosity and the Sensitivity of TNT to Shock", section of an NOLTR now in preparation.

ambiguous and such simple diagnostics fail, the tube must be instrumented (e.g., with ionization pins) to be sure that a shock-to-detonation transition has (has not) occurred.

In some cases, a shock-to-detonation transition occurs but under conditions such that the reaction is insufficiently powerful to punch a hole in the witness plate. In these cases, a more sensitive witness is used in the modified or extended tests which will be described in Section VI D.

As mentioned earlier, tests up to Test No. 440 were carried out with the first batch of tetryl pellets which was later assumed equivalent to all the subsequent batches. Hence their  $P_g$  values are in parentheses to indicate an assigned calibration (the present one) differing from what is now believed to have been an inaccurate one. Tetryl was the standard donor through Test 769, thereafter pentolite is the standard donor.

As in all tests, reproducibility of test values depends on reproducibility of test samples. It has been found that production propellants supplied by the manufacturer are generally uniform, nearly voidless, and reproducible from lot-to-lot. Military explosive samples, on the other hand, are generally prepared under less controlled conditions. With the exception of new explosives for which production control has been established, e.g., DATB, materials are generally supplied from old stores and are of unknown purity. Given the same batch of explosive, reproduction of the test charges will depend upon control of density, porosity, and particle size, which are interdependent variables. Such control is particularly difficult in preparing cast charges where radial variation in cooling rate and crystallization in the (cylindrical) mold is inevitable. A variation of five degrees in mold temperature will produce an easily detectable change in sample sensitivity of Comp B (2). Variations in the test results for cast TNT from the same explosive lot (see Appendix C) are probably caused by variations in the charge preparation although they may be caused by variations from box to box of the same explosive lot. For the former reason, pressed charges are considered more reproducible than cast. Two methods of pressing are available; these are, by increments on the hydraulic press and three-dimensionally in the isostatic press. The two methods produce density variations in the longitudinal and radial directions, respectively, but the latter (isostatic pressing) results in more reproducible charges. Method of preparation is shown for the explosives tested and listed in Appendix C.

Solid rocket propellants are, like military explosives, materials characterized by high and rapid energy releases; they are high explosives and have been omitted from the compilation only because those tested have had proprietary compositions. However, the compilation contains many propellant models (e.g., AP/wax) and it is possible to indicate the general propellant behavior without specifying the exact composition.

Propellants are manufactured with a great many combinations of various possible components. A representative sampling is given by the following typical classes:

- a. The simple composite propellant. It consists of an inorganic oxidizer combined with a fuel. The fuel may be an organic material only or that plus a finely divided metal. A typical example is ammonium perchlorate (AP)/polyurethane/aluminium.
- b. A member of Class a to which a solid high explosive (HE) has been added.
- c. The simple double-base propellant. This is essentially nitrocellulose (NC) colloided with nitroglycerin (NG). Similar series can be prepared using an explosive plasticizing agent other than NG.
- d. A member of Class c to which AP or Al or both has been added.
- e. A member of Class d to which a solid HE has been added.

It should be kept in mind that common explosives can also be classified in a similar manner. Only the pure organic HE such as TNT has no parallel class in the solid propellants. (There is a parallel among the monopropellants when liquid explosives are considered.) For example, mixtures of organic HE with Al are similar to Class d above and mixtures of ammonium nitrate (AN) and fuel oil, a widely used explosive, are members of Class a.

Generally, Classes b through e are detonable in the standardized LSGT whereas Class a, as manufactured\*, is not. However, simple composite propellants are detonable in large sizes ( $d \geq 7$  feet at 25°C) in the voidless condition or in the LSGT after introduction of about 10% porosity distributed so as to make the charge permeable. Table 4 gives representative values for a number of simple double-base propellants (Class c). The collection of compositions is not ideal for indicating effects of the components but does show the generally expected trends of increasing shock sensitivity with increasing NG content and decreasing content of non-explosive components.

At the present time, the production trend seems to be an increasing use of explosive components in both composite and double base matrices. As a result, many of the more recent propellant compositions exhibit a shock sensitivity comparable to that of established military explosives, e.g., cast TNT to cast Comp B.

\*Voidless solids only are considered; i.e., a slurry such as AN/FO is excluded.



Table 4  
LSGT RESULTS AT 25°C FOR SIMPLE DOUBLE BASE PROPELLANTS

Test No.	Propellant	Density g/cc	Composition			50% Point		
			NC%	NG%	Other %	NG/NC	No. Cards	Pg, kbar
364	ARP	1.61	46.10	39.10	14.80	0.85	40	(86)
270	JPN	1.62	51.40	42.90	5.70	0.84	65	(70)
48	AHH	1.60	54.63	32.08	13.29	0.59	35	(90)
362	OIO	1.55	59.10	25.20	15.70	0.43	16	(118)
16	OGK	1.53	57.28	24.30	18.42	0.42	9	(138)

\*Non-explosive

## V. EFFECT OF TEMPERATURE AND POROSITY ON LSGT RESULTS

## A. Temperature

Because most of our tests have been carried out at 25°C, they offer little information about the effect of temperature on the measured  $P_g$ . However, some work has been done in the range of -60° to 66°C on propellants, and other investigators have recently reported on the temperature effect.

If it is accepted that initiation to detonation is a thermal excitation of an exothermal reaction with pseudo-Arrhenius kinetics, the shock sensitivity should increase and  $P_g$  should decrease with increasing temperature. Propellants, detonable in the LSGT over the range -60° to 66°C, showed this behavior and exhibited a moderate temperature coefficient (13). Subsequently Roth (14) reported the same trend in four out of five pressed explosives; he tested each explosive at only two temperatures, 25°C and at > 100°C. Trott (15) has also used two test temperatures (25°C and liquid N<sub>2</sub>) to test Comp C-4 and smokeless powder (78/20, NC/NG), among other mixtures; he too found the same trend with temperature.

A very different situation arises when the explosive is originally in a subcritical or non-detonable condition. We are accustomed to a detonability limit line in the charge diameter ( $d$ )-loading density ( $\rho_0$ ) plane (at constant temperature, particle size, etc ...). Working at a constant  $\rho_0$ , the limiting (critical) diameter can be found or, at constant  $d$ , the critical density. The set of such pairs defines the limit line which divides the plane into an area where detonation can occur and another where it must fail. If, instead of the temperature, we hold the density constant, we find an analogous limit line in the temperature-diameter plane. The critical diameter would be expected to decrease with temperature increase [e.g., (15)] and for the effective diameter of the gap test there should be a critical temperature below which detonation fails. Thus, if, by varying the temperature, we cross from the failure area to the detonation area of the  $t$ - $d$  plane, we would expect to find  $P_g$  very high near the detonability limits, but rapidly decreasing as the temperature rises above its limit value. Thus AN prills at pour density are subcritical

(13) D. Price, I. Jaffe, and G. E. Roberson, "Shock Sensitivity of Solid Explosives and Propellants", Ind. Chim. Belge 1967, 32 (Spec. No.), 506.

(14) J. Roth, "Shock Sensitivity and Shock Hugoniot of High Density Granular Explosives", Fifth Symposium (International) on Detonation, ACR-184 (ONR), U.S. Gov. Print. Office, Washington, 1972; p 219.

(15) B. D. Trott, "Effect of Cryogenic Temperatures on the Performance of Selected Explosives", NAVEODFAC TR-144, Aug 1972.

under heavy confinement at 1.5 in. diameter until their temperature is increased to 140°C or higher (16); the LSGT on this material at 25°C is negative. Several propellants which gave negative results at low temperatures (-60° and -32°C) detonated at  $t \geq 25^\circ\text{C}$  (13). Moreover, one propellant exhibited the sharp gradient between 25° and 66°C that indicated its critical temperature was close to 25°C.

There is still a third temperature effect that has been reported but has not been observed here. Simple composite propellants when cooled below their glass temperature (generally -35° to -45°C) are, when shocked, capable of exhibiting violent explosions, though not true detonations. Since the glass temperature and the brittle temperature are nearly the same, it is believed that such explosions are caused by break-up of the embrittled material and consequent exposure of more burning surface. Break-up and irregular burning can result from a high loading rate of the igniter, and such trouble would be expected at low temperatures, even those above the brittle temperature. Plastic bonded explosives would also be expected to show this temperature effect. It has been reported (17) that an HMX/Viton, 85/15, exhibited detonation at -30°C, but only deflagration at -7°C when subjected to low velocity impact from a metal plate.

#### B. Porosity

The porosity of a material can be defined as the fraction of voids,  $(1 - \rho_o/\rho_v)$ , where  $\rho_o/\rho_v$  is the relative density,  $\rho_o$  is the charge density, and  $\rho_v$  is the voidless density. It can also be defined as the percentage  $(100 - \%TMD)$  where TMD is the theoretical maximum density ( $\rho_v$ ) and  $100(\rho_o/\rho_v) = \%TMD$ . The porosity does not exactly characterize the physical condition of the charge because porosity encompasses the interrelated factors of initial particle size; loading density; number, size, and shape of connected voids; permeability; and the specific surface area. It is, nevertheless, of major importance in determining detonability and shock sensitivity.

Figure 4 displays the shock sensitivity curves,  $P_g$  vs %TMD, for a number of organic HE; all data were obtained with the regular LSGT and are tabulated in Appendix C. Figure 5 shows analogous curves for 7 $\mu$  and 25 $\mu$  AP and AP mixtures with wax and Al. In this case, some of the data on charges of higher porosity were obtained with the modified or extended LSGT; however, this was done only on materials which had been completely surveyed for detonability, i.e., for which detonation at high porosities had been established by

(16) R. W. Van Dolah, C. M. Mason, F. J. Perzak, J. E. Hay, and D. R. Forshey, "Explosion Hazards of Ammonium Nitrate Under Fire Exposure", RI 6773, Bur. Mines, 1966.

(17) H. Napadensky, "Experimental Studies of the Effects of Impact Loading on Plastic-Bonded Explosive Materials", Final Report DASA-1391, Ill. Inst. Tech., Apr 1963.

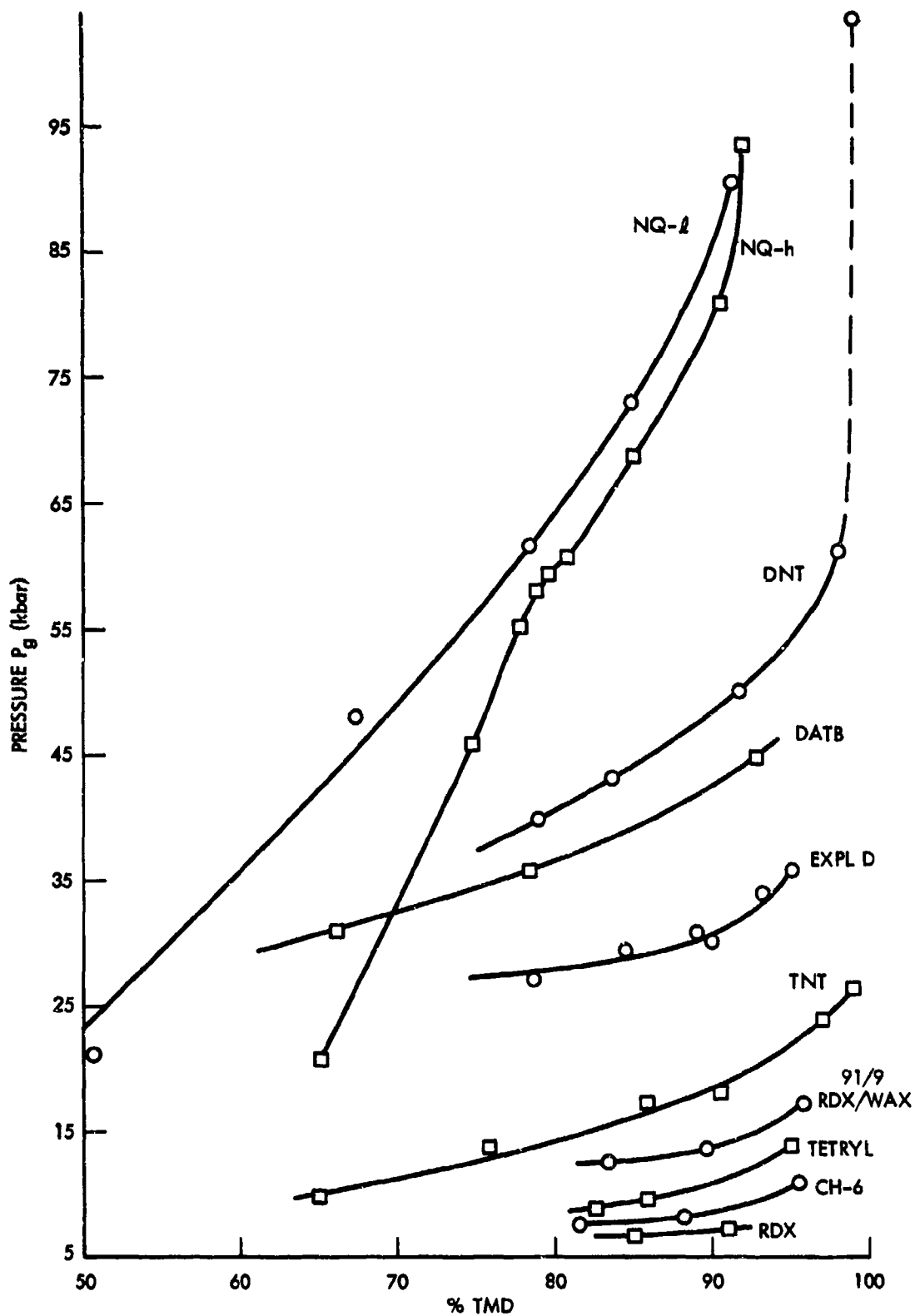


FIG. 4 LSGT RESULTS FOR PRESSED CHARGES OF ORGANIC HE

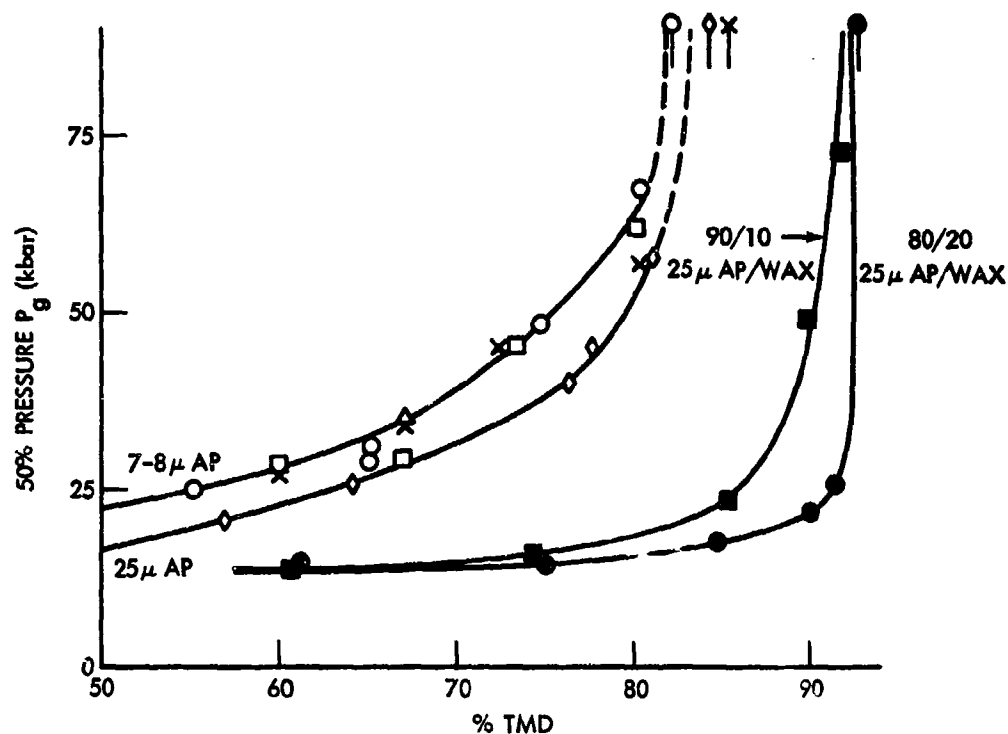


FIG. 5 LSGT RESULTS FOR PRESSED CHARGES OF AP AND AP/FUEL MIXTURES.  
(O AP 141,7 $\mu$ ;  $\square$  AP 145,8 $\mu$ ;  $\times$  AP 145/Al (7 $\mu$ ), 95/5;  $\Delta$  AP 145/Al (7 $\mu$ ), 90/10).

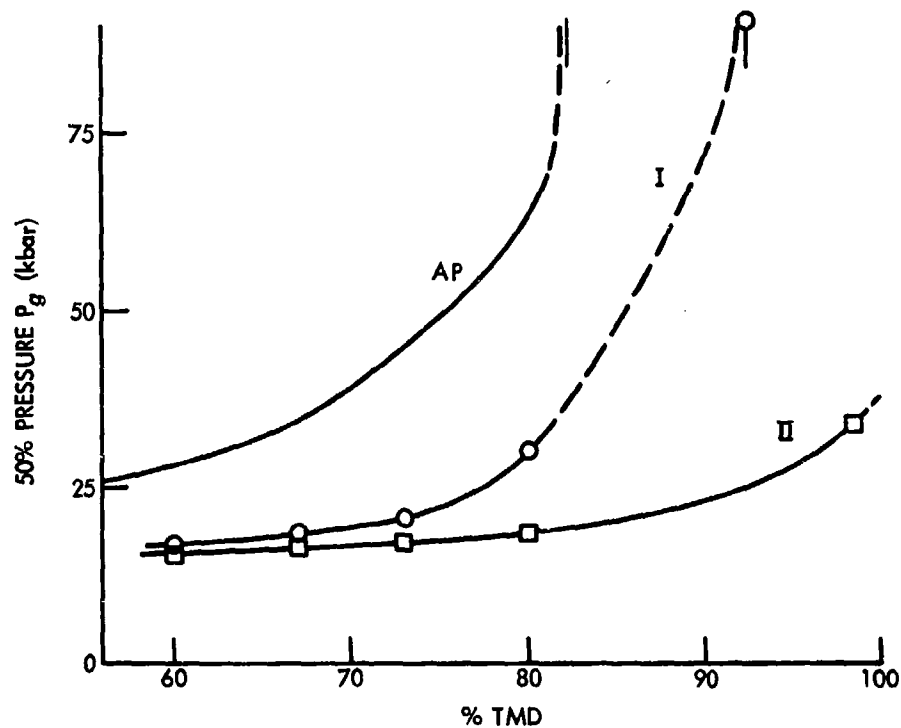


FIG. 6 LSGT RESULTS FOR TWO COMPOSITE PROPELLANT MODELS.  
(O AP/Al/WAX, 62.5/18.75/18.75;  $\square$  AP/Al/WAX/HMX, 50/15/15/20.)

supplementary measurements. The equivalence of the regular, modified, and extended tests where steady state detonation is known to occur has been established and will be described in Section VI D.

Since acceptable experimental Hugoniot data are not yet available for non-reacting porous explosives, we cannot determine the critical initiating pressure, i.e., that pressure  $P_i$  actually transmitted to the charge as a result of the 50% gap pressure on the attenuator side of the boundary PMMA/test material. It seems reasonable to assume, however, that their Hugoniots will show the qualitative trend with loading density that is found with material density in voidless charges. If so, at any given gap pressure, the pressure transmitted to the test charge will decrease as the loading density of the acceptor charge decreases. This means that the change in sensitivity, i.e., critical initiating pressure, with %TMD will be in the direction shown in Figures 4 and 5 for change in gap pressure, but it will be a relatively larger change.

Use of the 50% gap pressure contracts the true sensitivity scale (one based on pressure transmitted to the test material); use of the 50% gap length distorts the scale particularly in the higher sensitivity range where shock attenuation with increasing gap thickness is slow. Thus at 100 kbar the attenuation is about 5 kbar/mm whereas at 10 kbar it is about 0.3 kbar/mm.

Figures 4 and 5 show the generally accepted trends of decreasing sensitivity with decreasing porosity (or increasing compaction\*). Figure 4 arranges the organic explosives in their generally accepted order of shock sensitivity. It also shows the two least sensitive, NQ-h and DNT, approaching a dead-pressed\*\* form in the LSGT at about 92 and 99% TMD, respectively. This is in accord with the detonability curves of these materials (see Appendix D). The atypical lower branch of the curve for NQ-h (Figure 4) is attributed to a shift from steady

\*The degree of charge compaction will vary from zero at the pour density of the material to a value of one at the voidless density. Its variation should parallel that in relative density or %TMD.

\*\*In the preceeding section, the detonability or limit curves  $d$  vs  $\rho_0$  and  $d$  vs temperature ( $t$ ) were described. In this report the former is always presented as  $d$  vs %TMD at 25°C. At a given value of %TMD, the corresponding  $d$  value on the curve is called the critical diameter ( $d_c$ ) and it is that diameter below which steady state detonation cannot propagate in a cylindrical charge. "Subcritical" generally means  $d < d_c$ , but it can mean  $t < t_c$  for a given %TMD. Some HE have a limit curve showing an increase of  $d_c$  with increasing %TMD as it approaches  $\rho_v$ . Such HE under given dimensions and confinement, such as the LSGT, can sometimes be compacted until their effective diameter is smaller than the  $d_c$  of the limit curve, i.e., can become subcritical and non-detonable. When this occurs, the material is described as "dead pressed". Additional information on  $d_c$  appears in Appendix D.

state detonation to LVD which occurs in this relatively coarse material; in this particular case, it is difficult to distinguish between detonation and LVD by detonation velocity measurements (18).

Figure 5 shows the generally accepted trend of decreasing shock sensitivity with decreasing particle size for granular explosives (19). (It is important to remember that this trend is reversed when air is replaced by a condensed material (19). Thus in cast or plastic bonded explosives, the sensitivity increases with decreasing particle size.) Also shown in Figure 5 is that all of these AP charges dead press in the LSGT when the compaction becomes sufficiently great; this is in accord with their detonability limits. The bars at the right of the high pressure portions of the curve mark a %TMD above the critical at which reaction was still observed. Slow fading of shock induced reaction under subcritical conditions is typical of these group 2 explosives (see Appendix D).

Addition of wax to organic HE desensitizes the charge (e.g., RDX in Figure 4), but sensitizes AP (Figure 5). Addition of Al to organic HE desensitizes the charge (see TNT/Al series in Appendix C), and either has no effect on or sensitizes AP (Figure 5). Addition of 20% HMX to a composite propellant model gives a mixture which no longer exhibits dead pressing in the LSGT (see Figure 6).

Many military explosives are cast and can be considered essentially voidless materials. Any voids they contain will generally be unconnected and the charges will be impermeable. For such charges, the  $P_g$  vs %TMD relations shown by pressed charges are inapplicable, and the dominant variable becomes the homogeneity of the finished casting. We have already mentioned the effect of a small change in mold temperature on the sensitivity of cast Comp B (see Section IV). Similar small changes in procedure are probably responsible for the spread in  $P_g$  measured on various samples of cast TNT (31-52 kbar). There seems to be a continuous decrease in shock sensitivity with increasing homogeneity over the entire range of castings from hot pressed up to single crystal TNT (20).

- (18) D. Price and A. R. Clairmont, Jr., "Explosive Behavior of Nitroguanidine", Twelfth Symposium (International) on Combustion, The Combustion Institute, Pittsburgh, 1969; p 761. See also NOLTR 67-169
- (19) L. B. Seely, "A Proposed Mechanism for Shock Initiation of Low Density Granular Explosives", Proc. Fourth Elec. Initiation Symposium, Franklin Institute, Phila. 1963; Paper 27 of Rpt EIS-A 2357.
- (20) D. Price, "Shock Sensitivity, A Property of Many Aspects", Fifth Symposium (International) on Detonation, ACR-184 (ONR), U.S. Gov Print. Office, Washington, 1972; p 207. See also NOLTR 70-73.

Enough has been said to emphasize the difference between  $P_g$  and  $P_i$ . Relative sensitivity rating by  $P_g$  is least distorted when all materials are compared at the same %TMD. If the comparison is between (1) a voidless and (2) a very porous material, the difference indicated by the  $P_g$  values is less than that given by  $P_i$ . Where such a distortion is intolerable it is recommended that Hugoniot be obtained for both materials so that the respective values of  $P_i$  can be derived.

The critical diameter  $d_c$  of an explosive is, like  $P_g$ , a strong function of homogeneity of cast charges and of degree of compaction of pressed charges. The strongest relationship between these two parameters occurs when the charge properties approach the detonability limit (e.g.,  $d \rightarrow d_c$  in a cylindrical charge).  $P_g$  then increases rapidly until it can no longer be measured because the charge is no longer detonable, i.e., the charge has become subcritical. Even this relationship between  $P_g$  and  $d_c$ , however, is applicable only for different pressings or castings of the same explosive. There is no general relationship between  $P_g$  and  $d_c$  from explosive to explosive. Because so many investigators are still under the impression that such a relationship exists, Appendix D is devoted to a compilation of  $d_c$  measurements made at NOL and a demonstration of the lack of general relationship between  $d_c$  and  $P_g$ .

## VI. EFFECT OF CHANGING GAP TEST ELEMENTS

In general, any change in the test elements will shift the sensitivity scale of the test, and a new calibration will be required for each such change. Since the standardized test has proved satisfactory for most applications, very little work has been done on studying the effect of changing the test variables with the exception of the witness. However, practical problems seldom occur in the exact configuration of the LSGT, and hence require some conversion of the available information. The procedures used and relevant information will be summarized under the name of the test element considered.

### A. Donor

The donor used in the LSGT has an  $l/d$  of one. By studying the behavior of PMMA under shock loading by such a tetryl donor, we have found that the shock entering the PMMA gap is of very short duration. For example, 10 mm from the shocked surface, the shock pressure falls from 86 kbar to 0 in about one  $\mu$ sec (21). This is much shorter than the value computed by conventional one-dimensional detonation theory, and indicative of the important role of two-dimensional factors here. It is probably because of this steep pressure-time profile that the pressure amplitude alone seems to dominate the results; if pentolite is used in place of the tetryl donor, the measured 50% pressure is unchanged within experimental error. Of course, 50/50 pentolite

(21) I. Jaffe, J. Toscano, and D. Price, "Behavior of Plexiglas Under Shock Loading by a Tetryl Donor", NOLTR 64-66, 2 Jul 1964.



(1.56 g/cc) was chosen to replace tetryl (1.51 g/cc) because it was quite similar in its behavior; hence it is not surprising that the two donors seem nearly interchangeable. In principle, the entire pressure-time history of the stimulus, not merely its amplitude, should determine its initiating ability. Recent consideration of all available data on TNT (20) indicated that the principle does indeed apply and that the LSGT value lies on the critical curve in the pressure-time plane dividing the failure region from the region where detonation can occur.

As remarked in a previous section, the calibration curves for pentolite and tetryl donors do not differ significantly except at very low attenuations. However, the pentolite curve does lie consistently above the tetryl curve, i.e., the pentolite seems slightly more powerful. On the other hand the tetryl boosters (made in the U.S. Naval Ordnance Plant, Macon, Georgia) had more reproducible dimensions than do the present pentolite boosters which tend to be barrel shaped. This is reflected in greater scatter of the pentolite data than in that from the tetryl. [See Appendix of Reference (7).]

An investigation was also made of the effects of certain changes in size, shape, and confinement on the effectiveness of the tetryl booster (22). The two-inch dia of the donor at the booster/PMMA surface was kept constant. For a two-inch length of tetryl, confined and unconfined cylinders and truncated cones were found equivalent in boosting effectiveness. The effectiveness increased with increasing length (it was still increasing up to  $l/d$  of 4). For a given test material, a donor longer than 5.08 cm produced a 50% gap longer than that measured with the standard 5.08 cm long donor. But use of the calibration curves showed that the same 50% gap pressure was measured within the experimental error of that work.

#### B. Gap Material

The standard gap material (cellulose acetate and/or PMMA) was compared to several other gap materials. The data, given in Table 5, are not very precise since they were obtained before either the temperature or the preparation of the test charges was adequately controlled. In general, they confirm similar data of reference (1): many solids (wax, Al, Cu, polystyrene, and wood in reference (1); Al, glass, fiber glass and PMMA in Table 5) show about the same 50% gap thickness which, in the case of Comp B, is also comparable to the 50% air gap thickness. [For tetryl and pentolite, more shock sensitive materials, the air gap thickness is 2 to 3 times the gap thickness of the average solid attenuator (1).] The data of Table 5 include, however, two solids which vary significantly from the average behavior. Steel is a more effective shock attenuator and Mg a less effective one than the other materials tested.

(22) I. Jaffe and A. R. Clairmont, Jr., "The Effects of Configuration and Confinement on Booster Characteristics", NOLTR 65-33, 13 Apr 1965.

Table 5  
50% GAP THICKNESS FOR VARIOUS ATTENUATORS

Material	Attenuator Density, g/cc	50% Gap Thickness, in. x 100
Steel	7.84	99
Al	2.70	164
Glass	2.49	162
Fiberglass	1.84	139 < N < 145
Mg	1.74	211 < N < 218
PMMA	1.18	143
Air	~0.001	130 < N < 150

Acceptor: Unconfined cast Comp B (RDX/TNT/Wax, 60/40/1)

Temperature: Ambient

Familiar practical problems require estimating the effect of changing a booster's output by changing the attenuator used in a weapon. For example, the material or the thickness or both might be changed as a result of a revised engineering design. Rather than setting up an experimental model of the design, and running the tests, it is now customary to use the various one-dimensional (1-D) hydrodynamic codes that have become available. WONDY is such a code and includes a burn routine for the explosive (booster). With available input data for the booster and the Hugoniot ( $U, u$ ) data for the attenuator, behavior for point or plane wave initiation can be easily computed [e.g., particle velocity vs thickness of PMMA shocked by point initiated tetryl (7)]. In cases where 2-D effects are important, a correction can be made for them by introducing into the 1-D code a rarefaction traveling at a speed of  $(u + c)^*$  [e.g., reference (23)] rather than using the much more time-consuming and expensive 2-D codes. Where adequate input data are available for several candidate boosters, an estimate of the effects of interchanging them can also be obtained by calculations similar to the above.

### C. Confinement

It has been known since the earliest quantitative studies of shock sensitivity that the charge diameter affects the value of the measured  $P_i$ . This raises the question of what bare charge diameter would result in behavior equivalent to that exhibited by the explosive in the regular gap test confinement. We showed some time ago that this confinement on cast Comp B gave a gap pressure predicted for a bare charge of about twice the charge core diameter (ID of the confining tube) (24).\*\* More recently we found that 7 $\mu$  AP exhibits dead-pressing in the gap test at  $\rho_0 \geq 1.58$  g/cc (81% TMD; see Figure 3). Another fine AP (ca. 10 $\mu$ ) exhibited a critical dia of 80 mm at  $\rho_0 = 1.58$  g/cc (25). In this case too the standard confinement of the LSGT resulted in behavior exhibited by a 75 - 80 mm dia unconfined charge. On the basis of these two cases, the effective unconfined diameter ( $d_e$ ), assumed to produce the same behavior as that of the charge confined in the LSGT, is taken as 76.2 mm (3 inches).

\* $c$  is bulk sound speed in the shocked material.

\*\*The factor is quoted as 2.5 in reference (24); it should be 2.05.

(23) H. D. Jones, "Calculations of Induced Pressures in LE-3", Internal Memorandum, 19 Dec. 1972.

(24) D. Price and I. Jaffe, "Safety Information from Propellant Studies", AIAA Journal 1, 299 (1963).

(25) D. Price, A. R. Clairmont, Jr., & I. Jaffe, "Explosive Behavior of Ammonium Perchlorate", Combust. Flame 11, 415 (1967).

Although the regular confinement results in approximately the same effective dia ( $d_e$ ) for different explosives, the diameter effect on  $P_g$  (or  $P_i$ ) differs markedly with the sensitivity of the explosive. Thus  $(\Delta P_i / \Delta d^{-1})$  is 50, 189, and 210 kbar-cm, respectively, for cast DINA, cast Comp B, and creamed cast TNT. The gradient is determined from values measured on confined ( $d_e \sim 7.62$  cm) and unconfined charges ( $d = 3.81$  cm). See Table 6.

There are occasions in which we wish to predict the gap test value for the unconfined charge from that measured on the confined charge or vice versa. There appear to be several relationships between the two results, but the simplest is the linear relationship between gap thickness for the confined and unconfined charge. This is indicated when the data of Table 6 are plotted in Figure 7 to show the linear relation between the 50% gap thickness for the confined and unconfined charges of cast DINA, Comp B, and TNT. It should be mentioned that values for two pairs of cast pentolite do not fall on the curve, but the range covered by these two values (cross-hatched area) as well as that covered by six other pentolite samples in the LSGT (open area) is indicated. The upper part of this area lies quite close to the curve, and makes it probable that if the pentolite composition (PETN/TNT, 50/50) and casting had been as well controlled as those of Comp B, its data too would fall on the curve. (Many tests were made on pentolite castings because of difficulties encountered in trying to control the slurry viscosity.)

From the three measured values for Comp B in Table 6 the 50% gap thickness appears to vary linearly with the charge diameter. This confirms the trends from the data of reference (1) reported in reference (26). However, the present set cannot be linear for  $d < 3.81$  cm and still terminate at  $d = d_c$  for zero gap.

Data of Table 6 showed that confinement of the charge lowers the critical initiating pressure by an amount depending on the characteristics of the explosive. The 50% gap values for cast Comp B tested in casings of different materials were also determined; these values are listed in Table 7. The 50% gap pressures range from about 40 kbar (unconfined charge) to about 19 kbar (heaviest confinement in a Pb pipe).

Confining materials of shock impedance approximating that of the explosive (glass, PMMA, and Comp B) all have approximately the same effect on the 50% gap test value of Comp B. The metals (lead, steel, and aluminum) have an appreciably greater effect. As a first approximation, it is assumed that the confining tubes have a simple inertial effect. An "effective charge diameter" ( $d_e$ ) for the confined charge can then be computed by replacing the mass of the confining tube by an equal mass of Comp B in the cylindrical configuration.

(26) I. Kabik and S. J. Jacobs, Memo to 233 on PBXW-100 Booster Sensitivity Tests for Mk 46 Warhead, 6 Feb 1970.

Table 6  
DATA SHOWING EFFECT OF CONFINEMENT ON 50% GAP AND  $P_i$

Material <sup>a</sup>	Test No.	$\rho_o$ g/cc	$d_e$ cm	50% Point			Slope <sup>b</sup> $\Delta P / \Delta d^{-1}$ kbar-cm
				Gap in. x 10 <sup>2</sup>	$P_g$ kbar	$P_i$ kbar	
DINA	556	1.60	3.81	226	15.5	17.4	49.5
	556A		7.62C	279	10.0	10.9	
Comp B	339	1.70	3.81	143	39.8	49.0	189
	336		4.76	159	32.3	40.0	
	358		7.62C	201	19.7	24.2	
TNT	542	1.62	3.81	73	66.2	79.5	210
	548	1.61	7.62C	135	43.9	52.0	

a. All materials were cast. The casting of DINA was prepared with longitudinal wires and slow cooling.

b. Relationship  $P_i = a + b d^{-1}$  assumed; see reference (24).  $P_i$  was derived from Hugoniot of PMMA, TNT, and Comp B. The TNT Hugoniot was also used for DINA.

c. Standard LSCT confined charge assumed equivalent to 7.62 cm diameter unconfined charge.

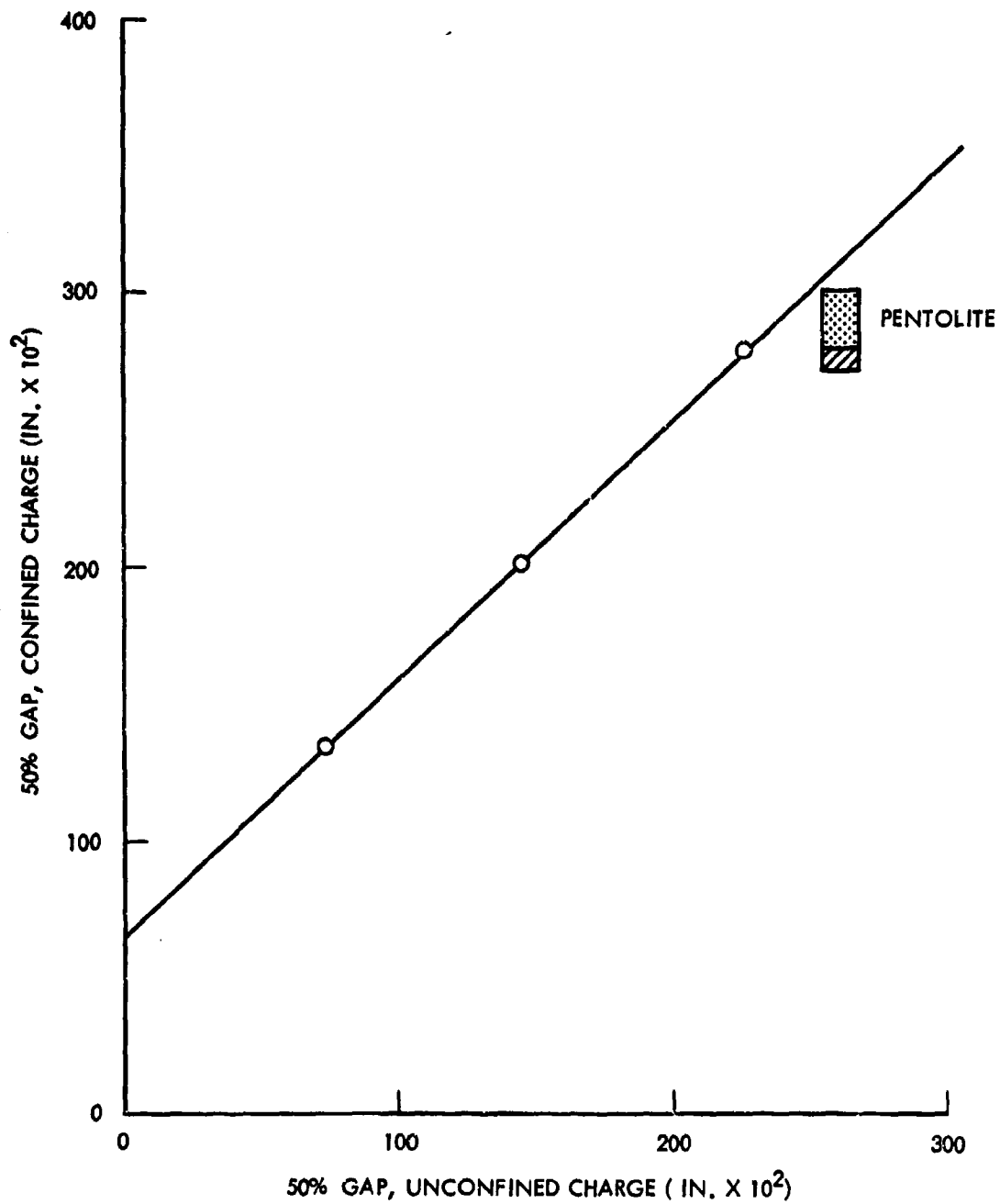


FIG. 7 EFFECT OF CONFINEMENT ON 50% GAP IN LSGT.

Table 7  
EFFECT OF CONFINEMENT ON TEST RESULTS FOR COMP B

Test No.	Confinement	Outer diameter, cm		Effective Charge diam*, de, cm	de <sup>-1</sup> cm <sup>-1</sup>	50% Point		Critical Initiating Pressure** (kbar)
		Test Charge	Container			in.x10 <sup>2</sup> No. Cards	Pg kbar	
344	Lead	3.66	4.76	8.68	0.115	204	(19.1)	23.3
358	Steel	3.66	4.76	7.50	0.133	201	(19.7)	24.2
343	Aluminum	3.66	4.76	5.30	0.189	179	(25.3)	31.4
336	None	4.76	-	4.76	0.210	159	(32.3)	40.0
340A	Glass	3.66	4.44	4.75	0.210	158	(32.7)	40.6
341	PMMA	3.66	4.76	4.45	0.225	156	(33.6)	41.7
339	None	3.81	-	3.81	0.262	143	(39.8)	49.0

Acceptor: Cast Comp B (RDX/TNT/Wax, 60/40/1) of  $\rho_0 = 1.704$  g/cc  
Temperature: Ambient

\*Effective charge diameter is charge diameter obtained when the confining tube mass is replaced by an equal mass of Comp B in the same cylindrical configuration.

\*\*From Hugoniot data for PMMA and for non-reacting Comp B (8).

Table 7 contains values of  $d_e$  and its reciprocal; Figure 8 shows the variation of 50% initiating pressure as a function of the reciprocal of the effective charge diameter.

The data of Table 7, like those of Table 5, were obtained before the present controls on test temperatures and casting procedures were used. The lower precision to be expected in the 50% gap values coupled with the few confining materials examined permit at least two interpretations of Figure 8: one linear relationship (solid line) for all materials, with the value for Al considered too low because of experimental error, or two linear relations, one for non-metals and one for metals (dashed line).

The  $P_i$  for cast Comp B measured under the standardized test conditions (23 kbar) is not significantly different from that measured under the highest confinement tested here (24 kbar for Pb). Use of the standardized confinement has increased the effective charge diameter by a factor of two and thereby decreased the  $P_i$  from 49 to 23.

#### D. Witness

1. Steel Plate. The standard witness plate can be replaced by a larger one (15.2 cm square) of the same thickness without affecting the 50% gap. This substitution is occasionally made when testing granular materials with which the standard witness plate shatters whereas the larger one does not; in such cases, use of the larger plate facilitates test interpretation.

The standard witness plate is 0.95 cm thick, and those plates first used showed a 50% probability of being punched when the standard tetryl donor was followed by a gap of 100 cards. For these plates it required a gap pressure of about 55 kbar and a transmitted pressure of about 120 kbar just to punch a hole in the witness plate. To transmit a pressure of 120 kbar or higher requires a pressure at the boundary determined by the second boundary material. In the case of PMMA, it must be 55 kbar or higher. For the average voidless propellant or explosive, it would have to be greater, say about 75 kbar; whereas for a granular material at  $\rho_0 = 1$  g/cc, the required pressure would be somewhat less than 55 kbar. Subsequent investigation (27) showed that there was a wide variation from lot to lot of the cold rolled plates used as witnesses. This is a matter of no consequence in testing high impulse reactions, e.g., a detonating explosive supplies far more force than the minimum required to punch any such plate. But it makes the limiting values quoted for punching the first lot of plates exactly applicable only to that one lot although its order of magnitude is representative of any similar witness plates. The high stress required to punch the plates as well as their variability from lot to lot make such witnesses quite inadequate for low impulse reactions.

(27) D. Price, Appendix A, "Some Properties of Various Steel Witness Plates", NOLTR 62-41, 20 Mar 1962.



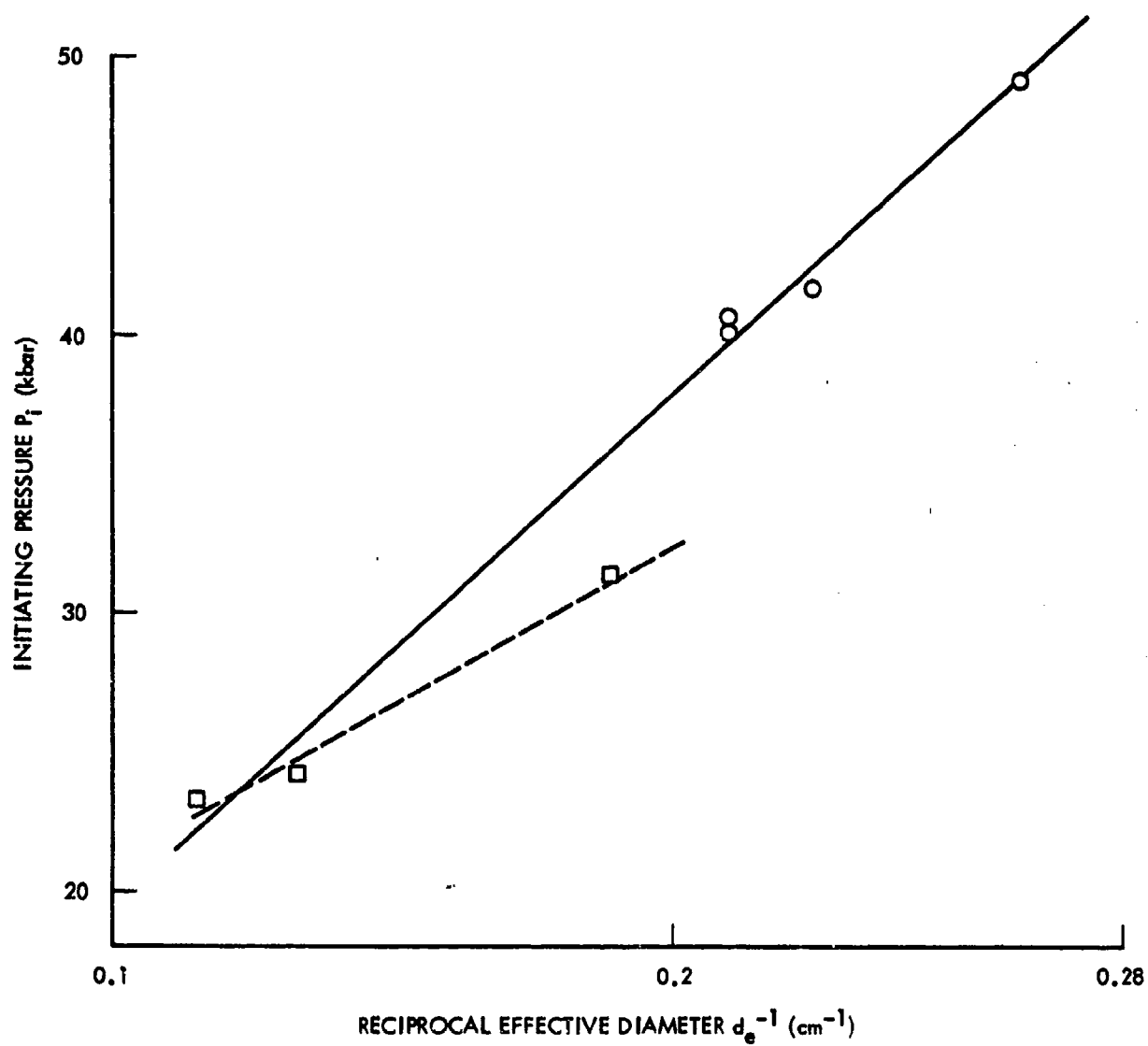


FIG. 8 VARIATION OF INITIATING PRESSURE OF CAST COMP B WITH RECIPROCAL EFFECTIVE CHARGE DIAMETER, (O NON-METAL CONTAINER; □ METAL CONTAINER)

The use of witness plates of varied thickness (0.95 to 0.16 cm) was also studied very briefly (27). The limits of practical thicknesses, 0.32 to 0.95 cm, resulted in a very narrow range of pressures required to punch the various plates. Again, plates of cold-rolled steel are shown inappropriate for witnessing low impulse reaction. It is necessary to replace the steel witness plate by a more responsive sensor to study such reactions.

2. Explosive Witness; Modified & Extended Tests. When essentially voidless test samples exhibit a no-go in the standard gap test the witness plate is generally undamaged just as it is when a condensed inert such as water is substituted for the test material. An undamaged witness plate seems conclusive evidence that no shock-induced reaction occurs under the test conditions. On the other hand, a go is interpreted as a "detonation"; although it may not be a steady state reaction, it is a powerful one propagated at supersonic speeds. This interpretation of a go has been supported by numerous experiments carried out with instrumented gap tests; in addition to determining the 50% gap, the propagation speed of the reaction has been followed with high speed cameras, ionization probes, or the continuous resistance wire technique. Consequently it is generally possible to classify voidless materials in the standard gap test as "detonable" or non-reactive under shock.

Granular materials, on the other hand, can exhibit, in the standardized test, a no-go for which the plate damage is extensive; the 0.95 cm thick steel plate will be greatly bulged and bent. Occurrence of such damage is strong evidence that a shock-induced reaction has occurred, but that it is of insufficient strength to punch a hole in the witness plate. When such a result is obtained, the material should be tested with more responsive sensors than the standard witness.

Low impulse reactions are obtained with low energy materials (AN, AP, or very low  $\rho_0$  charges of HE). Having established, by independent investigations, that such materials exhibit steady state reactions, we can assess their shock sensitivity by use of the "Extended Gap Test." The procedures for this test are those of the LSGT; only the witness is changed. The standard test is modified by placing a 14 cm tube of any powerful explosive between the test material and the witness plate of Figure 1. The modified test is shown in Figure 9; in it the low impulse reaction of the acceptor is used to initiate a high impulse reaction in the explosive witness which, in turn, punches a hole in the steel witness plate. Of course, the initiating pressure must be measured for each explosive sensor used. Data of Appendix C suggest appropriate witnesses ranging from cast TNT (50% gap pressure ca 44 kbar) to cast pentolite 60/40 (50% gap pressure ca 10 kbar). Only one explosive witness, capable of initiation by the low impulse reaction of the test material, is required to determine the 50% gap of the test material. If in addition, a measure of the reaction strength is desired, the critical explosive witness, i.e., one just initiated by the acceptor reaction, must be found by trying a graded series of witnesses at the

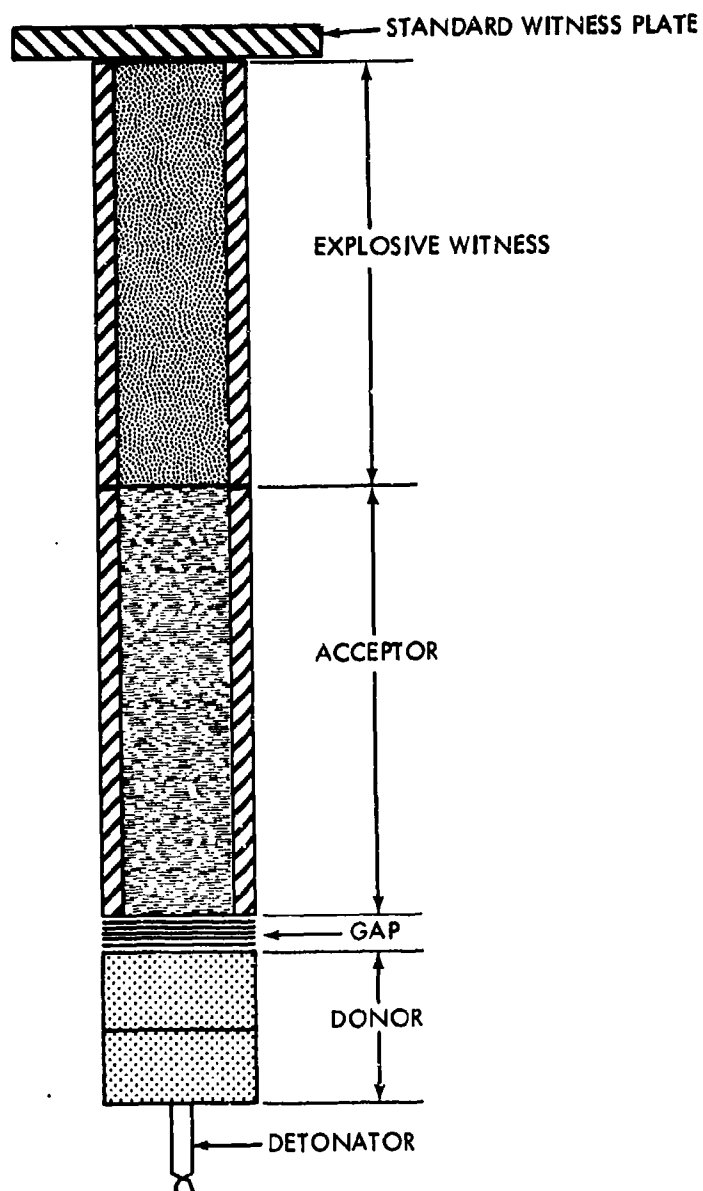


FIG. 9 EXTENDED GAP TEST ASSEMBLY

50% gap conditions. Reference (24) goes into some detail about measuring the 50% point and reaction strength of low impulse materials; reference (28) shows that a reaction pressure equal to or greater than the critical initiation pressure of the explosive witness is required to initiate the witness by gas loading from the reaction products.

One disadvantage of the extended test is its introduction of more steel fragments and consequent additional damage to the bombproof. To minimize such damage, the cased Comp B witness was replaced by unconfined cast Comp B (3.8 cm diameter x 6.4 cm length or 1.5 in. diameter x 2.5 in. length). As Table 6 shows, such an unconfined Comp B is approximately equivalent to a confined cast TNT. Both are, of course, more sensitive witnesses than the steel plate. The gap test with the unconfined cast Comp B witness is designated the "modified gap test" to distinguish it from the extended and the regular (LSGT).

As would be expected, the same  $P_g$  is measured whichever test is used for the organic HE. Thus cast Comp B (Test 522) has a 50% gap of  $218.5 \pm 1.5$  cards (Test Nos. 760 - 763) and DATB (Lot 315),  $139 \pm 1$  (Test Nos. 770 - 722). For 7 $\mu$  AP, the regular test shows negative results in the high porosity region although we know from numerous other studies that this AP does exhibit steady state detonation of the porous charges. As Figure 10 shows, the modified and extended tests give equivalent results in the high porosity region, and all three tests give equivalent results at 65% TMD and greater compaction. Since the curve of Figure 10,  $P_g$  vs %TMD, may be slightly distorted by changes in the method of charge preparation, the symbols for handpacking and the hydraulic press are shown where used on the more porous charges. All charges of 65% TMD or greater were prepared in the isostatic press.

#### VII. COMPARISON OF NOL LARGE SCALE AND SMALL SCALE GAP TEST VALUES

In earlier work (29), a comparison was made of the results obtained with the two NOL standardized gap tests: the LSGT and the small scale gap test (SSGT). Quantitative correlation was found between the two sets of test results provided explosives were tested at porosities of 10% or greater. (The limit seemed to be 6% for most organic HE and 10% for waxed HE.) At lower porosities, the more rapid approach to dead pressing in the SSGT than in the LSGT destroys any correlation.

(28) D. Price and F. J. Petrone, "Detonation Initiated by High-Pressure Gas Loading of a Solid Explosive", J. Appl. Phys., 35, 710 (1964).

(29) D. Price and T. P. Liddiard, Jr., "The Small Scale Gap Test: Calibration and Comparison with the Large Scale Gap Test", NOLTR 66-87, 7 Jul 1966.

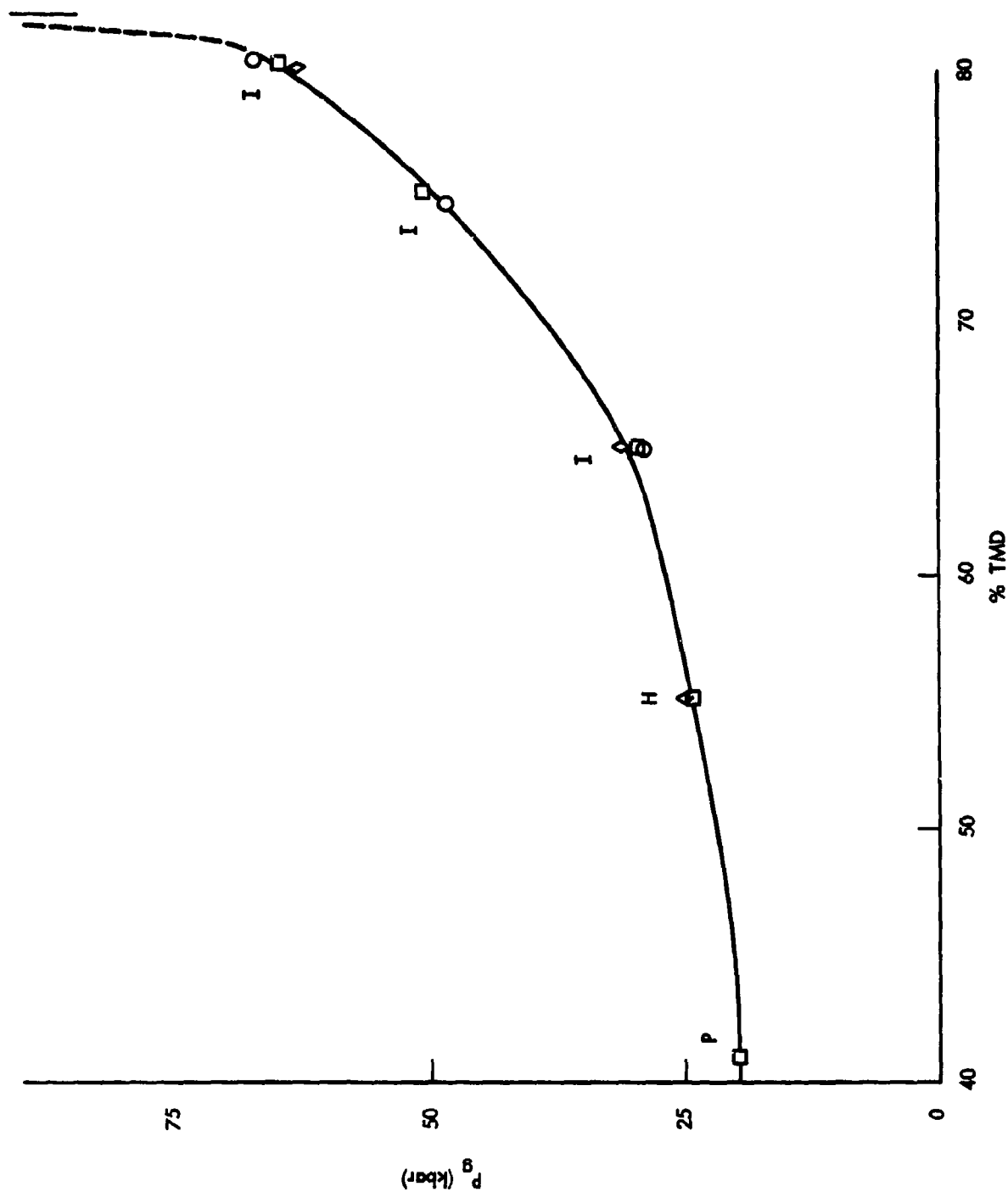


FIG. 10 COMPARISON OF EXTENDED, MODIFIED, AND REGULAR LSGT RESULTS FOR 7 $\mu$  AP 141.  
(O REGULAR; square MODIFIED; diamond EXTENDED; P HANDPACK; H HYDRAULIC PRESS; I ISOSTATIC PRESS)

The correlation undoubtedly still exists. It will be little affected by the improved Hugoniot chosen for PMMA because that changes  $P_g$  by 3% or less in the range of interest. But the LSGT results have also been corrected for error in the calibration measurements of  $u$  (errors up to 10% were introduced by measuring the free surface velocity and using Equation (4) to obtain  $u$ ). The SSGT calibration values are subject to the same error and have not been corrected since no direct measurements of  $u$  have been made. Hence our comparison is now made between uncorrected SSGT results and corrected LSGT results. Table 8 shows the present  $P_g$  values and Figure 11 illustrates the relationship between them. Table 8 is an updating of data given in Table 4 of reference (29) to take account of the improved PMMA Hugoniot and the corrections to the LSGT calibration. Figure 11 shows about the same degree of correlation as did the original data. In both cases the highest density NQ-1 point (72% TMD) lies above the curve. This could be the result of experimental error or the fact that this low energy HE dead presses in the SSGT at lower relative density than do higher energy HE.

#### VIII. RELATIONSHIP OF LSGT RESULTS TO WEDGE TEST DATA

The relationship of the LSGT results to all other sensitivity tests is believed to be shown by way the set of all tests maps out the critical curve in the pressure-time plane, as described in reference (20). In general, we do not have sufficient data to define this critical curve. Hence it is more common to compare the results of two tests directly, e.g., the LSGT and the SSGT in the preceeding section. Since the wedge test has been and is being widely used, its results too will be compared with the LSGT. The wedge test consists of shocking a wedge shaped charge with a plane wave, and observing the subsequent shock front as a function of path traveled.

A comparison of wedge test results with the NOL large scale gap test (LSGT) was given in the appendix of reference (30). The wedge data used were those of references (31) - (33); the pressure data as

- (30) D. Price, "Large Scale Gap Test: Interpretation of Results for Propellants", NavWep 7401, 15 Mar 1961.
- (31) J. M. Majowicz and S. J. Jacobs, Tenth Annual Meeting of Division of Fluid Dynamics of American Physical Society, Nov 1957. (See also NAVORD 5710).
- (32) N. L. Coleburn, B. E. Drimmer, and T. P. Liddiard, Jr., "The Detonation Properties of DATB", NAVORD 6750, 12 Oct 1960.
- (33) A. W. Campbell, W. C. Davis, J. B. Ramsay, and J. R. Travis, "Shock Initiation of Solid Explosives", Phys. Fluids 4 (4), 511 (1961).

Table 8

## COMPARISON OF LSGT AND SSGT RESULTS AT SAME RELATIVE DENSITY

Material	$\rho_{cc}$	%	50% Pressure $P_g$ (kbar)		Material	$\rho_{cc}$	%	50% Pressure $P_g$ (kbar)	
			LSGT	SSGT				LSGT	SSGT
NO-2	0.90	50.3	21.2	22.9**	Tetryl	1.43	82.4	9.0	9.9*
X547	1.20	67.4	48.0	57.4*	X460	1.49	86.0	9.7	10.8*
	1.27	71.5	51.8	80.2		1.64	94.9	13.9	16.4*
DATB	1.21	65.8	31.1	30.8**	CH-6	1.45	81.3	7.8	9.8**
X331	1.23	67.0	31.5*	31.5	X445	1.51	84.9	7.9*	10.4
	1.44	78.1	35.8	38.2		1.57	88.2	8.3	11.4*
	1.70	92.5	44.7	48.9		1.60	90.0	8.8*	12.4
						1.64	92.1	9.4*	14.2
TNT	1.35	81.8	14.9*	17.5		1.68	94.4	10.4*	18.0
X412	1.42	85.7	16.5	18.5*		1.70	95.5	11.0	20.2*
	1.45	87.4	17.3*	19.0					
	1.49	90.3	18.6	20.8*	RDX	1.53	85.0	6.8	9.3**
	1.55	93.6	21.0*	22.7	X189	1.64	91.8	7.4	11.8*
	1.60	96.9	24.1	27.6*					
	1.64	98.9	26.5	33.4*	EPM-2	1.72	91.7	14.7	15.9
TATB	1.82	93.9	64.0	102**	Comp C-3	1.61	--	23.3	38.6

\*Interpolated

\*\*Extrapolated

\*\*\*Nominal value, beyond range of calibration.

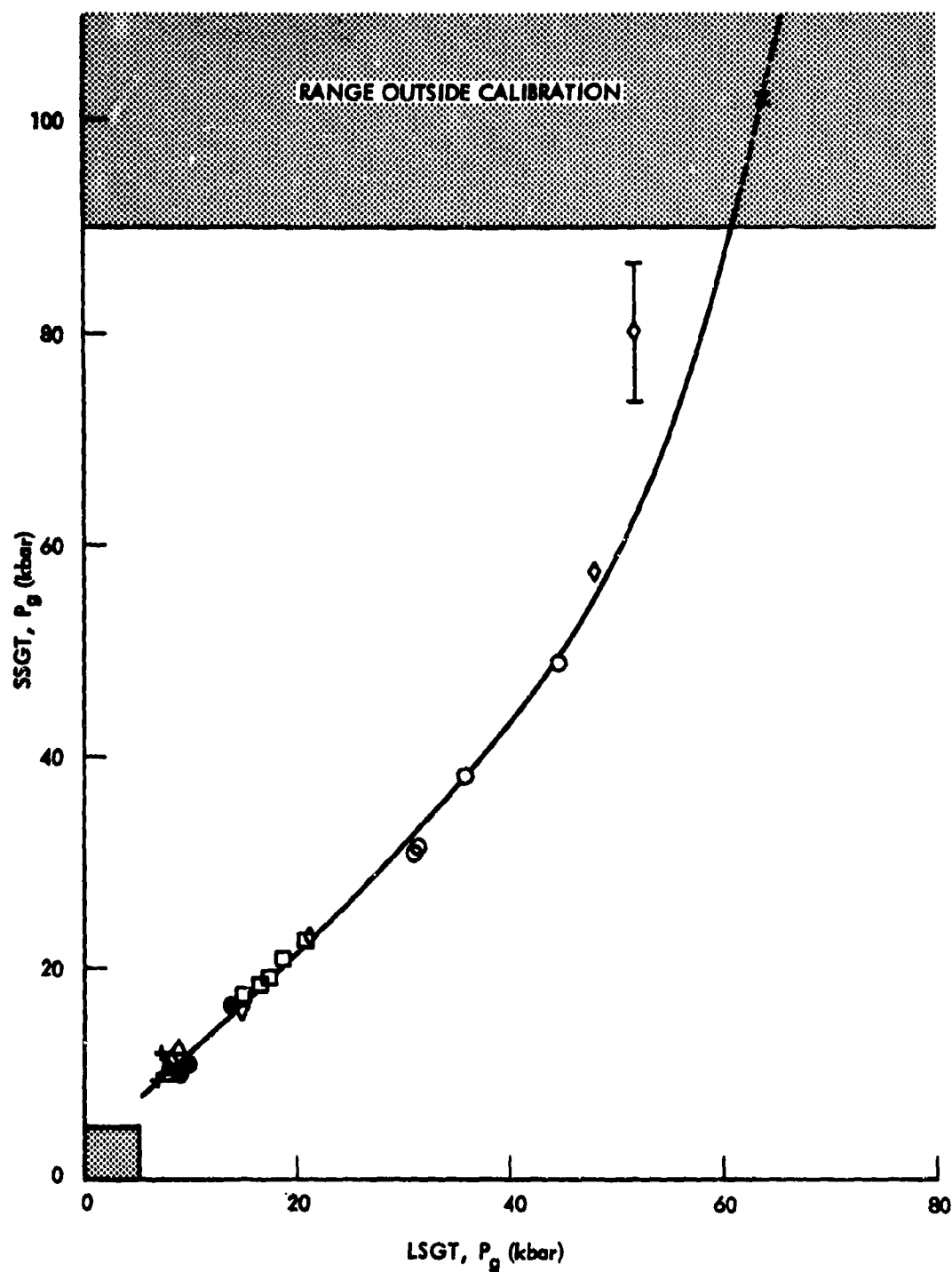


FIG. 11 CORRELATION OF SSGT AND LSGT VALUES.  
 (RANGE IN % TMD: + RDX 85-92;  $\Delta$  CH-6 81-90;  $\nabla$  EPM-2 92;  $\square$  TNT 82-94;  
 $\circ$  DATB 66-93;  $\diamond$  NQ-1 50-72;  $\bullet$  TETRYL 82-95;  $\times$  TATB 94)



listed in reference (31), were too large and had been corrected (see references (30) and (34)). The parameters considered in reference (30) were:

- $x_s$  Run length, distance from the shocked surface to the plane in which steady-state detonation is first established.
- $\tau_s$  Delay time, total time from entry of shock into the explosive until time steady-state detonation begins.
- $\Delta$  Excess delay time, amount by which  $\tau_s$  exceeds the time required for the detonation to travel distance  $x_s$ .  
 $\Delta = \tau_s - x_s/D$ .
- $P_g$  Pressure (50% point) in PMMA at gap/acceptor interface.
- $P$  Shock pressure.
- $P_i$  Threshold pressure in explosive required to initiate detonation in LSGT.

It was tentatively concluded that  $\Delta^{-1}$  vs  $P$ ,  $\tau_s^{-1}$  vs  $P$ , and  $x_s^{-1}$  vs  $P$  were all linear, and that, in the last case, the point ( $P_i$ ,  $0.02 \text{ mm}^{-1}$ ) fell on the curve. Moreover, it was pointed out that  $\log x_s$  vs  $\log P$  was also linear and, in some cases, extrapolated to reasonable values of  $P$  for  $x_s \sim$  reaction zone length whereas the  $x_s^{-1}$  vs  $P$  curves did not.

Because the average set of data (30) consisted of only three points, the suggested relationships were considered very tentative. However, Jacobs et al (34) working independently showed linearity of  $x_s^{-1}$  vs  $P$  for some nine points of data for cast Comp B-3. Somewhat later Ramsay and Popolato (35) published linear  $\log x_s$  vs  $\log P$  curves for five explosives. Since then both Los Alamos Scientific Laboratory and Lawrence Livermore Laboratory have used this empirical relationship for evaluating shock sensitivities.

(34) S. J. Jacobs, T. P. Liddiard, Jr., and B. E. Drimmer, "The Shock-to-Detonation Transition in Solid Explosives", Ninth International Symposium on Combustion, Academic Press, New York, 1963; p 517.

(35) J. B. Ramsay and A. Popolato, "Analysis of Shock Wave and Initiation Data for Solid Explosives", Fourth Symposium (International) on Detonation, ACR-126 (ONR), U.S. Gov. Print. Office, Washington, (1967); p 233.

At the time of the initial comparison, we used the first calibration of the LSGT (36) and the Russian data for the Hugoniot of non-reacting TNT (37). Now we have an improved calibration and Hugoniot data for PMMA (7). Moreover, we have improved Hugoniot data for a number of voidless explosives, (34), (8), (9). We also have a method of computing the Hugoniot of nonreacting pressed explosives from the Hugoniot of the voidless material (12), and thus avoid the complication caused by reaction of these relatively shock sensitive materials during attempts to measure the Hugoniot. For these reasons, we are now able to obtain better values of the 50% pressure  $P_g$  and to compute from it improved values of  $P_i$ .

In addition, we now have the results of a continuous wire study of the behavior of one explosive (DINA) for which  $x_s$  was measured over a range of  $P$  (38). Both confined and unconfined cast cylindrical charges were used with the donor/attenuator of the LSGT. Table 9 contains the data obtained.  $P$  in PMMA has been corrected according to the most recent LSGT calibration (7) and  $P$  in DINA was derived from the corrected values by using the NOL Hugoniot for cast TNT (8) which has about the same density as the cast DINA (1.59 - 1.63 g/cc). The run distance  $x_s$  is the value  $X_{\lambda C}$  of reference (38); it includes a correction for the width of the conducting zone of reacted explosive required to close the wire circuits. The correction is fully described and discussed in reference (38).

Figure 12 shows a plot of  $x_s^{-1}$  vs  $P$  for the unconfined charges. As found in the original examination of the data (38), there is a discontinuity in the slope which occurs after a certain run length. As Figure 12 is drawn, it appears at  $x = 21.5$  mm which is 0.565 of the charge diameter. Among the possible explanations offered for this discontinuity was the arrival at the charge axis of lateral rarefaction (release) waves. At the present time, this seems to be the best explanation, and has been reinforced with an examination of similar data from another investigation. Cosner and Sewell (39) worked with Comp B charges 54 mm diameter x 76.2 mm length.

- (36) I. Jaffe, R. L. Beauregard, and A. B. Amster, "The Attenuation of Shock in Lucite", NAVORD 6876, 27 May 1960.
- (37) V. S. Ilyukhin, P. F. Polhil, O. K. Rozanov and N. V. Shvedova, "Measurement of the Shock Adiabats of Cast Trinitrotoluene, Crystalline Hexogene and Nitromethane", Soviet Phys. Dokl. 5, 337 (1960).
- (38) D. Price, J. P. Toscano and I. Jaffe, "Development of the Continuous Wire Method. III. Measurements in Cast DINA", NOLTR 67-10, 20 Apr 1967.
- (39) L. N. Cosner and R. G. Sewell, "Initiation of Explosives through Metal Barriers", NAVWEPS Report 8507, China Lake, Cal., Apr 1964. (This report gives data obtained in 1956. In addition to these data, additional data were supplied by Cosner in 1962).

Table 9

DATA FOR SHOCK-TO-DETONATION TRANSITION IN CAST DINA<sup>a</sup>

	PMMA	DINA		
No. Cards	P (kbar)	P (kbar)	$x_s$ (mm)	$x_s^{-1}$ (mm <sup>-1</sup> )
Unconfined Charges (3.81 cm dia x 15.25 cm length)				
140	41.4	49.5	6.3	0.1587
164	30.3	35.7	11.5	0.0870
175	26.5	31.0	18.7	0.0535
200	19.9	23.0	25.0	0.0400
210	18.0	20.6	29.1	0.0344
220	16.3	18.4	43.0	0.0233
223	15.9	18.0	41.1	0.0243
225	15.6	17.6	43.9	0.0228
226	15.5	17.5 <sup>b</sup>	45.5 <sup>c</sup>	0.0220
Confined in Mild Steel (3.81 cm ID, 4.87 cm OD)				
164	30.3	35.7	10.7	0.0935
175	26.5	31.0	18.8	0.0532
180	25.0	29.2	19.5	0.0513
185	23.5	27.4	21.6	0.0463
191	21.9	25.4	22.3	0.0448
140	41.4	49.5	8.8	0.1136
150	36.3	42.8	9.9	0.1010
180	25.0	29.2	16.2	0.0617
227	15.3	17.3	32.7	0.0306
252	12.4	13.7	53.5	0.0187
265	12.1	13.4	60.9	0.0164
272	10.6	11.6	64.9	0.0154
276	10.3	11.35	67.1	0.0149
279	10.0	11.0 <sup>b</sup>	77 <sup>c</sup>	0.0130

a. Data from reference (38). P(PMMA) corrected by reference (7); P(DINA) derived from P(PMMA) and TNT Hugoniot (8);  $\rho_0$  of cast DINA 1.59 - 1.64 g/cc.

b. Value for  $P_i$ .

c. Extrapolated value.

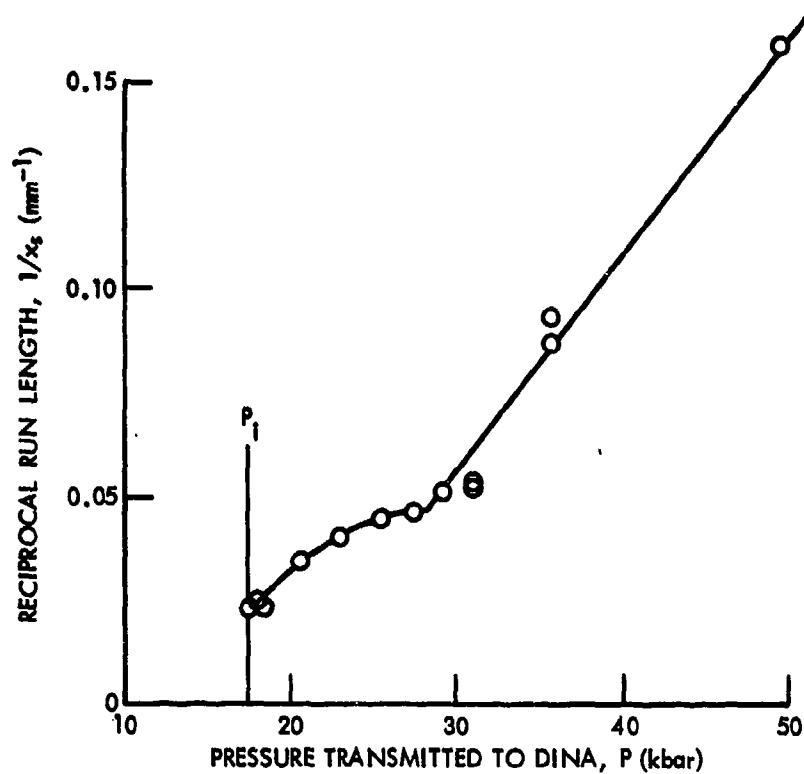


FIG. 12 RECIPROCAL RUN LENGTH VS. PRESSURE FOR UNCONFINED DINA.

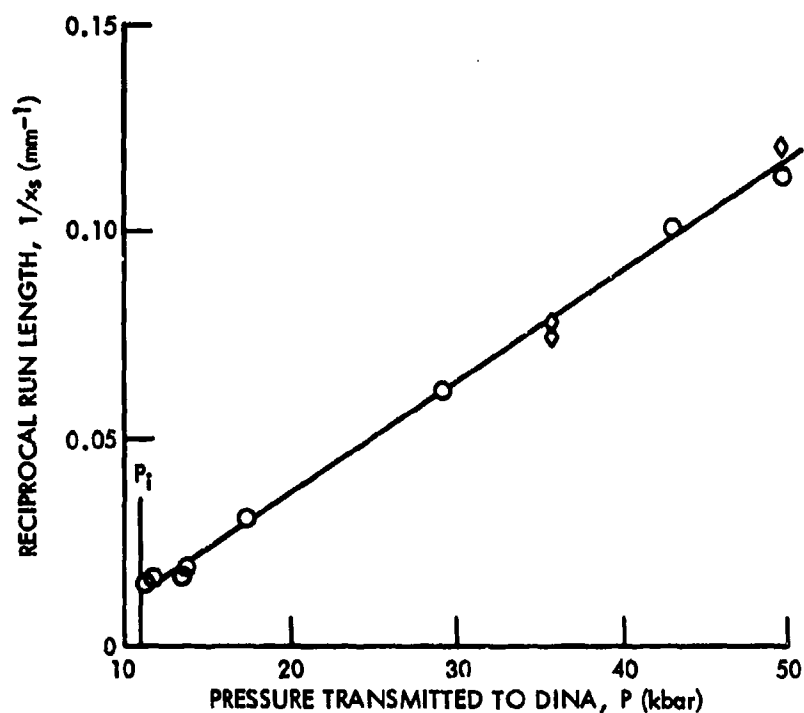


FIG. 13 RECIPROCAL RUN LENGTH VS. PRESSURE FOR CONFINED DINA.

(O CONFINED, CORRECTION OF 6.8mm;  $\diamond$  UNCONFINED, CORRECTION OF 6.8mm)

Their donor system differed from that of the LSGT and their attenuator (gap) was steel rather than PMMA. Run length was determined by streak camera records of the acceptor charge surface. An  $x_s^{-1}$  vs  $P$  plot of these data showed a discontinuity at  $x_s = 31$  mm or 0.57 of the charge diameter. The excellence of the agreement is entirely fortuitous (see later discussion), but it does appear that release waves play a role in determining the threshold pressure for initiating detonation in any unconfined cylindrical charge whose length is greater than about half a diameter. Hence such gap test values are not comparable to wedge test values; if properly designed, wedge tests are completed before release waves affect the detonation front.

Figure 13 displays the  $x_s^{-1}$  vs  $P$  curve for confined DINA; the confinement is mild steel 38.1 mm ID, 47.8 mm OD and very nearly the same as that of the standard LSGT (36.5 mm ID, 47.6 mm OD). As the plot shows, the relationship is linear and shows no sharp change in slope. It is comparable to the wedge test data in that measurements are completed before they are affected by the arrival of lateral rarefactions.

As the figures are drawn, the Figure 13 slope differs appreciably from the high pressure (low  $x_s$ ) portion of Figure 12, the analogous curve for unconfined DINA. Actually the first part (high pressure portion) of the two curves should coincide. That they do not is probably caused by a combination of errors. For example, to convert the raw value  $X_0$  to  $x_s$  in reference (38) the corrections used were 4.7 and 6.8 mm, respectively, for the unconfined and confined DINA. If the same correction (6.8 mm) is used for both sets of data, the two curves coincide for the data  $x_s < 14$  mm (see Figure 13). This probably means that the same correction should have been used in both cases but, of course, it does not reveal exactly what that correction should be. Fortunately, we can still benefit from the information of Figures 12 and 13 despite possible errors of the order of magnitude of 2 mm in  $x_s$ .

The fact that there is such an uncertainty should, however, be kept in mind. It certainly affects the value of  $x_s$  chosen for the arrival of the release wave at the axis. In this case, the way the curve is fitted to the data will also affect the value. Hence although the value picked was given above as "0.565 diameters", we can only be sure that it is about the value of a radius.

Data for the confined DINA were also examined in the other empirical relationships that have been mentioned ( $\log x_s$  vs  $\log P$ ,  $\log x_s$  vs  $\log \Delta$ ,  $\tau_s^{-1}$  vs  $P$ ,  $\Delta^{-1}$  vs  $P$ ). All showed some curvature when all eight pairs of data were included. However, if the first two pairs (i.e., at  $P$  values of 42.8 and 49.5 kbar) were discarded, the remaining six showed linearity for all the other relationships mentioned. Thus for the confined DINA and presumably any comparable data obtained in the LSGT set-up, the most successful linear relation is that of  $x_s^{-1}$  vs  $P$ .

This same relation ( $x_s^{-1}$  vs  $P$ ) has been used for reexamination of the wedge test data. These data for cast charges are given in Table 10. The corresponding critical initiating pressures of the same HE in the LSGT appear in Table 11. The transition data for cast pentolite and DINA are plotted in Figure 14; those for the remaining cast materials, in Figure 15. The data for pentolite and DINA have been plotted separately (1) to emphasize the similarity between the wedge test results and those from the regular LSGT configuration on similar explosives and (2) because these curves cross those of Figure 15 for the other TNT based castings. Both the pentolite and DINA data ( $x_s^{-1}$  vs  $P$ ) seem to terminate at  $P_i$ . The apparent crossing near  $P_i$  is probably fictitious. The  $P_i$  values of 11.9 (pentolite) and 11.0 kbars (DINA) are not significantly different and could be reversed by small errors in the measurements or the Hugoniot used or both. Moreover, unconfined pentolite showed  $P_i$  of 12 - 14 kbar as compared to 15 kbar for unconfined DINA, i.e., the reverse of the relative sensitivities of the confined charges. If the run length for the same shock amplitude is considered a measure of the shock sensitivity, then cast pentolite is more shock sensitive than cast DINA, probably over the entire pressure range. However, both curves of Figure 14 intersect some of the curves of Figure 15. Hence on the run-length criterion, reversals in relative sensitivity will occur between the higher and lower pressure ranges, e.g., for pentolite and Comp B-3 and for DINA and Octol 65/35.

In Figure 15, all five cast explosives show a satisfactory linear extrapolation of  $x_s^{-1}$  vs  $P$  to  $P_i$ , save possibly Comp B. Of course the data for Comp B-3 include only the higher pressure, shorter run length data. Reference (34) gives, in addition, lower pressure, longer run length data that resulted in an extrapolation to 28 kbar instead of the present 22 kbar. This difference is the order of magnitude of errors in  $P_i$  and possibly of the lower shock pressure measurements. It might also be caused by an unmonitored duration effect in the action of the shockwave; such an effect becomes more important at the lower amplitudes. Whatever the cause(s), the discrepancy cannot be resolved without further experimental work.

By the run-length criterion, the shock sensitivities of Figure 15, in descending order, are Comp B-3 (RDX/TNT, 60/40), Octol 65/35, Comp B (RDX/TNT/Wax, 60/40/1), Cyclotol 75/25, and TNT. This ordering of cast explosives is less mysterious than it seemed in 1961, chiefly because the role of particle size in affecting shock sensitivity has now been recognized. Seely (19) demonstrated in 1963 that shock sensitivity increased with increasing particle size if air were the continuous medium, but increased with decreasing particle size if the continuous medium were a condensed one. Cast explosives fall in the latter category and should show increasing sensitivity with decreasing particle size. RDX Class F is recommended for preparing Comp B-3; Class A for Comp B; and Class D for cyclotols. Figure 16 contains plots of relative particle size distribution made by using the screen openings and percentages required for each class in the specifications of MIL-R-398C. The relative weight mean diameters are 58, 130, and 740 $\mu$  respectively for Classes F, A, and D. It is

Table 10

## WEDGE TEST DATA FOR CAST CHARGES

Material	Density $\rho_o$ g/cc	Pressure P kbar	Run Length $x_s$ mm	$x_s^{-1}$ mm <sup>-1</sup>	Data Source
Pentolite	1.67	98	3.03	0.330	31, 30
50/50		79	3.64	0.275	
		68	4.31	0.232	
Comp B	1.71	95	2.86	0.350	34
		77	4.38	0.228	
		67	6.03	0.166	
Comp B-3	1.72	95	1.72	0.581	34
60/40		77	2.19	0.457	
		67	2.66	0.376	
Octol	1.79	105	1.94	0.515	31, 30
65/35		83	2.62	0.382	
		72	3.42	0.292	
Cyclotol	1.73	97	3.62	0.276	34
75/25		79	4.56	0.219	
		69	6.08	0.164	
TNT	~1.60	137	6.07	0.165	34
		75	18.6*	0.538	

\*Chosen beyond plateau and where steady state velocity is well established.

Table 11  
CRITICAL INITIATING PRESSURE ( $P_i$ ) FROM LSGT DATA

Cast Charges	Density $\rho_o$ g/cc	50% Point, LSGT		Critical Pressure $P_i$ (kbar)	HE Hugoniot Used	Comment
		in. x 10 <sup>2</sup> No. Cards	$P_g$ (kbar)			
Pentolite	1.67	278	10.1	11.9	Pentolite 50/50 (9)	$P_g$ average of 5 tests Comp B (9)
Comp B	1.70	201	19.7	24.1	Comp B-3 (8)	Comp B-3 (9) gives $P_i$ of 22.6
Comp B-3	1.72	209	18.1	22.0	Comp B-3 (8)	
Octol 65/35	1.79	214	17.3	22.0	Octol 75/25 (9)	
Cyclotol 75/25	1.73	182	24.4	30.0	Comp B-3 (8)	
TNT	~1.60	133	44.4	52.7	TNT (8)	



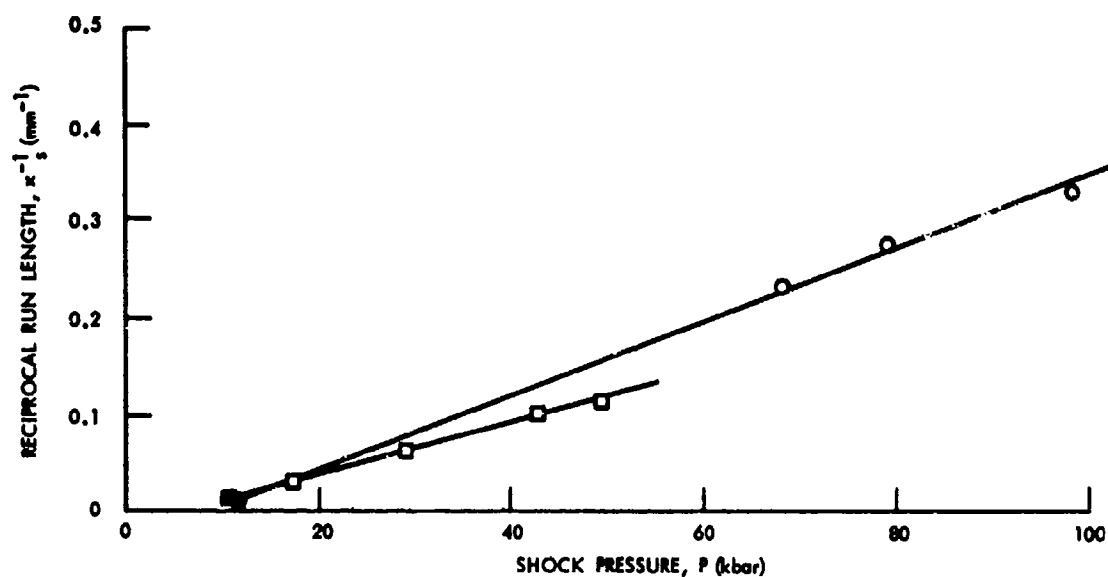


FIG. 14 SHOCK TO DETONATION TRANSITION FOR CAST PENTOLITE AND DINA.  
(O PENTOLITE, WEDGE DATA; □ DINA, REGULAR LSGT CONFIGURATION;  
×  $P_1$  VALUE)

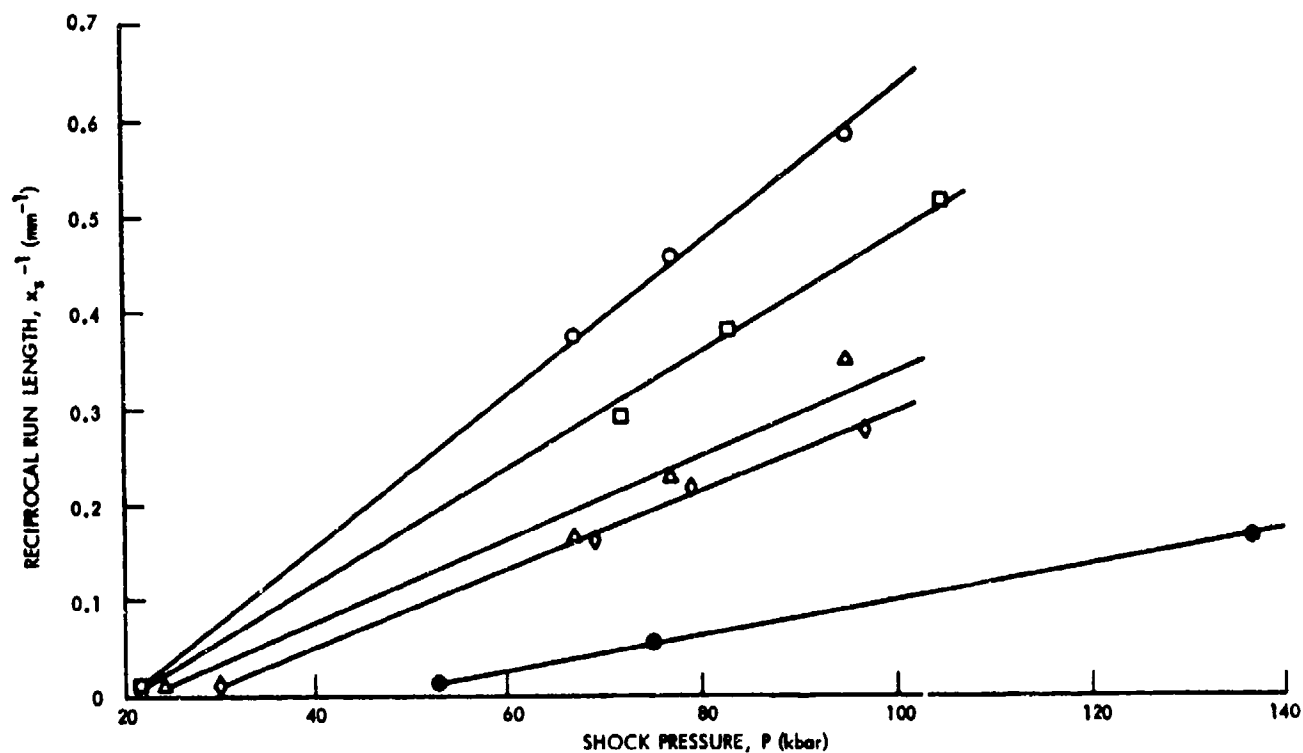


FIG. 15 SHOCK TO DETONATION TRANSITION FOR OTHER TNT BASED CAST EXPLOSIVES.  
(O COMP B-3; □ OCTOL 65/35; Δ COMP B; ◇ CYCLOTOL 75/25; ● TNT; ×  $P_1$  VALUE)

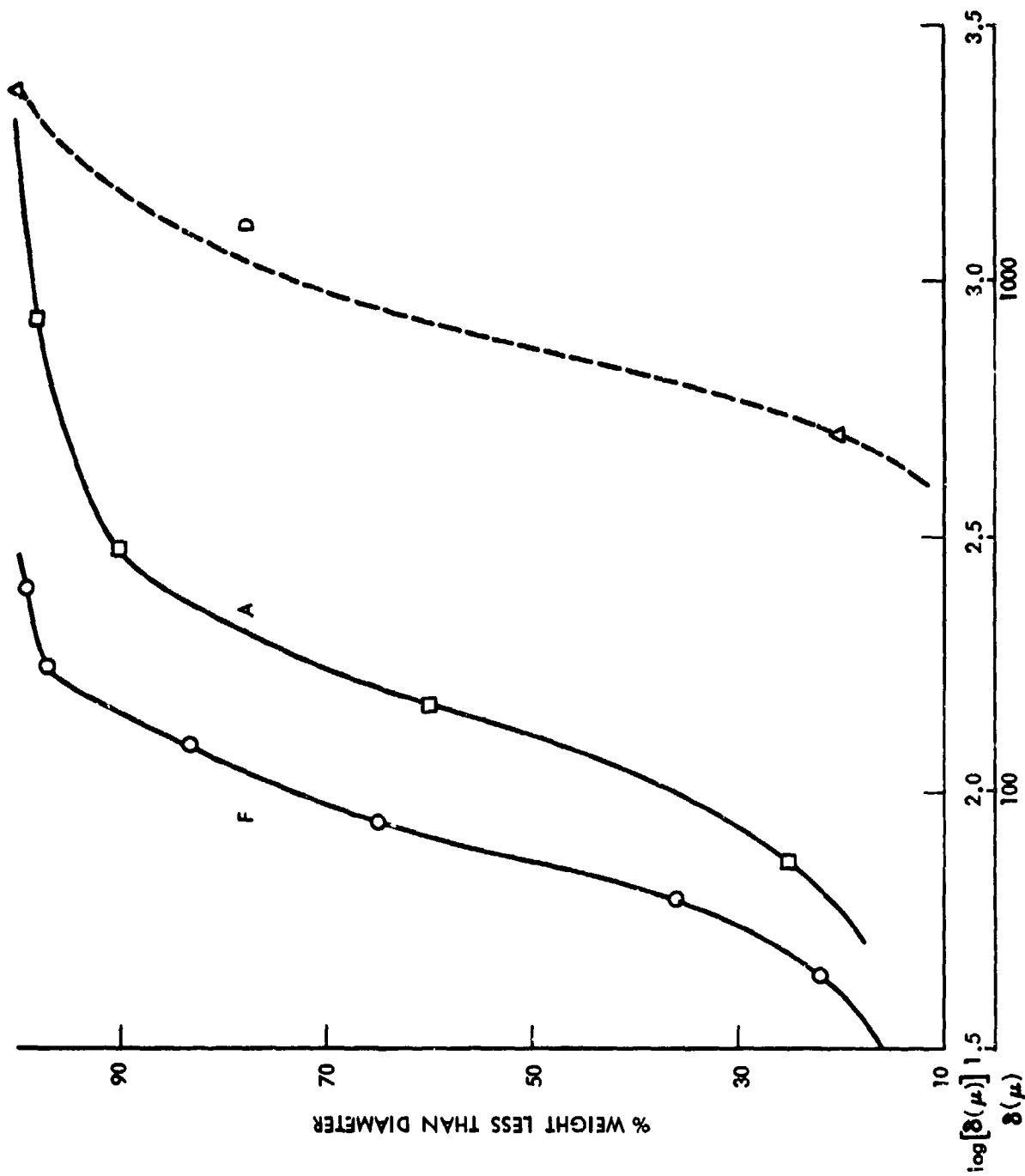


FIG. 16 APPROXIMATE PARTICLE SIZE DISTRIBUTION OF THREE CLASSES OF RDX

evident that the difference in the RDX particle size can account for the fact that Comp B-3 is more shock sensitive than Comp B. The difference between Classes A and D RDX can also account for the cyclotol (75% RDX) being less sensitive than Comp B (60% RDX).\*

It is a matter of interest that the relative ratings given by the 50% gap values (NOL's LSGT) of Table 11 are confirmed for all the cast materials (except Octol 65/35) by the 50% gap values reported for the LASL large scale test (40). The LASL test is on an unconfined charge of 1-5/8 inch diameter; data for Octol 65/35 were not tabulated.

Finally, Figures 14 and 15 reemphasize the inadequacy of an attempt to characterize shock sensitivity by measurement at only the 50% point. The curves  $x_s^{-1}$  vs  $P_i$  not only demonstrate differences in sensitivity much better than LSGT values alone can do; they also show reversals in behavior that cannot be predicted from the LSGT values. Even Figures 14 and 15 are incomplete descriptions of shock sensitivity. As discussed in reference (20), a limit curve in the pressure-time plane exists for the shock initiation of detonation in each charge, and as suggested in reference (41), a similar limit curve probably exists for the shock initiation of burning and sub-detonation reactions. Liddiard (42) has shown that threshold conditions for initiating such reactions can be defined and measured. Moreover such shock induced reactions are also an important aspect of a material's sensitivity to shock.

\*When pressed cyclotol 75/25 and pressed Comp B are compared at 96.4% TMD in the LSGT their respective 50% values of  $P_g$  are 12 and 18 kbar. By going to pressed charges, the particle size effect has been reversed and the chemical effect (75 vs 60% RDX) is still present. Hence the relative sensitivity has not only been reversed (compared to ratings of the cast materials), but the difference is significant.

- (40) A. Popolato, "Experimental Techniques Used at LASL to Evaluate Sensitivity of High Explosives", Proceedings of the International Conference on Sensitivity and Hazards of Explosives, London, 1963. Also private communication.
- (41) F. E. Walker and R. J. Wasley, "Critical Energy for Shock Initiation of Heterogeneous Explosives", Explosivstoffe 1969, 17(1), 9.
- (42) T. P. Liddiard, "The Initiation of Burning in High Explosives by Shock Waves", Fourth Symposium (International) on Detonation ONR ACR-126, U.S. Gov. Print. Office, Washington (1967); p 487.

## IX. SUMMARY

The present procedure for use of the standardized NOL large scale gap test is fully described. An improved method of assembly for firing is reported and the precision of the results (generally  $\pm 0.05$  cm in 50% gap thickness) reviewed. The best calibration data, gap pressure vs gap thickness, are presented for both the previous standard booster (tetryl,  $\rho_0 = 1.51$  g/cc) and the present one (pentolite,  $\rho_0 = 1.56$  g/cc).

Hugoniot data for representative voidless charges have been included as a basis for estimating the Hugoniot for any essentially voidless explosive; an estimated Hugoniot and the calibration data permit computation of the critical initiating pressure from the measured 50% gap value.

Compilations of all unclassified LSGT results to date are included. They are used to illustrate the change in sensitivity with propellant composition, e.g., increase with increased content of NG or HE, decrease with increased triacetin, and the changes effected by temperature and porosity. In general, shock sensitivity increases with increased temperature or increased porosity, but some results must be explained as effects on detonability or critical diameter as well.

The standardized gap test has been quite satisfactory in its present form. Hence only limited studies (reviewed here) have been made of the effect of changing any of the standard test elements. However, we have felt the need of a more sensitive witness than the standard steel plate. Both the modified and extended versions of the LSGT were developed to satisfy that need; they are described and their test results compared to those of the standard test.

The strong correlation between the SSGT and LSGT results for charges of 10% or greater porosity is documented. Wedge test results and shock-to-detonation transition studies on cylindrical charges of cast DINA showed strong similarities. It appears that the standard LSGT values lie on the low pressure end of the curve, reciprocal run length vs pressure defined by the wedge test data, whereas results from unconfined charges (non-standard test) do not.

Detonability measurements, particularly  $d_c$  values obtained at NOL have been compiled in Appendix D. Those data have been used to show that there is no general relationship between  $d_c$  and  $P_g$  from explosive to explosive.

# X. REFERENCES

- (1) E. A. Eyster, L. C. Smith, and S. R. Walton, "The Sensitivity of High Explosives to Pure Shocks", NOLM 10,336, 14 Jul 1949
- (2) I. Jaffe, A. R. Clairmont, Jr., and D. Price, "Large Scale Shock Sensitivity Test. Compilation of NOL Data for Propellants and Explosives", NOLTR 61-4, 15 May 1961 and NOLTR 65-177, 15 Nov 1965; NOLTR 65-177 supersedes NOLTR 61-4.
- (3) A. B. Amster, R. L. Beauregard, G. J. Bryan, and E. K. Lawrence, "Detonability of Solid Propellants. I. Test Methods and Instrumentation," NAVORD 5788, 3 Feb 1958
- (4) I. Jaffe, R. L. Beauregard and A. B. Amster, "The Attenuation of Shock in Lucite", NAVORD 6876, 27 May 1960. Also ARS Journal 32, 22-25 (1962)
- (5) G. D. Edwards and T. K. Rice, "Liquid Monopropellants; Detonation Sensitivity", NavOrd 2884, 25 Oct 1953
- (6) T. P. Liddiard, Jr. and D. Price, "Recalibration of the Standard Gap Test", NOLTR 65-43, 20 Aug 1965
- (7) J. O. Erkman, D. J. Edwards, A. R. Clairmont, Jr., and D. Price, "Calibration of the NOL Large Scale Gap Test; Hugoniot Data for Polymethyl Methacrylate", NOLTR 73-15, 4 Apr 1973
- (8) N. L. Coleburn and T. P. Liddiard, Jr., "Hugoniot Equations of State of Several Unreacted Explosives", J. Chem Phys. 44 (5), 1929 (1966)
- (9) V. M. Boyle, R. L. Jameson, and M. Sutanoff, "Determination of Shock Hugoniots for Several Condensed Phase Explosives", Fourth Symposium (International) on Detonation, ACR-126 (ONR), U.S. Gov. Print. Office, Washington, 1967; p 241
- (10) V. M. Boyle, W. G. Smothers, and L. H. Ervin, "The Shock Hugoniot of Unreacted Explosives", Fifth Symposium (International) on Detonation, ACR-184 (ONR), U.S. Gov. Print. Office, Washington, 1972; p 251
- (11) D. Price and I. Jaffe, "Large Scale Gap Test: Interpretation of Results for Propellants", ARS Journal 31, 595 (1961)
- (12) J. O. Erkman, "Porosity and the Sensitivity of TNT to Shock", section of an NOLTR now in preparation.
- (13) D. Price, I. Jaffe, and G. E. Roberson, "Shock Sensitivity of Solid Explosives and Propellants", Ind. Chim. Belge 1967, 32 (Spec. No.), 506
- (14) J. Roth, "Shock Sensitivity and Shock Hugoniots of High Density Granular Explosives", Fifth Symposium (International) on Detonation, ACR-184 (ONR), U.S. Gov. Print. Office, Washington, 1972; p 219
- (15) B. D. Trott, "Effect of Cryogenic Temperatures on the Performance of Selected Explosives", NAVEODFAC TR-144, Aug 1972

NOLTR 74-40

- (16) R. W. Van Dolah, C. M. Mason, F. J. P. Perzak, J. E. Hay, and D. R. Forshey, "Explosion Hazards of Ammonium Nitrate under Fire Exposure", RI 6773, Bur. Mines, 1966
- (17) H. Napadensky, "Experimental Studies of the Effects of Impact Loading on Plastic-Bonded Explosive Materials", Final Rept. DASA-1391, Ill. Inst. Tech., Apr 1963
- (18) D. Price and A. R. Clairmont, Jr., "Explosive Behavior of Nitroguanidine", Twelfth Symposium (International) on Combustion, The Combustion Institute, Pittsburgh, 1969; p 761. See also NOLTR 67-169
- (19) L. B. Seely, "A Proposed Mechanism for Shock Initiation of Low Density Granular Explosives", Proc. Fourth Elec. Initiation Symposium, Franklin Institute, Phila. 1963; Paper 27 of Rept EIS-A 2357
- (20) D. Price, "Shock Sensitivity, A Property of Many Aspects", Fifth Symposium (International) on Detonation, ACR-184 (ONR), U.S. Gov. Print. Office, Washington, 1972; p 207. See also NOLTR 70-73
- (21) I. Jaffe, J. Toscano, and D. Price, "Behavior of Plexiglas under Shock Loading by a Tetryl Donor", NOLTR 64-66, 2 Jul 1964
- (22) I. Jaffe and A. R. Clairmont, Jr., "The Effects of Configuration and Confinement on Booster Characteristics", NOLTR 65-33, 13 Apr 1965
- (23) H. D. Jones, "Calculations of Induced Pressures in LE-3", Internal Memorandum, 19 Dec. 1972.
- (24) D. Price and I. Jaffe, "Safety Information from Propellant Studies", AIAA Journal 1, 299 (1963)
- (25) D. Price, A. R. Clairmont, Jr., and I. Jaffe, "Explosive Behavior of Ammonium Perchlorate", Combust. Flame 11, 415 (1967)
- (26) I. Kabik and S. J. Jacobs, Memo to 233 on PBXW-100 Booster Sensitivity Tests for Mk 46 Warhead, 6 Feb 1970
- (27) D. Price, Appendix A, "Some Properties of Various Steel Witness Plates", NOLTR 62-41, 20 Mar 1962
- (28) D. Price and F. J. Petrone, "Detonation Initiated by High-Pressure Gas Loading of a Solid Explosive", J. Appl. Phys., 35, 710 (1964)
- (29) D. Price and T. P. Liddiard, Jr., "The Small Scale Gap Test: Calibration and Comparison with the Large Scale Gap Test", NOLTR 66-87, 7 Jul 1966
- (30) D. Price, "Large Scale Gap Test: Interpretation of Results for Propellants", NAVWEP 7401, 15 Mar 1961
- (31) J. M. Majowicz and S. J. Jacobs, Tenth Annual Meeting of Division of Fluid Dynamics of American Physical Society, Nov 1957. (See also NAVORD 5710)
- (32) N. L. Coleburn, B. E. Drimmer, and T. P. Liddiard, Jr., "The Detonation Properties of DATB", NAVORD 6750, 12 Oct 1960
- (33) A. W. Campbell, W. C. Davis, J. B. Ramsay, and J. R. Travis, "Shock Initiation of Solid Explosives", Phys. Fluids 4 (4), 511 (1961)

- (34) S. J. Jacobs, T. P. Liddiard, Jr., and B. E. Drimmer, "The Shock-to-Detonation Transition in Solid Explosives", Ninth International Symposium on Combustion, Academic Press, New York, 1963; p 517
- (35) J. B. Ramsay and A. Popolato, "Analysis of Shock Wave and Initiation Data for Solid Explosives", Fourth Symposium (International) on Detonation, ACR-126 (ONR), U.S. Gov. Print. Office, Washington, (1967); p 233
- (36) I. Jaffe, R. L. Beauregard, and A. B. Amster, "The Attenuation of Shock in Lucite", NAVORD 6876, 27 May 1960
- (37) V. S. Ilyukhin, P. F. Pokhil, O. K. Rozanov and N. V. Shvedova, "Measurement of the Shock Adiabats of Cast Trinitrotoluene, Crystalline Hexogene and Nitromethane", Soviet Phys. Dokl. 5, 337 (1960)
- (38) D. Price, J. P. Toscano and I. Jaffe, "Development of the Continuous Wire Method. III. Measurements in Cast DINA", NOLTR 67-10, 20 Apr 1967
- (39) L. N. Cosner and R. G. Sewell, "Initiation of Explosives through Metal Barriers", NAVWEPS Rept 8507, China Lake, Cal., Apr 1964. (This report gives data obtained in 1956. In addition to these data, additional data were supplied by Cosner in 1962)
- (40) A. Popolato, "Experimental Techniques Used in LASL to Evaluate Sensitivity of High Explosives", Proceedings of the International Conference on Sensitivity and Hazards of Explosives, London, 1963. Also private communication.
- (41) F. E. Walker and R. J. Wasley, "Critical Energy for Shock Initiation of Heterogeneous Explosives", Explosivstoffe 1969, 17(1), 9
- (42) T. P. Liddiard, "The Initiation of Burning in High Explosives by Shock Waves", Fourth Symposium (International) on Detonation ONR ACR-126, U.S. Gov Print. Office, Washington (1967); p 487
- (43) D. Price, "Contrasting Patterns in the Behavior of High Explosives", Eleventh Symposium (International) on Combustion, The Combustion Institute, Pittsburgh (1967); pp 693-701
- (44) I. Jaffe and D. Price, "Determination of the Critical Diameter of Explosive Materials", ARS Journal, 32, 1060 (1962)
- (45) L. A. Roslund and N. L. Coleburn, "Hydrodynamic Behavior and Equation of State of Detonation Products Below the Chapman-Jouguet State", Fifth Symposium (International) on Detonation, ONR Rept ACR 184, U.S. Gov. Print. Office, Washington, D.C. (1972); p 523
- (46) N. L. Coleburn and B. E. Drimmer, "Explosive Properties of the Amino-Substituted, Symmetrical Trinitrobenzene", NOLTR 63-81, May 1963
- (47) M. F. Murphy and N. L. Coleburn, "A Preliminary Evaluation of Tacot, A New Heat Resistant Explosive", NOLTR 61-155, 14 Nov 1961
- (48) D. Price, A. R. Clairmont, Jr., and J. O. Erkman, "Explosive Behavior of Aluminized Ammonium Perchlorate", Combust. Flame 20, 389 (1973). See also NOLTR 72-15

- (49) A. F. Belyaev and M. K. Sukoyan, "Detonability of Some Explosives with Increase in External Pressure", Combustion, Explosion and Shock Waves, 3 (1), 11 (1967)
- (50) D. Price, J. O. Erkman, A. R. Clairmont, Jr., and D. J. Edwards, "Explosive Characterization of Dinitrotoluene", Combustion and Flame 14, 145 (1970). See also NOLTR 69-92
- (51) V. A. Gor'kov and R. K. Kurbangalina, "Concerning the Detonation Ability of Ammonium Perchlorate", Combustion, Explosion, and Shock Waves 2 (2), 12 (1966)
- (52) D. Price, A. R. Clairmont, Jr., and J. O. Erkman, "Explosive Behavior of a Simple Composite Propellant Model", Combustion and Flame 17, 323 (1971)
- (53) P. B. Dempster, "The Effect of Inert Components in the Detonation of Gelatinous Explosives", Discussions Faraday Soc. 22, 196 (1956)
- (54) A. Ya. Apin and L. N. Stesik, "On the Mechanism of the Chemical Reaction at the Detonation of Compact Explosives", Zh. prikl mekh tekhn fiz No. 2, 146 (1965). Translation by J. O. Mulhaus
- (55) R. R. Elwell, O. R. Irwin and R. W. Vail, Jr. Project SOPHY-Solid Propellant Hazards Program AFRPL-TR-67-211 Vol II, App. I, Aug 1967
- (56) A. S. Derzhavets, "Increased Susceptibility of Explosives to a Detonation Impulse." Termostoikie Vzryvchatye Veshchestva Ikh Deistvie Glubokikh Skvazhinakh 1969, 37 Edited by F. A. Baum, Izd. "Nedra": Moscow; USSR. Only C. A. abstract available



APPENDIX A

Glossary

EMV	electromagnetic velocity
HE	high explosive
LSGT	large scale gap test
LVD	low velocity "detonation"
PMMA	polymethyl methacrylate
SSGT	small scale gap test
TMD	theoretical maximum density
c	sound velocity
d	diameter
$d_e$	effective diameter
$d_c$	critical diameter
D	detonation velocity
$h_{cr}^-$	critical height of slab of HE on a lead plate (48)
l	charge length
P	pressure
$P_g$	50% point pressure in PMMA in LSGT
$P_i$	initiating or critical pressure in HE; pressure transmitted to HE at 50% point in LSGT.
t	temperature ( $^{\circ}\text{C}$ )
$t_c$	critical temperature
u	particle velocity

NOLTR 74-40

$u_{fs}$	free surface velocity
$U$	shock velocity
$x$	coordinate along longitudinal axis
$x_s$	run length
$\delta$	particle size, particle diameter
$\rho_o$	charge loading density
$\rho_v$	voidless density
$\rho_o/\rho_v$	relative density
$100 \rho_o/\rho_v$	%TMD
$(1 - \rho_o/\rho_v)$	porosity, fraction of voids
$100(1 - \rho_o/\rho_v)$	% voids, % porosity
$\tau_s$	delay time
$\Delta$	excess delay time

APPENDIX B  
DENSITY OF EXPLOSIVE COMPONENTS  
DENSITY VALUES USED IN COMPUTING TMD'S OF MIXTURES

SYMBOL	NAMES OF PURE COMPOUNDS USED IN COMPOSITIONS	TMD (G/CC)
AN	AMMONIUM NITRATE	1.725
AL	ALUMINUM	2.699
AP	AMMONIUM PERCHLORATE	1.95
BA(NO <sub>3</sub> ) <sub>2</sub>	BARIUM NITRATE	3.24
BRL 2741	CURED PHENOLIC RESIN	*1.30
BTNEC	BIS(2,2,2-TRINITROETHYL) CARBONATE	1.88
C	GRAPHITE	2.25
CA STEARATE	CALCIUM STEARATE	1.04
CARNAUBA WAX		1.00
COMP D-2	GRADE A DENSITIZING WAX/LECITHIN/NC 12% N (84/2/14)	1.02
DATB	1,3-DIAMINO-2,4,6-TRINITROBENZENE	1.837
DINA	DI(2-NITROXYETHYL)NITRAMINE	1.67
DNB	M-DINITROBENZENE	1.566
DNT	2,4-DINITROTOLUENE	1.521
EDNA	ETHYLENE DINITRAMINE	1.71
EXPLOSIVE D	AMMONIUM PICRATE	1.72
HAP	HYDROXYLAMINE PERCHLORATE	2.06
HMX	CYCLOTETRAMETHYLENETETRANITRAMINE	1.903
KN	POTASSIUM NITRATE	2.109
LECITHIN	WETTING AGENT	1.04
LPT	LITHIUM PERCHLORATE TRIHYDRATE	1.841
NACL	SODIUM CHLORIDE	2.165
NC	NITROCELLULOSE (12 - 13.4% N)	1.58
NQ	NITROGUANIDINE	1.78
PETN	PENTAERYTHRITOL TETRANITRATE	1.78
PIB	POLYISOBUTYLENE (VISTANEX LM-MH 2620, ENJAY CO., N.Y.)	*0.835
RDX	CYCLOTRIMETHYLENETRINITRAMINE	1.802
TATB	1,3,5-TRIAMINO-2,4,6-TRINITROBENZENE	1.938
TCEP	TRICHLOROETHYL PHOSPHATE	1.45
TETRYL	2,4,6-TRINITROPHENYLMETHYLNITRAMINE	1.73
TNETB	2,2,2-TRINITROETHYL-4,4,4-TRINITROBUTYRATE	1.78
TNT	2,4,6-TRINITROTOLUENE	1.654
VITON	VITON A	1.85
WAX	MICROCRYSTALLINE WAX	0.95
ZYTEL	ZYTEL 63 (NYLON)	1.12

\*TMD COMPUTED BACKWARDS FROM EXPERIMENTAL TMD OF COMPOSITION

APPENDIX C

Compilation of LSGT Results

Note: All experimental densities were measured to four places although the fourth digit is not considered significant. For this reason as well as the fact that densities of some of the components\* are given to only three places, the density in the following tabulation is listed to only three figures. However, the initial measurement (four figures) was used in computing %TMD of the material and its mixtures\*. Differences caused by round-off sometimes introduce small discrepancies between the 3-figured  $\rho_0$  and the listed %TMD. When it is important to resolve such differences, the test number can be used to find the original data recorded in the shot notebook.

\*All component densities in computing densities of mixtures are listed in Appendix B.

# APPENDIX C

NOLTR 74-40

TEST	MATERIAL	DENSITY+ G/CC	STND KBAR	505 POINT++ CARDS	905 KBAR	PART. SIZE LOT NOS. MICRONS (NOL)	R E H A R K S	TEST
597 AN	(AMMONIUM NITRATE PRILLS)	0.86P	49.6	53	E	77	NO DETONATION. SEE NOLTR 67-112, DLT (DOUBLE LENGTH TUBE) X	597
603 AN		1.08P	62.4	35	E	90	NO DETONATION. SEE NOLTR 67-112	603
619 AN		1.13M	65.3	31	E	94	NO DETONATION. SEE NOLTR 67-112	619
615 AN		1.20M	69.6	1.1	E	175	NO DETONATION. SEE NOLTR 67-112	615
146	ANATOL (AN/TNT 60/40)	C		162		(31)	AMBIENT TEMPERATURE	146
758 AP	(AMMONIUM PERCHLORATE)	0.80P	41.0	202	M	20	ONLY 5 SHOTS	758
745 AP		1.07M	55.0	180	E	25		745
750 AP		1.07M	55.1	182	M	24		750
753 AP		1.271	65.1	168		29		753
752 AP		1.271	65.1	167.81	M	29		752
744 AP		1.271	65.2	162	E	31		744
746 AP		1.461	74.7	120		48		746
759 AP		1.461	75.1	113.51	M	51		759
768 AP		1.541	80.1	80	E	63		768
769 AP		1.541	80.3	76.2	M	65		769
767 AP		1.571	80.4	71.21		67		767
751 AP		1.601	82.2	Q			DAMAGE TO WITNESS PLATE	751
856 AP		1.17M	60.0	174	M	28		856
852 AP		1.51M	67.0	171		29		852
854 AP		1.43M	73.4	135		45		854
853 AP		1.56M	80.1	87		62		853
628 AP		1.251	64.1	178	E	26		628
693 AP		1.571	80.6	80		63		693
678 AP		1.321	70.7	150		36		678
690 AP		1.521	77.9	90.2		59		690
335A AP		0.75P	38.6	Q			MICROMILLED TO REDUCE PARTICLE SIZE, DAMAGE TO WITNESS PLATE	335A
656 AP		1.11M	56.9	198		20		656
631 AP		1.25M	64.2	178		26		631
633 AP		1.25M	64.4	178		28		633
637 AP		1.491	78.4	143		40		637
606 AP		1.501	76.7	143	E	40		606
635 AP		1.521	77.7	131		45		635
642 AP		1.581	81.1	98.21	E	56		642
658 AP		1.581	81.1	93		58		658
625 AP		1.601	81.9	98	E	56		625
634 AP		1.651	84.4	33	E	92		634
614 AP		1.671	85.5	32	E	93		614
335 AP		1.23P	63.0	Q			NON DETONATING, SEE NOLTR 67-112	335
646 AP		1.29P	66.0	153.21	E	35		646
648 AP		1.43M	73.2	98	E	56		648
334 AP		1.46M	75.0	Q			NON DETONATING, SEE NOLTR 67-112	334
645 AP		1.58M	80.3	74	E	66		645
346 AP		1.631	83.5	Q			NON DETONATING, SEE NOLTR 67-112	346
347 AP		1.691	96.7	X			NON DETONATING, SEE NOLTR 67-112	347

+ C = CAST, I = ISOSTATIC PRESS, M = HYDRAULIC PRESS, P = PACKED BY HAND  
 ++ AT Q CARD GAP X, G, AND Q INDICATE NO GO, GO, AND QUESTIONABLE  
 (X = FLAT PLATE, G = HOLE IN PLATE, AND Q = PLATE DAMAGE BUT NO HOLE)  
 \* TYPE OF TEST - REGULAR UNLESS LISTED AS E (EXTENDED) OR M (MODIFIED).  
 \*\* ALL CHARGES ARE CONDITIONED AND FIRED AT 25 DEG C EXCEPT WHERE NOTED.  
 PENTOLITE BOOSTERS REPLACED TETRYL BEGINNING WITH SHOT 770.

## APPENDIX C

TEST	MATERIAL	DENSITY, G/CC	50% POINT+ CARDS	50% POINT+ KBAR	PART, SIZE LOT NOS. MICRONS (MOL)	R E M A R K S **	TEST			
857	AP/AL-95/5	1.19H	60.0	176	M	28	8/7	145/HSD	SEE NOLTR 2-15 FOR AN ATYPICAL SERIES	857
848	AP/AL-95/5	1.32H	67.0	159		34	8/7	145/HSD		848
855	AP/AL-95/5	1.43H	72.4	137		45	8/7	145/HSD		855
849	AP/AL-95/5	1.59H	80.3	101		57	8/7	145/HSD		849
858	AP/AL-90/10	1.35H	67.1	158		35	8/7	145/HSD		858
732	AP/HML-80/20	1.56I	80.4	240±2		14	25/14	127/586		732
626	AP/MAX-90/10	1.08P	60.7	240		14	25/125	126/134		626
629	AP/MAX-90/10	1.32I	74.3	225±2		16	25/125	126/134		629
653	AP/MAX-90/10	1.34H	75.1	128		15	25/125	126/134		653
613	AP/MAX-90/10	1.52I	85.4	186		23	25/125	126/134		613
618	AP/MAX-90/10	1.60I	89.8	118±7	E	49	25/125	126/134	DENT IN PLATE AT 0 CARDS USING REGULAR TEST PROBABLY NO DETONATION. SEE NOLTR 49-16	618
632	AP/MAX-90/10	1.63I	91.8	59	E	73	25/125	126/134	SEE NOLTR 69-16	632
632U	AP/MAX-90/10	1.67I	93.8	X	E	20	200/125	126/134		632U
652	AP/MAX-90/10	1.42H	79.5	199	E	26	200/125	119/134	GO AT 0 GAP USING DLT (DOUBLE LENGTH TUBE)	652
651	AP/MAX-90/10	1.53H	85.5	175	E	26	200/125	119/134		651
668	AP/MAX-80/20	1.00P	61.2	236		14	25/125	126/134	NO. 6 DETONATOR WILL INITIATE CHARGE WITHOUT BOOSTER 0 GAP	668
669	AP/MAX-80/20	1.23H	75.0	236		14	25/125	126/134	NO. 6 DETONATOR WILL INITIATE CHARGE WITHOUT BOOSTER 0 GAP	669
670	AP/MAX-80/20	1.39H	84.7	213		17	25/125	126/134	NO. 6 DETONATOR WILL NOT INITIATE CHARGE WITHOUT BOOSTER 0 GAP	670
672	AP/MAX-80/20	1.48I	90.0	194	E	21	25/125	126/134		672
672U	AP/MAX-80/20	1.50I	91.5	178	E	26	25/125	126/134	SEE NOLTR 69-16	672U
676	AP/MAX-80/20	1.57I	95.6	X	E		25/125	126/134		676
773	AP/MAX/HMX-70/20/10	1.60I	97.8	157		35	22/125/14	142/134/586-2		773
762	AP/MAX/HMX-74/20/6	1.59I	97.0	144±1		39	22/125/14	142/134/586-1		762
787	AP/MAX/HMX-74/20/6	1.62I	98.8	130±5		47	22/125/14	142/134/586-2		787
765	AP/MAX/HMX-74/20/6	1.62I	99.0	122±3		48	22/125/14	142/134/586-2		765
766	AP/MAX/HMX-74/20/6	1.63I	99.6	106±2		53	22/125/14	142/134/586-2		766
797	AP/MAX/HMX-74/20/6	1.62I	99.0	G			22/125/14	142/134/586	2 SHOTS AT 0 GAP-FINE MMX (CLASS E)	797
795	AP/MAX/HMX-74/20/6	1.62I	99.1	K			22/125/640	142/134/585	2 SHOTS AT 0 GAP-COURSE MMX (CLASS D)	795
796	AP/MAX/HMX-74/20/6	1.62I	99.3	Q			22/125/MED.	142/134/689	2 SHOTS AT 0 GAP-MEDIUM MMX (CLASS A)-PLATE DAMAGE	796
148	BAROTOL BA10312/TNT/NC-73/27.1	C	11.8	(149)				AMBIENT TEMPERATURE		148
534	CH-6 (RDX/CALCIUM STEARATE/	1.45I	81.6	314		8		445		534
535	GRAPHITE/POLYISOBUTYLENE,	1.57I	88.0	308		8		445		535
533	97.5/1.5/0.5/0.5)	1.70I	95.8	267		11		445		533
140	COMP A-3 (RDX/MAX-91/9)	1.59H	92.4	210	(118)			72	AMBIENT TEMPERATURE	140
774	COMP A-3 (RDX/MAX-91/9)	1.45I	86.5	226±1		16		719	PRODUCTION LOT-FRECKLED APPEARANCE	774
775	COMP A-3 (RDX/MAX-91/9)	1.50I	89.9	230		15		719		775
776	COMP A-3 (RDX/MAX-91/9)	1.55I	92.8	240		14		719		776
777	COMP A-3 (RDX/MAX-91/9)	1.61I	96.2	242		14		719		777
778	COMP A-3 (RDX/MAX-91/9)	1.65I	98.7	228		15		719		778
805	COMP A-3 (RDX/MAX-91/9)	1.68I	99.8	253±2		12		719	NOS MIX-RDX SIZE GRADED TO GIVE HI DENSITY	805

\* C = CAST, I = ISOSTATIC PRESS, H = HYDRAULIC PRESS, P = PACKED BY HAND

\* TYPE OF TEST - REGULAR UNLESS LISTED AS E (EXTENDED) OR M (MODIFIED).

\*\* AT 0 CARD GAP X, G, AND Q INDICATE NO GO, GO, AND QUESTIONABLE

\*\* ALL CHARGES ARE CONDITIONED AND FIRED AT 25 DEG C EXCEPT WHERE NOTED.

(X = FLAT PLATE, G = HOLE IN PLATE, AND Q = PLATE DAMAGE BUT NO HOLE)

PENTOLITE BOOSTERS REPLACED TETRYL BEGINNING WITH SHOT 770.

## APPENDIX C

TEST	MATERIAL	DENSITY, G/CC	50% POINT CARDS	50% POINT KBAR	PART. SIZE LOT NOS. MICRONS (NOL)	REMARKS	TEST
309	COMP B (RDX/TNT/MAX,60/40/1)	1.661	96.5	238	(14)	CAST-GROUND, THEN PRESSED ISOSTATICALLY	309
358	COMP B (RDX/TNT/MAX,60/40/1)	1.70C	98.8	201	(20)	50 SHOTS IN SERIES	358
389	COMP B (RDX/TNT/MAX,60/40/1)	1.69C	98.2	207	18	CAST PENTOLITE WITNESS	389
390	COMP B (RDX/TNT/MAX,60/40/1)	1.69C	98.5	212	E 18	CAST PENTOLITE WITNESS	390
763	COMP B (RDX/TNT/MAX,60/40/1)	1.70C	98.7	220	16	STORED FOR 2 YEARS IN MAGAZINE	763
760	COMP B (RDX/TNT/MAX,60/40/1)	1.70C	98.7	217	E 17	STORED FOR 2 YEARS IN MAGAZINE	760
761	COMP B (RDX/TNT/MAX,60/40/1)	1.70C	98.7	218	M 17	STORED FOR 2 YEARS IN MAGAZINE	761
510	COMP B (RDX/TNT/MAX,60/40/1)	1.71C	99.4	135	44	UNCONFINED CHARGE	510
544	COMP B (RDX/TNT/MAX,60/40/1)	1.71C	99.4	145	39	UNCONFINED (CAST IN 5 CM MOLD, THEN MACHINED TO 3.6 CM DIAM)	544
847	COMP B/MAX, 100/4	1.65C	98.2	177	27	SPECIAL DESENSITIZED NOS MIX (RDX/TNT/MAX,60/40/5)	847
438	COMP B-3 (RDX/TNT,60/40)	1.71C	98.6	209	18		438
575	COMP C-3 (RDX/HE PLASTICIZER, 77/23)	1.60C	186	23			575
437	COMP C-4 (RDX/PLASTICIZER, 91/9)	1.41P	88.8	214	17	CONTAINS POLYISOBUTYLENE 2.1%, MOTOR OIL 1% AND	437
574	COMP C-4 (RDX/PLASTICIZER, 91/9)	1.56P	98.4	192	22	DI-(2-ETHYLHEXYL) SEBACATE 5.3%	574
257	CYCLOTOL (RDX/TNT, 75/25)	C	182	(24)		AMBIENT TEMPERATURE	257
389	CYCLOTOL (RDX/TNT, 75/25)	1.701	96.4	253	(12)		389
541	DATB	1.211	65.8	162	31	FROM HOLSTON ORDNANCE WORKS	541
539	DATB	1.441	78.1	151	36		539
540	DATB	1.701	92.5	132	45	BALL MILLED, FROM PICATINNY ARSENAL	540
326	DATB	1.711	92.9	135	(44)		326
770	DATB	1.671	90.7	139	44	0.37 G/CC BULK DENSITY, FROM HOLSTON ORD WORKS	770
772	DATB	1.671	90.9	140	M 44		772
771	DATB	1.671	91.0	139	E 44		771
346	DATB	1.671	91.1	138	(42)		346
255	DATB/BRL 2741, 95/5	1.76H	97.6	120	(48)	32 DEG C, CHARGES CONTAINED SMALL IMPERFECTIONS	255
256	DATB/BRL 2741, 95/5	1.76H	97.6	119	(49)	66 DEG C, CHARGES CONTAINED SMALL IMPERFECTIONS	256
331	DATB/ZYTEL 65, 95/5	1.691	95.1	129	(46)		331
845	DESTEX (TNT/AL/MAX/C/LEC/TIN)	1.61C	93.1	116.2	51	6 SHOT SERIES, FOR V-RINGBLOOM	845
846	DESTEX 74.68/18.68/4.68/1.89/.07	1.62C	93.6	107	54	6 SHOT SERIES, FOR V-RINGBLOOM	846
275	DINA	C	330	(17)		AMBIENT TEMPERATURE, CREAM CAST	275
556A	DINA	1.60C	95.8	279	10	CHARGE CONTAINED CONTINUOUS RESISTANCE WIRES, DATA IN TR-67-10	556A
556	DINA	1.60C	95.8	226	16	UNCONFINED CHARGE, SAME VALUE FOUND WITH WIRES, SEE TR-67-10	556

\* C = CAST, I = ISOSTATIC PRESS, H = HYDRAULIC PRESS, P = PACKED BY HAND  
 \*\* AT 0 CARD GAP X, G AND Q INDICATE NO GO, GO, AND QUESTIONABLE  
 (K = FLAT PLATE, G = HOLE IN PLATE, AND O = PLATE DAMAGE BUT NO HOLE)

\* TYPE OF TEST - REGULAR UNLESS LISTED AS E (EXTENDED) OR M (MODIFIED).  
 \*\* ALL CHARGES ARE CONDITIONED AND FIRED AT 25 DEG C EXCEPT WHERE NOTED.  
 PENTOLITE BOOSTERS REPLACED TETRYL BEGINNING WITH SHOT 770.

# APPENDIX C

TEST	MATERIAL	DENSITY G/CC	STMD KBAR	50% POINT CARDS	POINT KBAR	PART. SIZE LOT NOS. MICRONS (NOL)	R E M A R K S **	TEST
813 DMB		1.51C	96.4	32	95		CREAM CAST, FOR L-STARR	813
814 DMB	RDH/MAX-60/40/1	1.61C	96.3	156	36		CREAM CAST, FOR L-STARR	814
661A DNT		0.71P	46.5	192±2	E	22	GO AT 0 GAP DLT EXTENDED (DLT = DOUBLE LENGTH TUBE)	661A
665 DNT		1.00H	85.7	181	E	25		665
665A DNT		1.501	98.9	24	103	150	2 DLT EXTENDED TESTS FAILED AT 0 GAP	665A
664 DNT		1.45C	95.5	12	E	128		664
695 DNT		1.10H	72.3	143±1	40	350	PROBABLY NOT DETONATING (SEE NOLTR 69-92)	695
696 DNT		1.20H	79.1	144	39	350		696
697 DNT		1.27H	83.6	137	43	350		697
709 DNT		1.40H	91.8	115	50	350	23 DEG C	709
712 DNT		1.451	98.1	85±2	61	350	23 DEG C	712
333 EDNA		1.551	90.7	250	(13)	14		333
516 EPM-2 (97.5% HMX)		1.721	92.4	232	15		HMX ANALOG OF CH-6	516
139 EXPLOSIVE D		1.59H	92.6	150	(36)	185	AMBIENT TEMPERATURE	139
783 EXPLOSIVE D		1.55H	78.7	177	27	720	PRODUCTION LOT	783
781 EXPLOSIVE D		1.46H	84.6	171	30	720	PRODUCTION LOT	781
775 EXPLOSIVE D		1.53H	89.0	163	31	720	SAMPLE FROM YORKTOWN, FIRED FOR M.HELLER	775
779 EXPLOSIVE D		1.55H	90.0	169	30	720	PRODUCTION LOT	779
782 EXPLOSIVE D		1.60H	93.2	160	34	720	PRODUCTION LOT	782
780 EXPLOSIVE D		1.64H	95.1	156	36	720	PRODUCTION LOT	780
313 H-6 (RDH/TNT/AL/MAX-47/31/22/5)		1.761	97.6	197	(20)		LOT 279 COMP B USED TO MAKE H-6	313
311 H-6 (RDH/TNT/AL/MAX-47/31/22/5)		1.75C	97.3	166	(30)		LOT 279 COMP B USED TO MAKE H-6	311
593 HAP		0.97P	47.1	363±1	E	6	DENSITY 0.93-1.0 G/CC, SIEVED THRU NO. 16 SCREEN	593
144 HMX-1 (RDH/TNT/AL/MAX-40/38/17/5)		C		154	(34)		AMBIENT TEMPERATURE, MADE FROM LOT 268 COMP B AND LOT 203 TNT	144
296 HMX-3 (RDH/TNT/AL/MAX-31/29/35/5)		1.85C	97.9	161	(41)			296
557 HP-61 (NITROCARBONITRATE)		0.8P		D			PLATE DAMAGES, CONTAINS AN-COAL-OIL, MANUFACTURED BY HERCULES POWDER CO	557
558 HP-61 (NITROCARBONITRATE)		0.8P		121	E	48	CONTAINS AN-COAL, AND OIL, MANUFACTURED BY HERCULES POWDER CO	558
401 HYDROGEN PEROXIDE/WATER-98/2		1.438		35	90		LIQUID TESTED AT 13 DEG C	401
627 LITHANOL (LPT/AL-69/31)		1.25P	61.2	176	E	26	YORKTOWN, LPT DENOTES LITHIUM PERCHLORATE TRIHYDRATE	627
684 LITHANOL		1.25P	61.2	145±7	39		OLD BATCH	684
684A LITHANOL		1.32P	64.4	66±3	E	70	OLD BATCH	684A
683 LITHANOL		1.25P	61.2	55±2	76		NEW BATCH, SMALLER PARTICLE SIZE	683
682A LITHANOL		1.31P	64.2	X	E		NEW BATCH, SMALLER PARTICLE SIZE, DLT (DOUBLE LENGTH TUBE)	682A

\* C = CAST, I = ISOSTATIC PRESS, H = HYDRAULIC PRESS, P = PACKED BY HAND  
 \*\* AT 0 CARD GAP X, G, AND D INDICATE NO GO, GO, AND QUESTIONABLE  
 (X = FLAT PLATE, G = HOLE IN PLATE, AND Q = PLATE DAMAGE BUT NO HOLE)

\* TYPE OF TEST - REGULAR UNLESS LISTED AS E (EXTENDED) OR M (MODIFIED).  
 \*\* ALL CHARGES ARE CONDITIONED AND FIRED AT 25 DEG C EXCEPT WHERE NOTED.  
 PENTOLITE BOOSTERS REPLACED TETRYL BEGINNING WITH SHOT 770.

NOLTR 74-40



## APPENDIX C

TEST	MATERIAL	DENSITY G/CC	DE POINT CARDS	DE POINT CARDS	PART. SIZE LOT NOS. MICRONS	REMARKS	TEST
432	LK-030-N (HMX/DATB/VITON-70/20/10)1.83H	98.6	188	23			432
434	LX-040-0 (HMX/VITON-85/15)	1.85H	98.0	165	30		434
706	MINOL II (AN/TMT/AL+0/40/20)	1.59C	87.5	151	36	0.4% WATER ADDED, 23 DEG C, FOR D-RICH	706
704	MINOL II	1.64C	90.1	149.1	37	0.2% WATER ADDED, 23 DEG C, FOR D-RICH	704
705	MINOL II	1.67C	91.8	183	24	TEMP CYCLED -65F TO 160F FOR 4 DAYS, 23 DEG C, FOR D-RICH	705
718	MINOL II	1.69C	92.7	167	29	70 DEG C, FOR D-RICH	718
719	MINOL II	1.69C	92.9	139	42	25 DEG C, SAME MIX AS TEST 718, FOR D-RICH	719
699	MINOL II	1.70C	93.3	118	49	23 DEG C, STANDARD CASTING, FOR D-RICH	699
710	MINOL II	1.70C	93.5	132	35	23 DEG C, FROM CORNHUSKER MAP, FOR D-RICH	710
701	MINOL II	1.71C	93.7	161	32	60 DEG C, FOR D-RICH	701
707	MINOL II	1.73C	95.3	147	38	23 DEG C, MELTED IN VACUUM, FOR D-RICH	707
323	NC (NITROCELLULOSE)	1.45H	91.8	197	(20)	CONTAINS 12.6% NITROGEN	323
596	NO-L (NITROGUANIDINE, LBD)	0.56P	31.2	216.1	17	CRYSTALS NEEDLE-LIKE AND FREQUENTLY HOLLOW	596
602	NO-L	0.90P	50.6	194	21	LBD DENOTES LOW BULK DENSITY	602
604	NO-L	1.20I	87.4	121	48		604
605	NO-L	1.40I	78.5	84.1	61		605
607	NO-L	1.51I	85.0	60	73		607
594	NO-L	1.63I	91.4	35	90		594
677	NO	1.39I	78.0	109	52	GROUND 589, 50-60% 10 MICRON	677
679	NO	1.44I	81.0	98	56		679
680	NO	1.50I	84.5	81	63		680
317	NO-M (NITROGUANIDINE, HBD)	1.35H	75.9	150	(41)	FROM NPP, DENSITY VARIED FROM 1.33 AND 1.37 G/CC	317
332	NO-M	1.44I	80.9	85	(61)	SCREENED	332
319	NO-M	1.64I	92.1	36	(89)	HBD DENOTES HIGH BULK DENSITY	319
552	NO-M	1.16P	65.1	196	21	FROM NPP	552
524	NO-M	1.35H	74.2	128	46		524
524	NO-M	1.40I	78.9	90-95	58		524
525	NO-M	1.51I	85.1	68	69		525
546	NO-M	1.61I	90.6	47	81		546
518	NO-M	1.64I	92.1	32	93		518
673	NO-M	1.39I	78.0	98	56		673
674	NO-M	1.44I	80.7	80	63		674
681	NO-M	1.44I	80.8	79	64	REPEAT TEST	681
675	NO-M	1.52I	85.4	68	69		675
644	NO-M	1.33I	74.9	128	46		644
617	NO-M	1.39H	77.9	100	55		617
616	NO-M	1.44I	80.7	86	60		616
577	NO-M	1.42I	79.7	94	59	PENTOLITE BOOSTER	577
691	NO/500IUM CHLORIDE-90/10	1.70I	93.6	272.2	99	95/NA 589/NONE DLT WENT AT 25 CARDS	691

\* C = CAST, I = ISOSTATIC PRESS, H = HYDRAULIC PRESS, P = PACKED BY HAND \* TYPE OF TEST - REGULAR UNLESS LISTED AS E (EXTENDED) OR M (MODIFIED).  
 \*\* AT 0 CARD GAP X, G, AND Q INDICATE NO GO, GO, AND QUESTIONABLE. \*\* ALL CHARGES ARE CONDITIONED AND FIRED AT 25 DEG C EXCEPT WHERE NOTED.  
 (X = FLAT PLATE, G = HOLE IN PLATE, AND Q = PLATE DAMAGE BUT NO HOLE) PENTOLITE BOOSTERS REPLACED TETRYL BEGINNING WITH SHOT 770.

## APPENDIX C

TEST	MATERIAL	DENSITY+ G/CC	50% POINT+ KBAR	PART. SIZE LOT NOS. MICRONS (NOL)	R E M A R K S **	TEST
316	OCTOL (HMX/TNT+55/35)	1.78C	98.9 214	(17)	293	316
305	PBX-9404-03 (HMX/NC/TECP+94/3/3)	1.77H	94.9 235	(14)	TECP IS TRICHLOROETHYL PHOSPHATE	305
532	PENTOLITE (PETN/TNT+50/50)	1.64C	95.9 301	9	HEATED TO REDUCE SLURRY VISCOSITY	532
377	PENTOLITE (PETN/TNT+50/50)	1.661	97.1 280	(10)		377
588	PENTOLITE (PETN/TNT+50/50)	1.67C	97.7 284	10		588
591	PENTOLITE (PETN/TNT+50/50)	1.67C	97.7 287	E 10	CAST PENTOLITE WITNESS SAME AS MAIN CHARGE (DLT)	591
529	PENTOLITE (PETN/TNT+50/50)	1.67C	97.7 282	10		529
561	PENTOLITE (PETN/TNT+50/50)	1.67C	97.7 278	10		561
511	PENTOLITE (PETN/TNT+50/50)	1.67C	97.7 273	10		511
509	PENTOLITE (PETN/TNT+50/50)	1.67C	97.7 272	11		509
354	PENTOLITE (PETN/TNT+50/50)	1.68C	98.2 266	(11)	UNCONFINED, 1.5 IN DIAM X 6 IN LONG	354
505	PENTOLITE (PETN/TNT+50/50)	1.68C	98.2 255	12	UNCONFINED	505
512	PETN/TNT+55/45	1.67C	97.1 290	9		512
530	PETN/TNT+55/45	1.67C	97.1 292	9	PETN LOT 321 ADDED TO PENTOLITE LOT 408	530
515	PETN/TNT+60/40	1.59C	91.9 364	6	PETN LOT 321 ADDED TO PENTOLITE LOT 408-CASTING POOR (LCM DENSITY). THIS MAY ACCOUNT FOR HIGH SENSITIVITY	515
142	PICRATOL (EXPLOSIVE D/TNT+52/48)	C	148	(37)	185/203 AMBIENT TEMPERATURE	142
361	RDX	1.531	85.1 336	(7)	FROM HOLSTON	361
359	RDX	1.641	91.0 323	(7)	CLASS B	359
360	RDX	1.641	91.0 284	(10)	CLASS B	360
714	RDX/TNT/AL/MAX+25.6/26.4/45/5	1.85C	94.2 139	42	BARE CHARGE, 1.415 IN DIAMETER	714
698	RDX/TNT/AL/MAX+25.6/26.4/45/5	1.88C	95.3 137±1	43	23 DEG C, FOR PHILLIPS FIRED FOR PHILLIPS	698
799	RDX/MAX+91/9	1.401	83.3 251	13	SPECIAL NOL DRY MIX	799
800	RDX/MAX+91/9	1.501	89.7 243	14	CLASS E/125 659/134	800
798	RDX/MAX+91/9	1.601	95.8 217	17	CLASS E/125 659/134	798
499	TATB	1.821	94.2 78	64	TWO UNCONFINED CHARGES ALSO DETONATED AT 0 AND 25 CARDS	499
537	TETRYL	1.431	82.6 294	9	CHARGES CONTAIN 0.5% GRAPHITE	537
536	TETRYL	1.491	86.0 283	10		536
300	TETRYL	1.62H	93.4 261	(12)		300
538	TETRYL	1.641	94.9 238	14		538
303	TNETB	1.64C	92.6 277	(10)		303
733	TNETB/8TNEC+75/25	1.61C	89.0 350	6	563/HUMMEL POURING TEMP 90 DEG C, MOLD TEMP 65 DEG C, ONLY 6 SHOTS	733

\* C = CAST, T = ISOSTATIC PRESS, H = HYDRAULIC PRESS, P = PACKED BY HAND  
 \*\* AT 0 CARD GAP, G, AND Q INDICATE NO GO, GO, AND QUESTIONABLE  
 (X = FLAT PLATE, G = HOLE IN PLATE, AND Q = PLATE DAMAGE BUT NO HOLE)

\* TYPE OF TEST - REGULAR UNLESS LISTED AS E (EXTENDED) OR M (MODIFIED)  
 \*\* ALL CHARGES ARE CONDITIONED AND FIRED AT 25 DEG C EXCEPT WHERE NOTED.  
 PENTOLITE BOOSTERS REPLACED TETRYL BEGINNING WITH SHOT 770.

## APPENDIX C

TEST	MATERIAL	DENSITY+ G/CC	506 POINT+ CARDS + KBAR	PART. SIZE LOT NOS. MICRONS (HOL)	R E M A R K S **	TEST
550 TNT		1.07P	65.0 262	412		550
551 TNT		1.25H	75.8 239	412		551
792 TNT		1.321	80.2 234	200	COURSE TNT (RETAINED ON 200 MESH SCREEN)	792
793 TNT		1.331	80.4 231	100	FINE TNT (THRU 200 MESH SCREEN)	793
314 TNT		1.33H	80.6 224	277	GRANULAR TNT FROM YORKTOWN	314
521 TNT		1.421	85.6 213	412		521
522 TNT		1.491	90.5 208	412		522
304 TNT		1.581	95.7 193	277	GRANULAR TNT FROM YORKTOWN	304
565 TNT		1.581	95.7 198	517	GRANULAR TNT FROM DUPONT	565
517 TNT		1.601	97.1 183	412		517
545 TNT		1.641	99.0 173	412	WATER HEATED TO 88 DEG C DURING PRESSING. NO EVIDENCE OF MELTING ON SURFACE OF CHARGE. DENSITY VARIED BETWEEN 1.63-1.64	545
498 TNT		1.62C	98.1 124	412		498
526 TNT		1.61C	97.5 124	412	REPACKED-DIFFERENC. FROM TEST ABOVE ATTRIBUTED TO DIFFERENCE IN CASTING OR IN SAMPLE TAKEN FROM DIFFERENT BOX OF THIS LOT	526
544 TNT		1.60C	97.1 162	412		544
520 TNT		1.61C	97.3 133	277	GRANULAR TNT FROM YORKTOWN	520
548 TNT		1.61C	97.3 135	457	FLAKE TNT FROM YORKTOWN	548
542 TNT		1.62C	98.1 73	457	FLAKE TNT FROM YORKTOWN, UNCOMFIRMED	542
531 TNT		1.58C	96.0 145	470	GRANULAR TNT FROM HOLSTON, RECRYSTALLIZED	531
567 TNT		1.59C	96.6 133	517	GRANULAR TNT FROM DUPONT	567
586 TNT		1.62C	98.1 108	517		586
587 TNT		1.62C	98.1 121	517	GRANULAR TNT FROM DUPONT, CAST PENTOLITE WITNESS	587
688 TNT		1.56C	94.8 96	57	STAND CAST, 2 IN DIAM BARE CHARGES, FOR DAHLGREN	688
689 TNT		1.56C	94.8 98	56	STAND CAST, 1-1/2 IN DIAM BARE CHARGES, FOR DAHLGREN	689
686 TNT		1.62C	98.1 38	88	VAC CAST, 2 IN DIAM BARE CHARGES, FOR DAHLGREN	686
687 TNT		1.62C	98.1 47	81	VAC CAST, 1-1/2 IN DIAM BARE CHARGES, DLT 60 0 CARDS, DAHLGREN	687
546 TRITONAL (TNT/AL+95/5)		1.621	96.3 190	517/121	GRANULAR TNT FROM DUPONT	546
576 TRITONAL (TNT/AL+90/10)		1.651	95.6 185	517/121		576
583 TRITONAL (TNT/AL+80/20)		1.721	95.8 181	517/121		583
581 TRITONAL (TNT/AL+70/30)		1.791	95.7 168	29		581
585 TRITONAL (TNT/AL+60/40)		1.871	95.6 162	31		585
145 TRITONAL (TNT/AL+80/20)		C	114	203/	AMBIENT TEMPERATURE, FLAKE TNT FROM KEYSTONE ORDNANCE WORKS	145
258 TRITONAL (TNT/AL+90/10)		C	126	277/	AMBIENT TEMPERATURE, GRANULAR TNT FROM YORKTOWN	258
702 TRITONAL (TNT/AL+80/20)		1.72C	96.0 100	55	60 DEG C, FIRED FOR D-RICH	702
703 TRITONAL (TNT/AL+80/20)		1.73C	96.8 101	55	23 DEG C, FIRED FOR D-RICH	703
700 TNT/AL/MAX/GRAPHITE, 80/20/5/2		1.68C	97.0 109	52	23 DEG C, FOR ROGERS AT RWS	700
812 TNT/MAX, 98/2		1.471	90.2 198	21	FIRED FOR B-WHITE	812
811 TNT/MAX, 95/5		1.461	91.5 191	23	FIRED FOR B-WHITE	811
734 TNT/MAX, 95/5		1.58H	97.4 176	26	FROM YORKTOWN, FIRED FOR H-MELLER	734

\* C = CAST, T = ISOSTATIC PRESS, M = HYDRAULIC PRESS, P = PACKED BY HAND  
 \*\* AT 0 CARD GAP X, G, AND Q INDICATE NO GO, GO, AND QUESTIONABLE  
 (X = FLAT PLATE, G = HOLE IN PLATE, AND Q = PLATE DAMAGE BUT NO HOLE)

\* TYPE OF TEST - REGULAR UNLESS LISTED AS E (EXTENDED) OR M (MODIFIED).  
 \*\* ALL CHARGES ARE CONDITIONED AND FIRED AT 25 DEG C EXCEPT WHERE NOTED.  
 PENTOLITE BOOSTERS REPLACED TETRYL BEGINNING WITH SHOT 770.

## APPENDIX D

Summary of NOL Measurements of Critical  
Diameter for Detonation

The critical diameter ( $d_c$ ) for detonation is defined as the minimum diameter of an unconfined cylindrical charge at which steady state detonation can propagate. Because a positive result in the LSGT requires detonation of the test charge, it also requires that the effective diameter of the LSGT (i.e., the equivalent diameter of an unconfined charge) be supercritical. As noted in Section VI C, this effective diameter appears to be about 7.6 cm.

There is a widespread misconception that the critical diameter and the shock insensitivity of a material are directly related. This idea still persists despite the fact, established years ago, that for pressed charges of organic HE,  $d_c$  decreases and  $P_g$  increases with increasing compaction (e.g., reference (43)). It has also been established for granular charges (with gas at 1 atm. in the interstices) that decreasing the initial particle size decreases  $d_c$  but increases the 50% point value of  $P_g$ . To be sure, there seems to be a complicated relationship between  $d_c$  and  $P_g$  for a single material, as follows.

At  $d_c$  the pressure pulse between the von Neumann shock front and the C-J plane is just critical for initiating detonation after a run length equal to the reaction zone length and a total delay time equal to the reaction time (20). In other words, the C-J pressure and reaction time of a charge at its critical diameter would lie at the upper end of the critical curve in the pressure-time plane above which initiation and propagation of detonation can occur and below which detonation must fail. The critical initiating pressure in the LSGT and its duration define a point on the lower end of the same critical curve. We sometimes find that the same explosive will show (1) increasing  $d_c$  with increasing  $P_g$  in one part of the compaction range and (2) increasing  $d_c$  with decreasing  $P_g$  in another part of the range. But, as our accumulated data show, there is no ordering at all of  $d_c$  vs  $P_g$  from explosive to explosive.

Measurements of  $d_c$  at single densities have been collected in Table D-1. Most of these data are from early work in which the importance of particle size was not recognized. Although of restricted

(43) D. Price, "Contrasting Patterns in the Behavior of High Explosives," Eleventh Symposium (International) on Combustion, The Combustion Institute, Pittsburgh (1967); pp 693-701.

Table D-1

## NOL DETERMINATIONS OF CRITICAL DIAMETER AT ONLY ONE DENSITY

Material & Form	$\rho_o$ g/cc	$d_c$ cm	Ref	Gap Test No.	$\rho_o$	50% Point		Pg kbar	Comment
						% TMD	in.x 10 <sup>2</sup> , No. cards		
Cast HE Cyclotol 75/25	*	0.81	44	257	*		182	24	
Cyclotol 60/40	*	0.62	44	438	1.71	98.6	209	18	For B-3; Comp B: 201 cards & 20 kbar
HBX-1	1.72	>0.64	45	144	*		154	34	
HMX/TNT/AL									
56.5/30.4/13.1	*	0.70	44	-			-	-	
TNT	*	2.69	44	520	1.61	97.3	133	44	Typical value for creamed cast TNT
Tritonal 95.2/4.8	*	2.26	44	-			-	-	
Tritonal 80/20	*	1.83	44	145,258	*		120	48	Average of two deter- mination

\* $\rho_o$  not reported; method used underestimates  $d_c$ .

Table D-1 (Cont.)

Material & Form	$\rho_0$ g/cc	% TMD	$d_c$ cm	Ref	Gap Test No.	$\rho_0$	50% Point		Pg No. cards	Comment
							in. x 102,	TMD		
Pressed HE**										
DATB	1.800	97.9	0.53	46	-	1.80	-	97.9	-	53 By extra- polation in Fig. 4
HBX-1	1.72	97.7	~0.6	45	-	-	-	-	-	-
TACOT	1.45	78.8	<0.3	47	-	-	-	-	-	-
TATB	1.802	92.7	1.3	46	499	1.82	78	94.6	78	64
TNA	1.74	98.8	0.3	46	-	-	-	-	-	-
TNB	1.64	97.2	≤0.3	46	-	-	-	-	-	-
7 $\mu$ AP/Al, 90/10	1.42	70.8	2.54	48	858	1.35	158	67.1	158	35

\*\*Particle size distribution not reported.

- (44) I. Jaffe and D. Price, "Determination of the Critical Diameter of Explosive Materials," ARS Journal, 32, 1060 (1962).
- (45) L. A. Roslund and N. L. Coleburn, "Hydrodynamic Behavior and Equation of State of Detonation Products Below the Chapman-Jouguet State," Fifth Symposium (International) on Detonation, ONR Rpt. ACR 184, U.S. Gov. Print. Office, Washington D.C. (1972); p 523.
- (46) N. L. Coleburn and B. E. Drimmer, "Explosive Properties of the Amino-Substituted, Symmetrical Trinitrobenzene," NOLTR 63-81, May 1963.
- (47) M. F. Murphy and N. L. Coleburn, "A Preliminary Evaluation of Tacot, A New Heat Resistant Explosive," NOLTR 61-155, 14 Nov 1961.
- (48) D. Price, A. R. Clairmont, Jr., and J. O. Erkman, "Explosive Behavior of Aluminized Ammonium Perchlorate," Combust. Flame 20, 389 (1973). See also NOLTR 72-15.

value, the data serve to indicate the order of magnitude of  $d_c$  for some common explosives. Where available, a representative value for  $P_g$  is also listed. No correlation between  $d_c$  and  $P_g$  for this group of explosives is evident.

It should be noted, from the data for cast TNT and the tritonals in Table D-1, that as aluminum is added,  $d_c$  decreases. This is also reported to be the case for aluminized plastisol NC propellants.

Available data ( $d_c$  vs %TMD) for TNT were reviewed in reference (20). Figure D-1 shows the smoothed curves derived from that study. They illustrate:

1. The large effect of the initial particle size.
2. The U shaped limit curve which is the general form to be expected for any explosive.
3. The decrease in  $d_c$  with increasing compaction (over most of the range) which is typical of TNT-like explosives classified as group 1(43).
4. The small  $d_c$  (1 - 10 mm) to be expected for the most common, porous HE.

Because it is difficult to prepare charges as cylinders of very small diameter, it is useful to know the approximate relation between the critical (confined) layer height ( $h_{cr}$ ) and  $d_c$ . This is given as

$$d_c \approx 2h_{cr}$$

by Belyaev & Sukoyan (49), and by means of it they report the following values.

Reference (49) Data

HE	Particle size ( $\mu$ )	$\rho_0$	Approx. $d_c$ (mm)
TNT	20-70	1.60	3.25
TNT	400-800	1.57	3.30
PETN	1-10	1.68	0.18-0.19
Tetryl	50-150	1.65	0.55-0.58
	50-150	1.58	0.70
	1-10	1.16	0.94

(49) A. F. Belyaev and M. K. Sukoyan, "Detonability of Some Explosives with Increase in External Pressure", Combustion, Explosion and Shock Waves, 3 (1), 11 (1967).

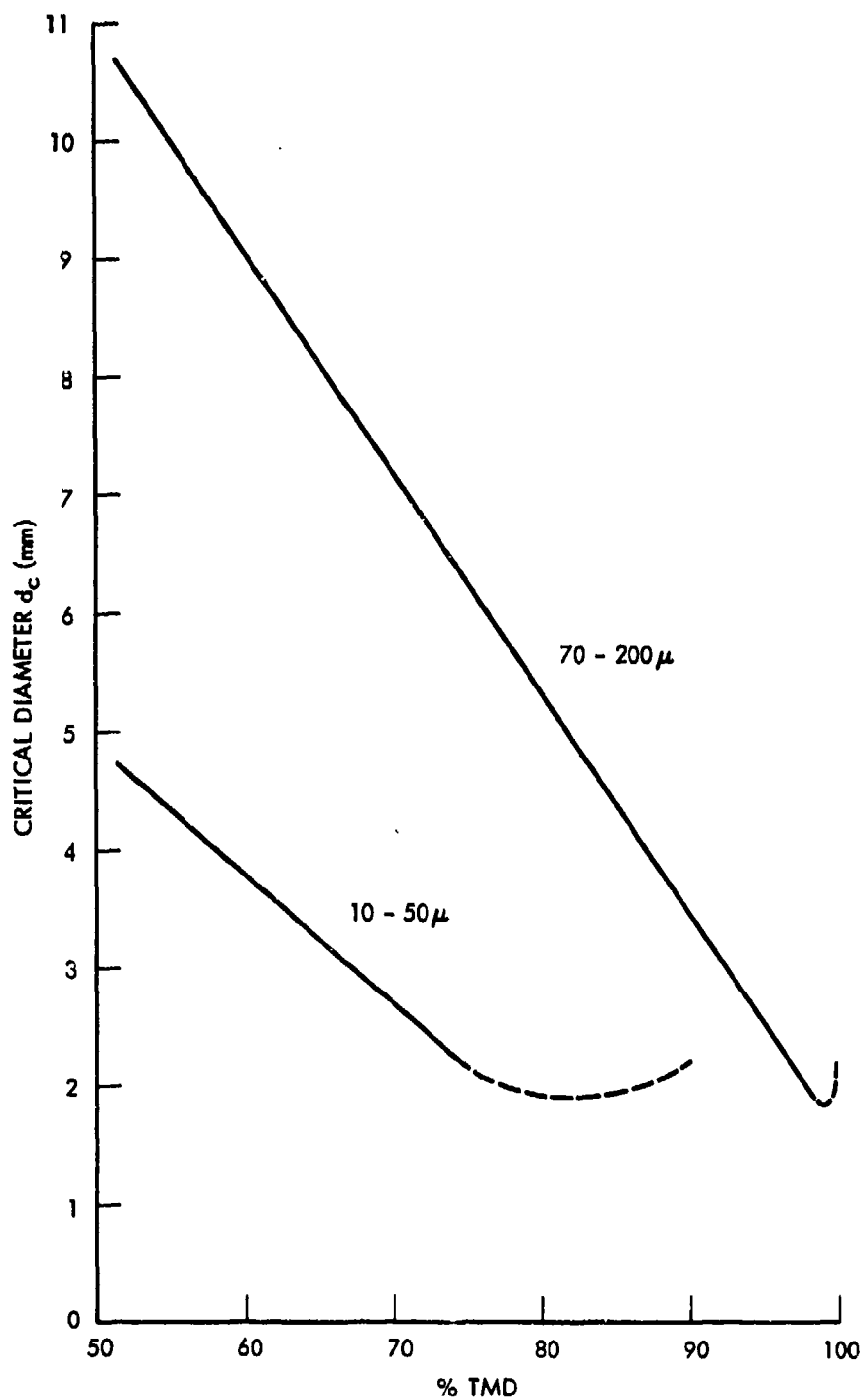


FIG. D-1 DETONATION FAILURE LIMIT CURVES FOR TNT.



We obtained the detonability curves of several other group 1 HE. They were low and high bulk density nitroguanidine (18) and 10 $\mu$  dinitrotoluene (50). The data were reported in the references shown, and the smoothed limit curves appear in Figure D-2. The minimum for NQ-h is obvious; that for DNT is not so evident since it is just being approached at 100% TMD. However, the sharp rise in  $P_G$  at 99% TMD (Figure 4) and the fact that DNT dead presses in the 0.7 scale version of the LSGT both indicate the existence of a minimum near 100% TMD.

In contrast to Group 1 material, Group 2 explosives (typified by AP and its mixtures) (43) exhibit an increase in  $d_c$  with increasing compaction over most of the range. This is illustrated in Figure D-3 which displays the detonability curves for various APs and two AP/wax mixtures. Here too there is a large effect of particle size ( $\delta$ ) and as in Group 1,  $d_c$  decreases with  $\delta$ . Here too the U shaped curve is the general form (see 10 $\mu$  AP) although the minimum occurs at lower %TMD rather than at higher, as in Group 1. Finally all of the curves of Figure D-3 show a very steep slope at some high compaction; it is in this region that these materials become subcritical (or dead-press) in the LSGT.

The failure curve of 10 - 80 $\mu$  AP in Figure D-3 comes from reference (51). The AP used in that work was obtained from a sieve cut; it had a microscopically observed particle size range of 10 - 80 $\mu$ , but the particle size distribution and median were not determined. The weight median particle size would of course be smaller than the mean of the projected area diameter of microscopic observations. Hence it is not surprising that this curve lies between those for the weight median particle sizes of 10 and 25 $\mu$ .

Reference (51) also reports a large effect of initial temperature on  $d_c$  of AP, one comparable to the temperature effect on AN quoted in Section VA. Finally, reference (51) describes the decrease in  $d_c$  of AP with the addition of fuel or with glass confinement as well as the increase in  $d_c$  of both AP and TNT with the addition of water; the effect of moisture is much more pronounced for AP than for TNT.

At the time that the minimum in the NQ-h curve (Figure D-2) and that in the 10 $\mu$  AP curve (Figure D-3) were observed, there was some question of the validity of such curves. Consequently the work was repeated on new batches of the explosives: NQ-h' Lot 589 (Curve of Figure D-2 is for NQ-h Lot 530) and 7.7 $\mu$  AP Lot 133.

(50) D. Price, J. O. Erkman, A. R. Clairmont, Jr., and D. J. Edwards, "Explosive Characterization of Dinitrotoluene", Combustion and Flame 14, 145 (1970). See also NOLTR 69-92.

(51) V. A. Gor'kov and R. K. Kurbangalina, "Concerning the Detonation Ability of Ammonium Perchlorate", Combustion, Explosion, and Shock Waves 2 (2), 12 (1966).

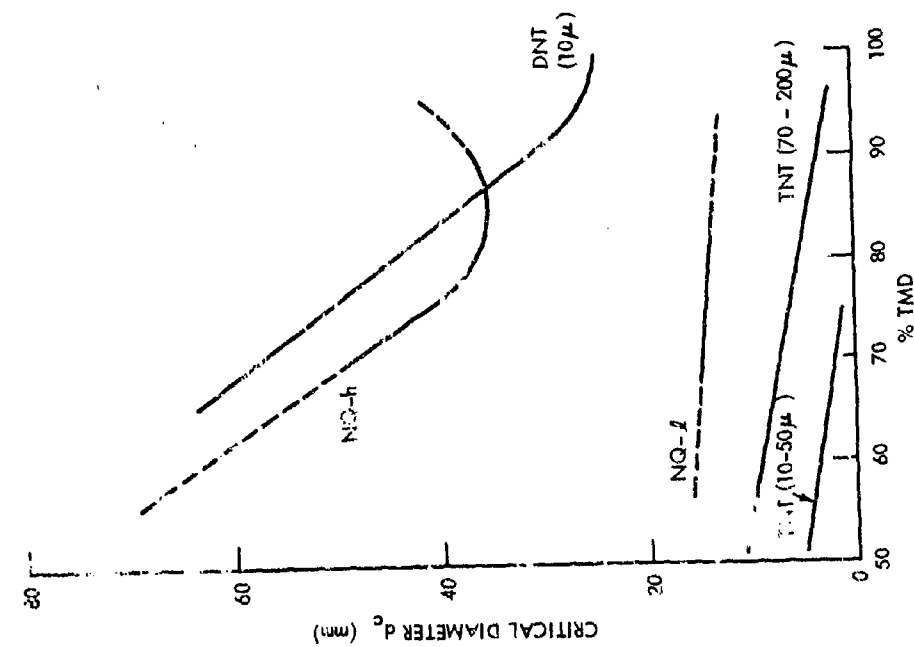


FIG. D-2 DETONABILITY CURVES (GROUP 1)

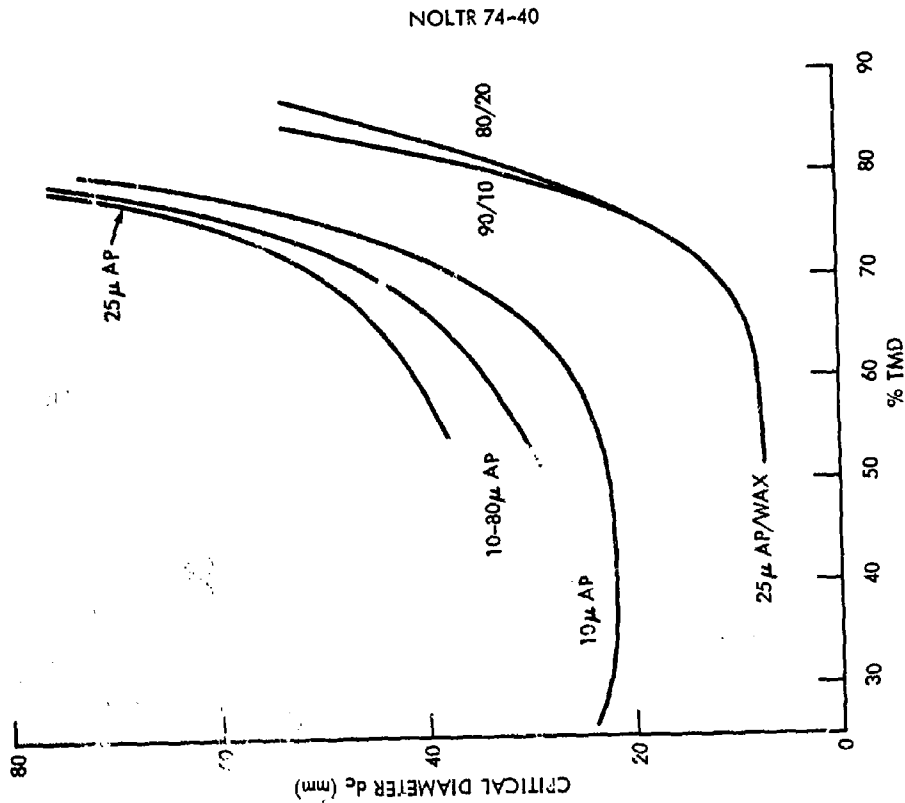


FIG. D-3 DETONABILITY CURVES (GROUP 2)

The latter data have been reported (52), but the former are reported here for the first time. In both materials, the existence of a minimum in the detonability curve was confirmed. Figure D-4 shows the new curves compared to those of Figures D-2 and D-3. These results again confirm that the general failure curve is U shaped although both branches are not generally found in easily accessible experimental ranges.

Figure D-5 contains the  $d$  vs %TMD limit curves for the remaining series that have been run: 9 $\mu$  AP/Al, 95/5 (53), and the two propellant models, Mod I and Mod II. The limit curve for 10 $\mu$  AP is also shown for comparison. Evidently the addition of 5% Al to AP decreases the critical diameter significantly; the difference at 50% TMD is about twice that found between 10 and 7.7 $\mu$  AP (Figure D-4).

From the shock sensitivity curves (Figures 4-6) and the detonability curves (Figures D-1 to 5), it is possible to pick pairs of  $P_g$ ,  $d_c$  corresponding to the same %TMD\*. We already know that Group 1 materials show opposite trends in  $d_c$  and  $P_g$  with compaction, and that Group 2 materials show the same trends. We also know that particle size has about twice the effect on  $d_c$  that it has on  $P_g$  (e.g., 8 and 25 $\mu$  AP). Hence we cannot expect a general relationship between  $d_c$  and  $P_g$  over all the materials studied or even for batches of the same material of different particle size. Within single batches, however, there seems to be a relationship between  $d_c$  and  $P_g$ .

Figure D-6 illustrates the relationships for various Group 1 explosives. To the left of the minimum in  $d_c$  vs %TMD, the trend is decreasing  $d_c$  with increasing  $P_g$ ; in fact, much of the data in this range can be fit to linear relationships between  $d_c^{-1}$  and  $P_g$  (a different curve for each HE). To construct Figure D-6, values of  $d_c$ ,  $P_g$  at intervals of about 5% in %TMD were used. Only one relative density (85% TMD) common to each curve is indicated by the dashed line. The corresponding set of curves for Group 2 HE is shown in Figure D-7; here the common value of 80% TMD is indicated by arrows.

\*It should be kept in mind that the same batches of HE were seldom used for both curves. Thus, the TNT detonability curve is from the literature; two lots of DNT (150 - 350 $\mu$ ) were used to obtain the shock sensitivity curve and a third (3 - 10 $\mu$ ) to obtain the detonability curve; and AP (7 $\mu$ ) was used for  $P_g$  vs %TMD whereas AP (10 $\mu$ ) was used for  $d_c$  vs %TMD.

- (52) D. Price, A. R. Clairmont, Jr., and J. O. Erkman, "Explosive Behavior of a Simple Composite Propellant Model", Combustion and Flame 17, 323 (1971).
- (53) P. B. Dempster, "The Effect of Inert Components in the Detonation of Gelatinous Explosives", Discussions Faraday Soc. 22, 196 (1956).

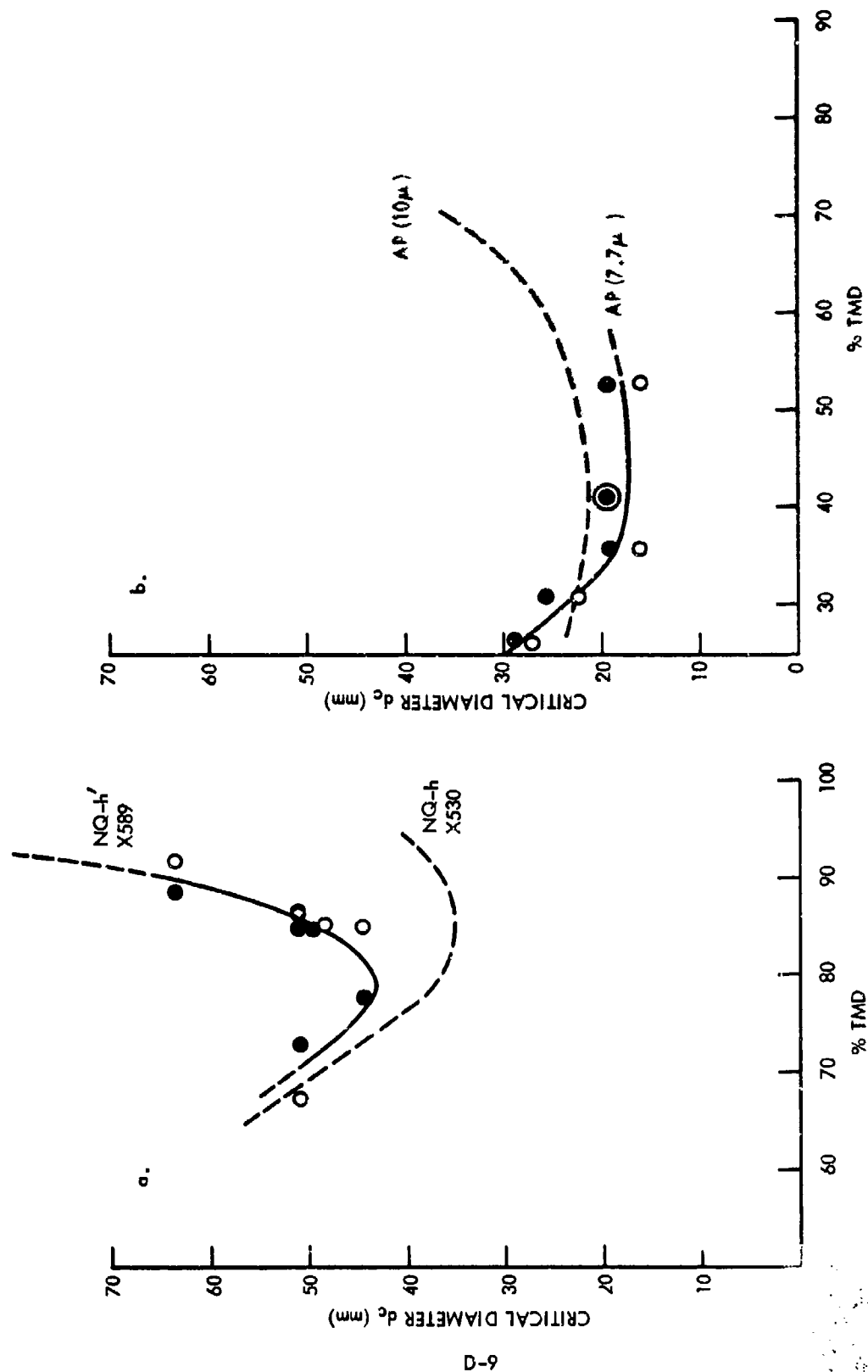
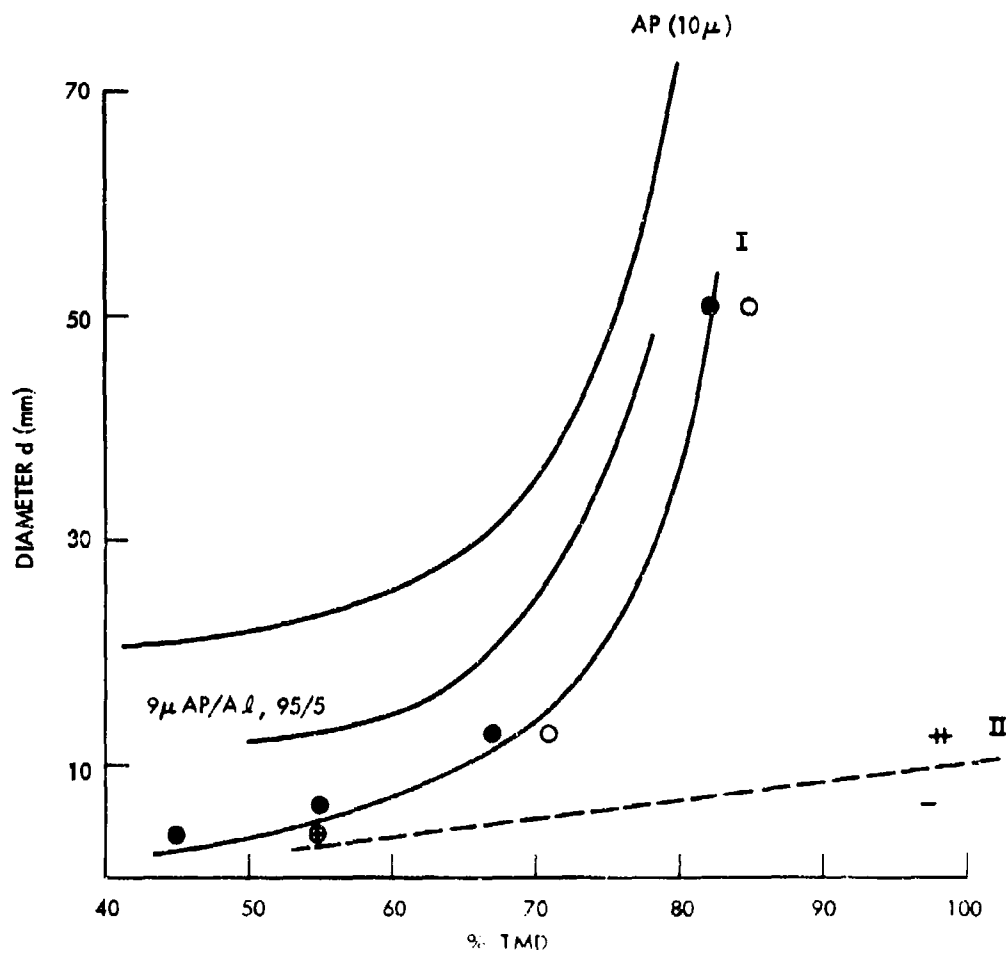


FIG. D-4 MINIMA IN DETONABILITY CURVES. (● DETONATION; ○ FAILURE)



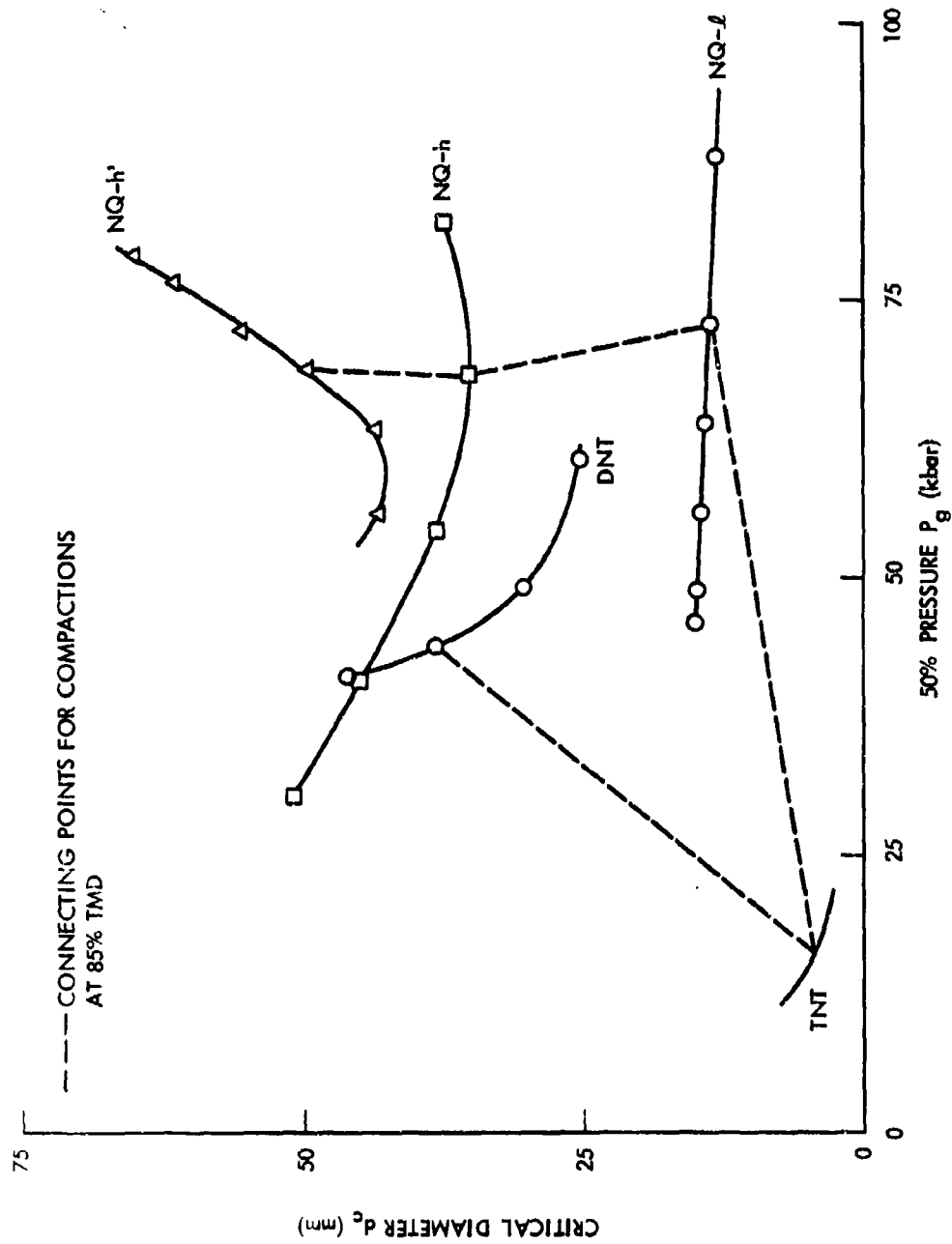


FIG. D-6 RELATIONS  $d_c$  vs  $P_g$  FOR GROUP I HE

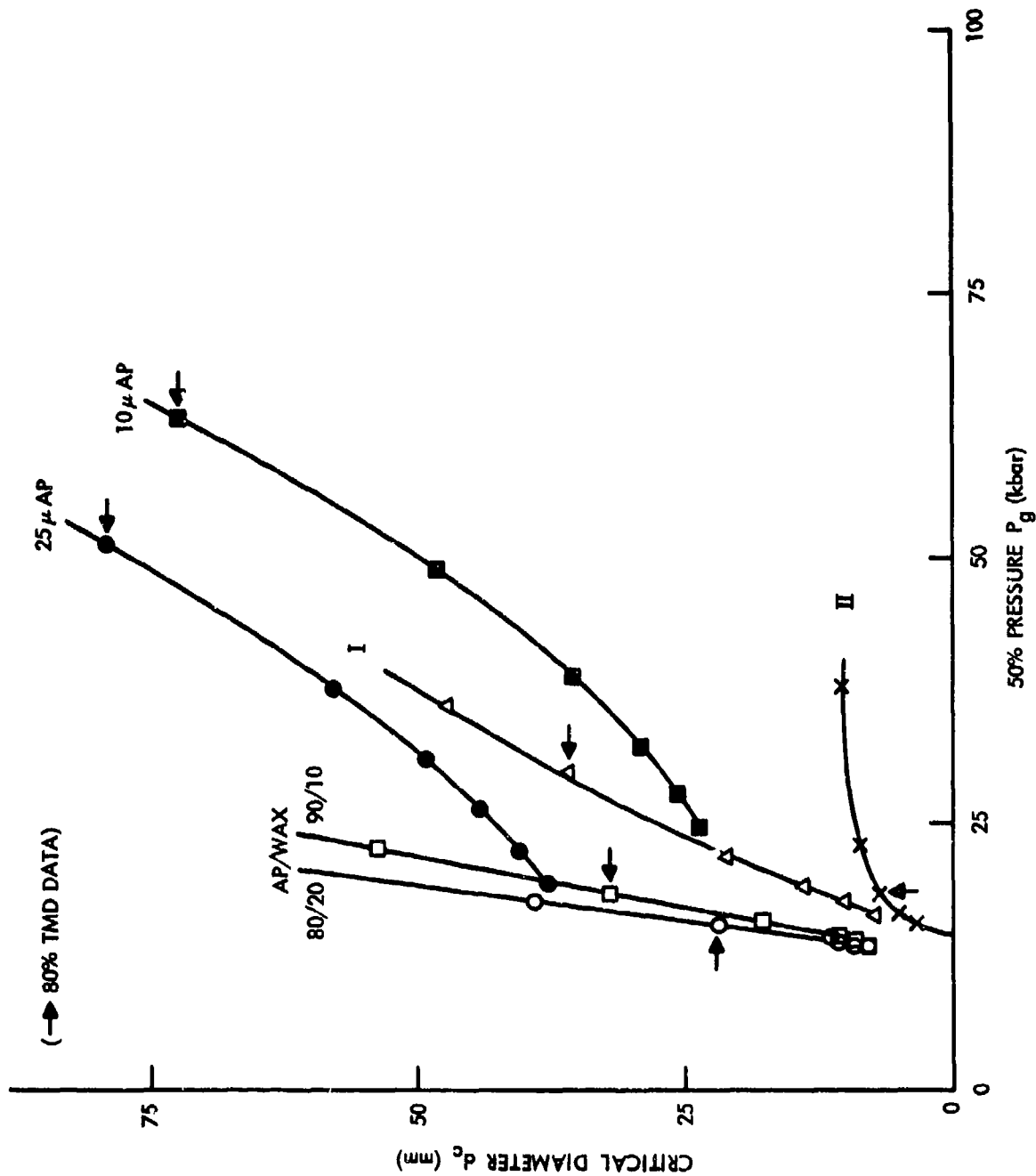


FIG. D-7 RELATIONS  $d_c$  VS.  $P_g$  FOR GROUP 2 HE  
(I AP/AE/WAX, 62.5/18.75/18.75; II AP/AE/WAX/HMX, 50/15/15/20)

Note that there is some relationship between  $d_c$  and  $P_g$  in every case, but there is no general relationship. Moreover the trends found appear to be dominated by the location of the minimum  $d_c$  in the detonability curve. Thus,

Material	Min. $d_c$ at % TMD of	Dead Press at % TMD	Ignitability (Impact) cm	Q cal/g
10 $\mu$ AP	44	80	100-133	405
NQ-h,h'	79-84	92	>320	921
DNT	~100	>99	>320	1151
TNT-p	>100	>100	160	1297

It seems probable that the same factors are responsible for dead pressing and the occurrence of a minimum in the failure limit curve. Two likely factors are ignitability and energy release Q of the subsequent exothermic reaction. Consequently approximate values for these factors have also been listed.

Finally, it should be noted that the addition of inert materials can change the value of  $d_c$ . Dempster (53) showed that 0.5 - 10 $\mu$  particles of inert of density > 2.8 g/cc (e.g., BaSO<sub>4</sub>) sensitized blasting gelatine to shock initiation whereas those greater in size than 10 $\mu$  sensitized it to initiation by impact (dropweight) or friction. The first effect seemed to be that of reducing  $d_c$ ; that this effect did occur was shown by Apin & Stesik (54) working with pastisol type propellants. Using relatively dense powdered diluents (CaCO<sub>3</sub>, MgO, Bi<sub>2</sub>O<sub>3</sub>, PbO, HgO, & W), they found,

$$d_c = \frac{A}{(n + n_0)^{1/3}} + B \quad (11)$$

where A & B are functions of the diluent,

$n$  = concentration of additive particles,

$n_0$  = concentration of reaction foci in matrix before addition of inert. The first term of Equation (11) is the average distance between foci. It was assumed that the inert particles of  $\rho > \rho_{\text{matrix}}$  afforded a focus where shock reflection and intensification could produce a hot spot.

(54) A. Ya. Apin and L. N. Stesik, "On the Mechanism of the Chemical Reaction at the Detonation of Compact Explosives," Zh. prikl mekh tekhn fiz No. 2, 146 (1965). Translation by J. O. Mulhaus.



Interestingly enough, Irwin of Aerojet (55) added finely divided RDX to a simple composite propellant ( $d_c \sim 65-72$  in.) and found,

$$d_c = \frac{a}{(x_{RDX} + C)^{1/3}} + B \quad (12)$$

where  $x_{RDX}$  is mass fraction of RDX particles and  $a$ ,  $B$ , &  $C$  are arbitrary constants; each particle is considered a hot spot which seems reasonable.

Both Equations (11) and (12) are for voidless materials and suggest that the greater the number of hot spots, the easier the propagation and the smaller  $d_c$ . This is quite reasonable but incomplete. For example, the greater the number of hot spots, the greater the burning area, the more rapid the acceleration of burning under confinement and hence the more easily transition to detonation can occur. Therefore as  $n$  increases,  $d_c$  decreases and  $P_g$  decreases if the number of hot spots were the only factor. But as we have seen above,  $d_c$  and  $P_g$  do not show the same trend over the range of relative density studied.

Other workers (56) investigated the effect of additives on minimum initiating charge (booster test) and on  $d_c$ . They reported the same effect of the additive on both, but added that they were effective only in the case of explosive charges with a high density and low porosity - in other words, Equations (11) and (12) seem inapplicable to granular porous charges.

(55) R. R. Elwell, O. R. Irwin and R. W. Vail, Jr. Project SOPHY-Solid Propellant Hazards Program AFRPL-TR-67-211 Vol II, App. I, Aug 1967.

(56) A. S. Derzhavets, "Increased Susceptibility of Explosives to a Detonation Impulse." *Termostoikie Vzryvchatye Veshchestva Ikh Deistvie Glubokikh Skvazhinakh* 1969, 37 Edited by F. A. Baum, Izd. "Nedra": Moscow; USSR. Only C. A. abstract available.